Inaugural dissertation

for

obtaining the doctoral degree

of the

Combined Faculty of Mathematics, Engineering, and Natural Sciences

of the

Ruprecht-Karls-University

Heidelberg, Germany

Presented by

Luísa Vieira Codeço Marques, MSc

Born in: Rio de Janeiro, 1993

Oral examination: May 28th, 2024

Identification of small molecules and miRNA inducing M1-like polarisation in murine and human macrophages

Referees: Prof. Dr Viktor Umansky

Prof. Dr Stefan Eichmüller

Abstract

Macrophage activation plays a pivotal role in the immune response, with the M1-like and M2-like phenotypes orchestrating pro-inflammatory and anti-inflammatory actions, respectively. The dynamic ability of macrophages to shift between these states underpins their significance in pathophysiological conditions, including cancer, where repolarisation towards an M1-like state could potentiate anti-tumour immunity. This study aimed to explore the repolarisation potential of murine bone marrow derived macrophages (BMDMs) and human monocyte derived macrophages (MdMs), focusing on identifying and testing functional molecules capable of inducing shifts toward an M1-like activation state.

Through RNA and miRNA sequencing, shared and species-specific pathways in gene expression were identified, facilitating the selection small molecule inhibitors (SMIs) targeting transcription regulators associated with the M2-like phenotype and miRNAs over-expressed in M1-like macrophages and *in silico* analysed to target transcription regulators. My results revealed that miR-155-5p, along with a pool of SMIs targeting Stat6, Myc, Stat3, and HDACs, effectively repolarised macrophages towards an M1-like phenotype, albeit with notable differences in the extent of repolarisation and functional outcomes between murine and human models.

Functional assays assessing the anti-tumour activity and T-cell activation potential of repolarised macrophages demonstrated that IFN-ɣ+LPS treatment significantly enhanced these capabilities in both species. However, despite molecular indications of repolarisation with miR-155-5p and the inhibitor pool, these did not translate into expected functional outcomes, highlighting the complexity of macrophage biology and the nuanced interplay of molecular and functional repolarisation mechanisms.

This study contributes significantly to our understanding of macrophage polarisation and repolarisation, emphasising the translational relevance of shared pathways across species and identifying potential therapeutic targets for manipulating macrophage states. The findings underscore the importance of evaluating both molecular changes and functional implications of repolarisation strategies, paving the way for the development of targeted therapies that leverage the immune system's intrinsic anti-tumour potential.

Zusammenfassung

Die Aktivierung von Makrophagen spielt eine entscheidende Rolle in der Immunantwort, wobei die M1-ähnlichen und M2-ähnlichen Phänotypen jeweils pro-entzündliche und anti-entzündliche Aktionen orchestrieren. Die dynamische Fähigkeit von Makrophagen zwischen diesen Zuständen zu wechseln, unterstreicht ihre Bedeutung bei pathophysiologischen Zuständen, einschließlich Krebs, wo eine Repolarisation in Richtung eines M1-ähnlichen Zustands die Anti-Tumor-Immunität potenzieren könnte. Diese Studie zielte darauf ab, das Repolarisationspotenzial von murinen knochenmarkabgeleiteten Makrophagen (BMDMs) und von menschlichen monozytenabgeleiteten Makrophagen (MdMs) zu erforschen, wobei der Fokus auf der Identifizierung und Prüfung von Kandidaten lag, die in der Lage sind, Verschiebungen in Richtung eines M1-ähnlichen Aktivierungszustands zu induzieren.

Durch RNA- und miRNA-Sequenzierung wurden gemeinsame und speziesspezifische Wege der Genexpression identifiziert, was die Auswahl kleiner Molekülinhibitoren (SMIs) erleichterte, die auf Transkriptionsregulatoren abzielen, die mit dem M2-ähnlichen Phänotyp assoziiert sind, und miRNAs, die in M1-ähnlichen Makrophagen überexprimiert sind und *in silico* analysiert wurden, um Transkriptionsregulatoren zu zielen. Meine Ergebnisse zeigten, dass miR-155-5p zusammen mit einem Pool von SMIs, die auf Stat6, Myc, Stat3 und HDACs abzielen, Makrophagen effektiv in Richtung eines M1-ähnlichen Phänotyps repolarisierten, allerdings mit bemerkenswerten Unterschieden im Ausmaß der Repolarisation und funktionellen Ergebnissen zwischen murinen und menschlichen Modellen.

Funktionelle Untersuchungen zur Bewertung der Anti-Tumor-Aktivität und des T-Zell-Aktivierungspotenzials von repolarisierten Makrophagen zeigten, dass eine Behandlung mit IFN-γ+LPS diese Fähigkeiten in beiden Spezies signifikant verstärkte. Trotz molekularer Anzeichen einer Repolarisation mit miR-155-5p und dem Inhibitorpool führten diese jedoch nicht zu den erwarteten funktionellen Ergebnissen, was die Komplexität der Makrophagenbiologie und das nuancierte Zusammenspiel von molekularen und funktionellen Repolarisationsmechanismen hervorhebt.

Diese Studie trägt wesentlich zu unserem Verständnis der Makrophagenpolarisation und Repolarisation bei und betont die translationale Relevanz gemeinsamer Pfade über Spezies hinweg und identifiziert potenzielle therapeutische Ziele zur Manipulation von Makrophagenzuständen. Die Ergebnisse unterstreichen die Wichtigkeit, sowohl molekulare Veränderungen als auch funk-

tionelle Implikationen von Repolarisationsstrategien zu bewerten, was den Weg für die Entwicklung von zielgerichteten Therapien ebnet, die das intrinsische Anti-Tumor-Potenzial des Immunsystems nutzen.

Acknowledgements

This journey towards completing my doctoral thesis has been an incredible learning experience, and it would not have been possible without the support and guidance of several key individuals and institutions. I extend my deepest gratitude to:

Prof. Dr. Stefan Eichmüller, for welcoming me into his team and providing me with the opportunity to embark on this fascinating project. His invaluable scientific discussions and unwavering support have been pivotal throughout my research.

Dr. Wolfram Osen, whose mentorship and scientific insights have significantly shaped my laboratory experience and thesis writing. His constant supervision has been a cornerstone of my development as a researcher.

Prof. Dr. Viktor Umansky and **Prof. Dr. Adelheid Cerwenka**, members of my TAC committee, for their consistent engagement with my work and their constructive scientific feedback, which has enriched my research immensely.

Prof. Dr. Alexander Dalpke and **Prof. Dr. Ilse Hofmann**, for their willingness to be part of my examination committee and support my journey towards obtaining my doctoral degree.

I am also grateful to:

Dr. Theresa Kordaß, for her collaboration on work with human MdMs and assistance with bioinformatic analysis, offering me both knowledge and support.

Elke Dickes, for her guidance in the activation and culture of CTLs and for being an exemplary mentor in the lab.

Alicia Avenhaus, for introducing me to the Incucyte® S3, and **Dr. Angelika Riemer** and **Kathrin Wellach**, for allowing me access to the Incucyte® SX5.

Dr. Moritz Mall, for the use of the QuantStudio 5 Real-Time PCR System 384-well, a crucial tool in my research.

GENEWIZ Multiomics & Synthesis Solutions from Azenta Life Sciences, for their expertise in library preparation, sequencing, and bioinformatic analysis of RNA and miRNA sequencing.

Melanie Bewerunge-Hudler from the **Microarray Core Facility**, for her support with Microarray analyses.

The dedicated individuals at the **FACS Core facility**.

Dr. Rainer Will, for his contribution to the production of RFP cell lines.

The **animal caretakers**, whose efforts have been essential to the progress of this research.

Tim Wagner and the students involved in this project: **Ida**, **Masooma**, and **Anni**, for their contributions and teamwork.

Each of you has played a significant role in my academic journey, providing support, inspiration, and expertise that have been instrumental in the completion of my thesis. I am profoundly grateful for your generosity and mentorship.

Furthermore, I would like to thank my friends and family:

Minha mãe, meu pai, minha irmã, Breno e a pequena Manu. Amo vocês.

Bryce and Inu, you are also my family.

My friends from Brasil and from Germany, thank you all.

Contents

List of Figures

List of Tables

List of Acronyms

ABCA1	ATP-binding cassette transporter
AF488	Alexa Fluor 488 dye
AGM	aorta-gonads-mesonephros
Ago	Argonaute
ALI	acute lung injury
ALOX15	arachidonate 15-lipoxygenase
AMPK	AMP-activated protein kinase
APC	Allophycocyanin
APCs	antigen-presenting cells
APC-Cy7	Allophycocyanin-Cyanine 7
Arg1	arginase 1
ATP	adenosine triphosphate
BCL6	B-cell lymphoma 6
BM	bone marrow
BMDMs	bone marrow-derived macrophages
bp	base-pair
BSA	bovine serum albumin
BV421	Brilliant Violet 421
cAMP	cyclic AMP
CAR	chimeric antigen receptor
CCL	C-C Motif Chemokine Ligand
CCR	C-C motif chemokine receptor
CD	Cluster of differentiation
CDPs	common dendritic cell progenitors
CEA	Carcinoembryonic antigen
CFB	Complement Factor B
CFSE	Carboxyfluorescein succinimidyl ester
Chil3	chitinase-like 3 or Ym1
c-Maf	proto-oncogene c-Maf
cMoPs	common monocyte progenitors
CMPs	common myeloid progenitors
c-Myc	Cellular Myelo-Cytomatosis Proto-Oncogene

CNS	central nervous system
CR	Complement receptor
CSF1	Colony-stimulating factor 1
CTLs	Cytotoxic T lymphocytes
CTLA-4	cytotoxic T-lymphocyte-associated protein 4
CTV	CellTrace Violet
COX2	Cyclooxygenase 2
CX3CL1	C-X3-C Motif Chemokine Ligand 1
CX3CR1	C-X3-C motif chemokine receptor 1
CXCL	C-X-C Motif Chemokine Ligand
Cy3	Cyanine3
CyTOF	Cytometry by time of flight
DAMPs	damage-associated molecular patterns
DC	dendritic cell
DCs	dendritic cells
DEG	differentially expressed gene
DMEM	Dulbecco's modified Eagle medium
DNA	deoxyribonucleic acid
DRAM2	DNA damage regulated autophagy modulator 2
DTT	dithiothreitol
EBI	erythroblastic island
EGF	epithelial growth factor
ELISA	enzyme-linked immunosorbent assay
EMPs	erythro-myeloid progenitors
EMT	epithelial-to-mesenchymal transition
FACS	Fluorescence-activated cell sorting
FBS	fetal bovine serum
Fc	fragment crystallizable region
FcαRI	Fc alpha receptor I
FcγR	Fc gamma receptor
FcεRI	Fc epsilon receptor I
FGF	fibroblast growth factor
FL	fetal liver
FSC	forward scatter
GBM	Glioblastoma
GFP	green fluorescent protein
GM-CSF	Granulocyte-macrophage colony-stimulating factor
GMPs	granulocyte-macrophage progenitors
GO:BP	Gene Ontology:Biological Process
GPCRs	G protein-coupled receptors
GSK-3β	Glycogen synthase kinase-3beta

HBSS	Hanks' buffered saline solution
HCC	hepatocellular carcinoma
HDACs	Histone deacetylases
HGF	Hepatocyte Growth Factor
HIF-1α	hypoxia-inducible factor 1-alpha
HIFs	hypoxia-inducible factors
HNF4α	Hepatocyte Nuclear Factor 1-Alpha
HNSCC	head and neck squamous cell carcinoma
HSCs	hematopoietic stem cells
IA^b	MHC Class II Allele IAb
iC3b	inactivated C3b
IDO1	Indoleamine 2,3-dioxygenase 1
IF	immunofluorescence
IFN-γ	Interferon Gamma
Ig	Immunoglobulin
IHC	immunohistochemistry
I-κB	inhibitor of kappa B
IKK	inhibitor of kappa B kinase
IL	Interleukin
iNOS	inducible nitric oxide synthase
integrin αVβ3	integrin alfa V beta 3
IRF	interferon regulatory factor
JAK	Janus kinase
JUN	Jun Proto-Oncogene, AP-1 Transcription Factor Subunit
KLF4	Kruppel-like factor 4
LBP	lipopolysaccharide-binding protein
LLC	Lewis lung carcinoma
LNPs	lipid nanoparticles
LPS	lipopolysaccharide
MCPIP1	monocyte chemotactic protein-induced protein-1
M-CSF	Macrophage colony-stimulating factor
MdMs	monocyte-derived macrophages
MDPs	monocyte-macrophage DC progenitors
MFI	Median Fluorescence Intensity
MHC	major histocompatibility complex
MIF	macrophage migration inhibitory factor
miRISC	miRNA-induced silencing complex
miRNAs	MicroRNAs
MMPs	Matrix metalloproteinases
MRC1	Mannose Receptor C-Type 1 or CD206
Mrc1	Mannose Receptor C-Type 1 or CD206

mRNAs	messenger RNAs
MS	multiple sclerosis
Mtb	*Mycobacterium tuberculosis*
MYC	Myelo-Cytomatosis Proto-Oncogene
NF-kB	Nuclear factor kappa-light-chain-enhancer of activated B cells
NK	natural killer
NLRs	NOD-like receptors
NO	nitric oxide
Nos2	Nitric oxide synthase 2
OA	osteoarthritis
OVA	Ovalbumin
P2Y2R	P2Y purinoceptor 2
PAMPs	pathogen-associated molecular patterns
PBS	phosphate-buffered saline
PDAC	pancreatic ductal adenocarcinoma
PDE4B	Phosphodiesterase 4B
PDGF	platelet-derived growth factor
PD-L	Programmed death-ligand
PE	Phycoerythrin
PE-Cy7	Phycoerythrin-Cyanine7
Pen-Strep	Penicillin-Streptomycin
PerCP-Cy5.5	Peridinin-chlorophyll-protein
PO	Pacific Orange
PPAR	Peroxisome Proliferator-Activated Receptor
pre-miRNAs	precursor miRNAs
pri-miRNAs	primary miRNAs
PRRs	pattern recognition receptors
qRT-PCR	quantitative real time polymerase chain reaction
RA	rheumatoid arthritis
RAGE	Receptor for Advanced Glycation Endproducts
Retnl1	resistin like alpha or Fizz1
RFP	Red Fluorescent Protein
RLRs	RIG-I like receptors
RNA-Seq	RNA-sequencing
RNA	ribonucleic acid
RNS	Reactive nitrogen species
ROS	Reactive oxygen species
RPKM	Reads Per Kilobase per Million mapped reads
Rpl19	Ribosomal Protein L19
RT	room temperature
SCARB1	Scavenger receptor class B member 1

scRNA-seq	single cell RNA-sequencing
SH2	Src Homology 2
SHIP1	SH-2 containing inositol 5' polyphosphatase 1
SIRPα	Signal Regulatory Protein Alpha
SIRT1	Sirtuin1
SLC2A6	Solute carrier family 2, facilitated glucose transporter member 6
SMIs	small molecule inhibitors
SOCS1	suppressor of cytokine signaling-1
Sod2	SOD2 superoxide dismutase 2
SSC	side scatter
STAT	Signal Transducers And Activators Of Transcription
STING	Stimulator of interferon genes
TAMs	tumour associated macrophages
TAK1	Transforming growth factor-β-activated kinase 1
TCR	T cell receptor
TF	transcription factor
TGF-β	Transforming Growth Factor Beta
Th1	Type 1 T helper
Th2	Type 2 T helper
Th17	Type 17 T helper
TLRs	Toll-like receptors
TME	tumour microenvironment
Tnf	Tumor Necrosis Factor
TNF-α	Tumor Necrosis Factor alpha
Tnfaip3	Tumor necrosis factor alpha-induced protein 3
TRAF1	TNF receptor-associated factor 1
Tregs	regulatory T cells
Trem2	Triggering Receptor Expressed On Myeloid Cells 2
Trim24	Tripartite Motif Containing 24
Trp53	Transformation-Related Protein 53
TSS	transcriptional start site
UTP	Uridine triphosphate
UTRs	untranslated regions
VEGF	vascular endothelial growth factor
WT	wild-type
YS	yolk sac

Chapter 1

Introduction

Macrophages are tissue resident immune cells and an essential component of innate immunity. These mononuclear phagocytes are the first line of defence against infection, sensing diverse microenvironmental stimuli and adapting their response accordingly. Their main function is immune surveillance and tissue homeostasis. Their innate immune sensors can recognise pathogen-associated molecular patterns (PAMPs) and damage-associated molecular patterns (DAMPs), resulting in a complex signalling cascade and their activation. They neutralise pathogens in tissue via phagocytosis and secretion of pathogen killing substances, while secreting mediators that call and activate other immune cells, starting inflammation. As phagocytic cells, they also have an antigen processing and antigen presentation role, where they then crosstalk with cells of the adaptive immune response, being a mediator between innate and adaptive response. In parallel, macrophages also help with tissue remodelling and wound healing by clearing apoptotic cells and production of extracellular matrix components and angiogenic factors. They can also mitigate the inflammatory response for the resolution of the immune response, being then regarded as anti-inflammatory (Murphy & Weaver, 2016).

Macrophages respond to various environmental signals and with different functional phenotypes, called activation states. These phenotypes can also be reversed, demonstrating these cells capability for plasticity and heterogeneity. This plasticity is orchestrated by complex gene networks, signalling cascade and epigenetic regulation. Multiple transcription factors and differential expression of MicroRNAs (miRNAs) influence these states (Geiß et al., 2022). The plasticity and versatility of macrophages make them attractive targets for therapeutic intervention, and understanding the mechanisms underlying macrophage activation and polarisation is critical for the development of new strategies for the treatment of immune-related diseases.

Macrophage activation is typically into divided into two broad and simplified categories: classical activation (M1) and alternative activation (M2), mirroring the Th1 and Th2 response. M1 macrophages are characterised by a pro-inflammatory phenotype and are involved in host defence against intracellular pathogens, such as viruses and bacteria. In contrast, M2 macrophages are associated with anti-inflammatory and tissue repair functions and are involved in the resolu-

tion of inflammation and tissue remodelling. The imbalance between these activation states has been implicate implicated in a range of diseases and pathologies (Kloc, 2017). Unchecked chronic inflammation is the cause of multiple autoimmunity disorders, such as multiple sclerosis (MS) and rheumatoid arthritis (RA). In parallel M2 macrophages are implicates in excessive fibrosis and airway hyperreactivity (Funes et al., 2018).

One of the hallmarks of cancer is immune evasion (Hanahan & Weinberg, 2011). Macrophages are one of the most abundant immune cells infiltrating solid tumours, and they help establish an immunosuppressive milleu, helping the tumour cells escape the adaptive immune system. These tumour associated macrophages (TAMs) could be new targets for cancer immunotherapy, where their ability to repolarise into immunostimulatory activated macrophages could then facilitate the immune system to fight and neutralise the tumour (Kumar et al., 2020).

My objective is to delve into and harness the mechanisms of macrophage activation, focusing on exploring repolarisation strategies via inhibiting transcription factors and applying miRNAs.

1.1 Macrophages - Origin

The origins of macrophages, critical components of the immune system, are traced back to the intricate processes of hematopoiesis, which occurs in multiple waves throughout embryonic development and into adulthood. This developmental journey shapes the diverse roles that macrophages play in tissue homeostasis, inflammation, and disease response. Initially, macrophage progenitors emerge from primitive hematopoiesis in the yolk sac (YS), marking the earliest phase of immune cell development. This is followed by a transition to fetal hematopoiesis, where the fetal liver (FL) becomes a key site for the generation of hematopoietic stem cells (HSCs) that will eventually seed the bone marrow, setting the stage for adult hematopoiesis (Kloc, 2017).

The embryonic development of macrophages begins with the formation of early erythromyeloid progenitors (EMPs) in the YS, which give rise to the first tissue resident macrophages without transitioning through a monocytic stage. As development progresses, a second wave of hematopoiesis introduces late EMPs capable of migrating to the FL, contributing to a pool of progenitors that include lymphoid elements. This phase, termed transient hematopoiesis, is crucial for expanding and diversifying the types of immune cells that can be produced. Concurrently, a third wave originates from the intraembryonic hemogenic endothelium, leading to the maturation of HSCs in the aorta-gonads-mesonephros (AGM) region, which then populate the FL and eventually the fetal bone marrow (Kloc, 2017) (Fig 1). These processes underscore the complexity and coordination required to establish the immune system's cellular components before birth (Figure 1.1.1left).

Upon birth, the differentiation of macrophages progresses through definitive haematopoiesis within the bone marrow (BM), leading to the production of monocytes and monocyte-derived macrophages (Figure 1.1.1 right). These cells are essential for responding to inflammatory condi-

tions and are characterised by their ability to be recruited to tissues, where they perform various effector functions. While there is no strict division of labour based on their origins, evidence suggests that tissue resident macrophages, seeded pre-natally, are mainly responsible for maintaining tissue homeostasis. In contrast, monocyte-derived macrophages, emerging from adult haematopoiesis, are particularly active in directing responses to pathological signals, underlining their critical role in inflammation.

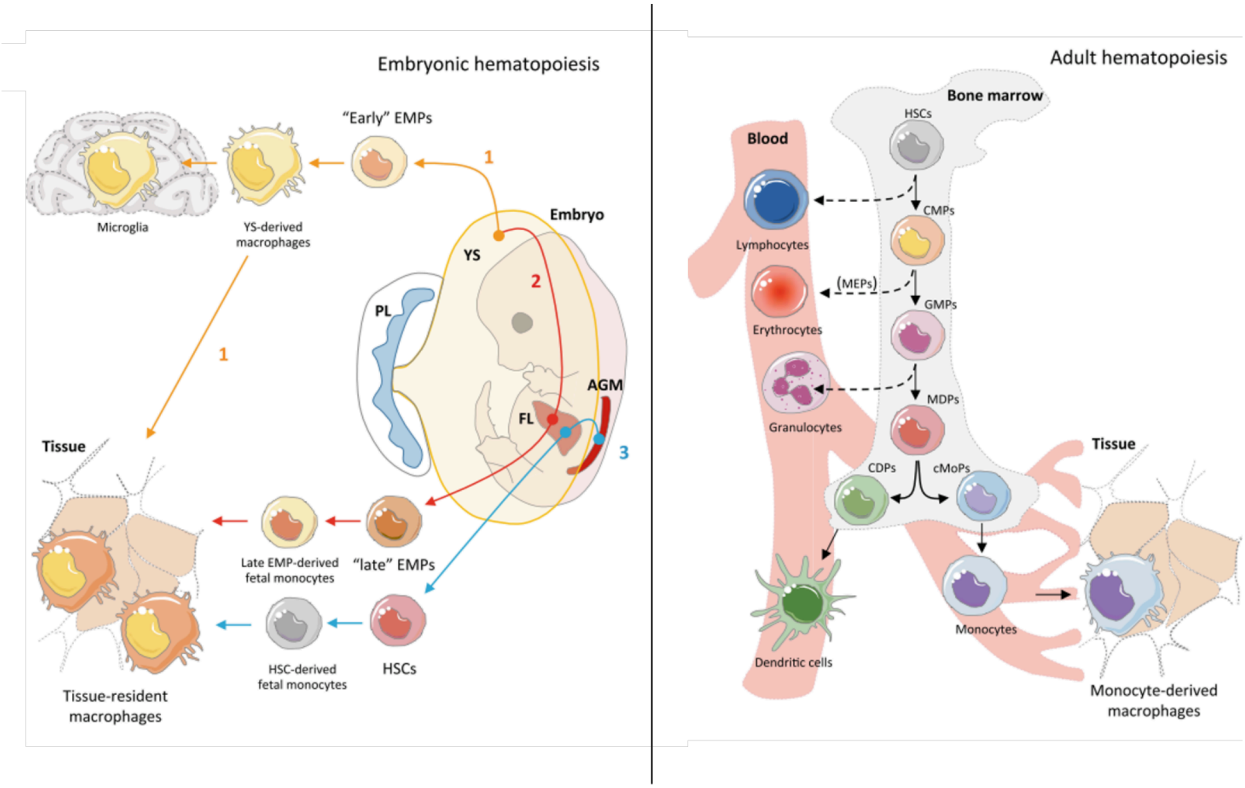

Figure 1.1.1. Origins of tissue-resident macrophages and monocyte-derived macrophages. On the left, tissue-resident macrophages originate from several embryonic sources, following a sequence that includes the YS, FL, and the AGM regions, unfolding through three principal waves of embryonic haematopoiesis. The initial wave commences in the YS, leading to the formation of "early" EMPs through "primitive haematopoiesis," from which YS-derived macrophages emerge. These YS-derived macrophages are posited as the predominant precursors for most tissue derived macrophages, such as microglia. The subsequent wave introduces "late" EMPs, potentially moving from YS to FL, considered as transient definitive progenitors. The final wave involves the creation of immature HSCs within the AGM, which then populate the FL, initiating "definitive haematopoiesis" and potentially seeding fetal BM to produce HSC-derived fetal monocytes. Following this embryonic development, monocyte-derived macrophages (on the right) are produced in the BM from the differentiation process of HSCs through stages of increasingly specific cell types, culminating in monocytes. This process is termed "definitive haematopoiesis". Once in the bloodstream, monocytes can migrate into tissues, differentiating into macrophages. This pathway involves a progression from HSCs to common myeloid progenitors (CMPs), granulocyte-macrophage progenitors (GMPs) and monocyte-macrophage DC progenitors (MDPs), which can differentiate into common dendritic cell progenitors (CDPs), giving rise to dendritic cells (DCs), or to common monocyte progenitors (cMoPs), which give rise to the monocytes. Image from (Kloc, 2017)

1.2 Tissue specific macrophages

The tissue-specific functions of macrophages reflect their remarkable adaptability and essential roles in maintaining physiological homeostasis, regulating inflammation, and responding to disease states across various organ systems. Each macrophage population is finely tuned to the unique demands of its residing tissue, showcasing a wide array of specialised functions that are crucial for the health and proper functioning of the organism (Figure 1.2.1) (Mass et al., 2023; Saraiva Camara & Braga, 2022).

In the central nervous system (CNS), microglia are pivotal for neuroprotection, development, and maintaining neural homeostasis. Microglia, the resident macrophages of the CNS, are involved in synaptic pruning, supporting neuronal survival, and modulating inflammatory responses within the brain and spinal cord (Paolicelli et al., 2011). They continuously survey the CNS environment, ready to respond to injury or disease by engulfing cellular debris and secreting neurotrophic factors. These macrophages rely on niche-specific factors like Colony-stimulating factor 1 (CSF1) and Interleukin (IL)34 for their maintenance (Mass et al., 2023; Saraiva Camara & Braga, 2022).

In the bone marrow, macrophages such as erythroblastic island (EBI) macrophages, osteal macrophages (osteomacs), and osteoclasts play critical roles in haematopoiesis, bone remodelling, and the maintenance of the HSC niche. EBI macrophages facilitate erythropoiesis, osteomacs regulate osteoblast function and contribute to bone health, and osteoclasts are involved in bone resorption (Mass et al., 2023; McDonald et al., 2021; Saraiva Camara & Braga, 2022). These functions are essential for the dynamic process of bone formation and degradation, which is crucial for skeletal integrity and the creation of space within the bone marrow for HSCs and other haematopoietic activities.

Liver macrophages, called Kupffer cells, play vital roles in detoxification, immune surveillance, and metabolic regulation. Kupffer cells, residing within the liver sinusoids, are crucial for clearing pathogens, dead cells, and debris from the blood. They also contribute to the liver's metabolic functions, including iron and cholesterol homeostasis (Bonnardel et al., 2019; Mass et al., 2023; Saraiva Camara & Braga, 2022). The liver's unique exposure to gut-derived antigens and metabolic products positions these macrophages as key players in maintaining immune tolerance and metabolic balance.

Lung macrophages, primarily alveolar macrophages, are essential for respiratory health. Alveolar macrophages patrol the air spaces, clearing inhaled particles and pathogens, and modulating inflammation to prevent tissue damage (Aegerter et al., 2022). Their ability to self-renew and their dependency on Granulocyte-macrophage colony-stimulating factor (GM-CSF) signal for maintenance are crucial for sustaining lung function (Mass et al., 2023; Saraiva Camara & Braga, 2022).

The specialisation of macrophages within these diverse tissues highlights their indispensable roles in tissue integrity, immune defence, and the maintenance of homeostasis. Their capacity to adapt to the specific needs of each tissue underlines the complexity of the immune system and the importance of macrophages in health and disease.

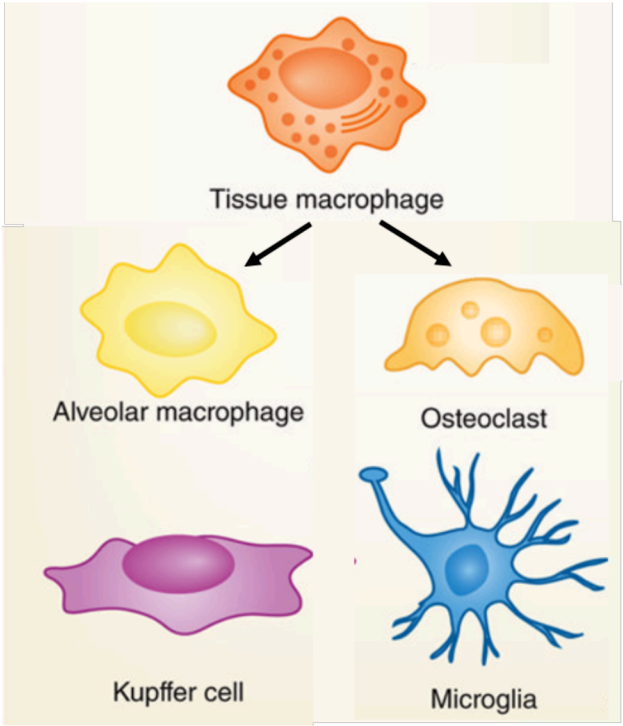

Figure 1.2.1. Tissue-specific macrophages.
Each of these macrophage populations is adapted to its specific environment, capable of responding to local cues, and performing functions that contribute to the health and defence of the organism. Examples of tissue-specific macrophages: Alveolar Macrophages in the lung, Kupffer Cells in the liver, osteoclasts in bone and microglia in the central nervous system. Modified from (Galli et al., 2011).

1.3 Macrophages – Main Functions

Macrophages exhibit a broad spectrum of functions, from phagocytosis and antigen presentation to the modulation of immune responses through cytokine signalling. They adeptly internalise and digest particulate matter, such as pathogens, through phagocytosis, This ability underscores their vital role in host defence, leading to the Reactive oxygen species (ROS) mediated killing and enzymatic digestion of pathogens in the phagolysosome and the presentation of antigenic peptides to T helper cells, bridging innate and adaptive immunity.

Complement receptors, including Complement receptor (CR)1, 2, 3 and 4, are crucial for the recognition and clearance of pathogens and apoptotic cells (Ley et al., 2016). These receptors bind to complement proteins that have been deposited on the surface of such targets, opsonising them and facilitating their phagocytosis and removal. For instance, CR1, or Cluster of differentiation (CD)35 is involved in the clearance of immune complexes, while CR3, composed of CD11b and

CD18 and CR4, composed of CD11c and CD18 are important for binding to inactivated C3b (iC3b), a cleavage product of the complement component C3, enhancing the phagocytosis of coated pathogens (Taylor et al., 2005; Walport, 2001) (Figure 1.3.1A).

The fragment crystallizable region (Fc) receptor family, consisting of at least six members including Fc gamma receptor (FcγR) I, II, IIc, IIIa, Fc alpha receptor I (FcαRI), and Fc epsilon receptor I (FcεRI), represents a diverse group of transmembrane glycoproteins. These receptors specifically bind to the Fc region of antibodies that have attached to antigens, forming immune complexes (Guilliams et al., 2014; Ley et al., 2016; Taylor et al., 2005). FcγR target various subclasses of Immunoglobulin (Ig)G, with each receptor showing specificity for different IgG subclasses, while FcαRI is dedicated to recognising IgA antibodies, playing a crucial role in mucosal immunity and the neutralisation of pathogens. FcεRI, with its high affinity for IgE, is integral to the defence against parasitic infections and the mediation of allergic responses (Das et al., 2020; Guilliams et al., 2014) (Figure 1.3.1A). The engagement of Fc receptors on macrophages triggers phagocytosis of antibody-coated pathogens and activation of intracellular signalling pathways that lead to the release of inflammatory mediators.

The clearance of apoptotic cells by macrophages is another critical function for maintaining tissue homeostasis and preventing inflammation. Through receptors that recognise ”eat-me” signals, like phosphatidylserine, calreticulin and CD47, macrophages efficiently engulf apoptotic cells in a non-inflammatory manner (Lendeckel et al., 2022; Ley et al., 2016; Taylor et al., 2005). Key receptors involved in this process include the integrin alfa V beta 3 (integrin αVβ3), Receptor for Advanced Glycation Endproducts (RAGE), stabilin 2, Tyro3, Axl, and Mer, which recognise phosphatidylserine. CD91 acts as a receptor for calreticulin. Meanwhile, healthy cells express CD47 as a “don’t eat me” signal, which is detected by Signal Regulatory Protein Alpha (SIRPα) on macrophages (Gordon & Plüddemann, 2018; Van Duijn et al., 2022). Apoptotic cells also release ”find-me” signals, including adenosine triphosphate (ATP) and Uridine triphosphate (UTP), which attract macrophages via receptors, such as P2Y purinoceptor 2 (P2Y2R), and C-X3-C Motif Chemokine Ligand 1 (CX3CL1), which binds to C-X3-C motif chemokine receptor 1 (CX3CR1) (Ley et al., 2016), ensuring prompt clearance (Figure 1.3.1C).

Beyond the clearance of apoptotic cells, macrophages are equipped with an array of pattern recognition receptors (PRRs), that enable them to detect and respond to bacterial, viral, fungal, and parasitic infections, through PAMPs and DAMPs, such as double-stranded ribonucleic acid (RNA), unmethylated CpG deoxyribonucleic acid (DNA), lipoproteins, and lipopolysaccharide (LPS) (Murphy & Weaver, 2016). These sensors, including Toll-like receptors (TLRs), NOD-like receptors (NLRs), RIG-I like receptors (RLRs), receptors for intracellular DNA such as Stimulator of interferon genes (STING), C-type lectins, and scavenger receptors, recognise both direct pathogen components and products (Creagh & O’Neill, 2006). TLRs, for example, are critical in recognising microbial products across a broad spectrum of pathogens, initiating signals that lead to Nuclear factor kappa-light-chain-enhancer of activated B cells (NF-kB) activation or type

I interferon production depending on the pathway engaged (Kawasaki & Kawai, 2014; Ley et al., 2016; Taylor et al., 2005). This activation not only boosts phagocytic activity and pathogen killing but also enhances the production of ROS and Reactive nitrogen species (RNS), crucial for the effective elimination of phagocytosed pathogens (Figure 1.3.1B).

One well-studied example of TLR signalling is the interaction between TLR4 and LPS, a component found on the outer membrane of Gram-negative bacteria. TLR4 specifically binds to LPS, and this interaction is facilitated by CD14, a co-receptor that binds to lipopolysaccharide-binding protein (LBP), helping to present LPS to TLR4. This engagement triggers a cascade of signalling events leading to the immune response against the invading pathogen (Das et al., 2020).

In addition to TLRs, other receptors such as the mannose receptor (CD206) play significant roles in pathogen recognition. CD206 is capable of recognising polysaccharides present on the surfaces of yeast cells, among other pathogens (Das et al., 2020). This receptor is prominently expressed on M2 macrophages, a subset of macrophages associated with tissue repair, resolution of inflammation, and immunoregulation. The expression of CD206 and its role in pathogen recognition exemplifies the diverse mechanisms through which the immune system identifies and responds to various microbial threats (Figure 1.3.1B).

Chemokine receptors, part of the G protein-coupled receptors (GPCRs) family, are pivotal in directing macrophage responses to chemokine—signalling proteins released in response to inflammation. These receptors equip macrophages to migrate towards and address inflammatory sites or tissue injuries by responding to chemokines such as C-C Motif Chemokine Ligand (CCL)1, 2, 3, 4, and 5, which they themselves can produce. Key among these receptors are C-C motif chemokine receptor (CCR)2, 5, and CX3CR1, each playing unique roles in macrophage function and movement. CCR2 facilitates the release and trafficking of monocytes from the bone marrow to inflamed areas, while CCR5 attracts monocytes to vascular walls, aiding their penetration into inflamed tissues (Ley et al., 2016; Mantovani et al., 2004; Taylor et al., 2005).

The role of macrophages extends beyond mere pathogen elimination. They are instrumental in presenting antigen fragments, derived from digested proteins of pathogens, on major histocompatibility complex (MHC) class II molecules (Muntjewerff & Meesters, 2020; Roche & Furuta, 2015). This antigen presentation on the cell surface activates T helper cells in an antigen-specific manner, bridging innate and adaptive immunity.

This bridging role is further enhanced by the cytokine receptors on macrophages, which are pivotal in sensing and responding to signals from the adaptive immune system. These receptors detect the ongoing immune reactions, such as Type 1 T helper (Th1), Type 2 T helper (Th2), or Type 17 T helper (Th17) responses, allowing macrophages to adapt their functions to the prevailing cytokine environment, primarily influenced by activated T cells. Among the key receptors, the Interferon Gamma (IFN-ɣ) receptor stands out for promoting the M1-like phenotype, known for its role in pro-inflammatory responses and defence against microbes, while the IL4 receptor

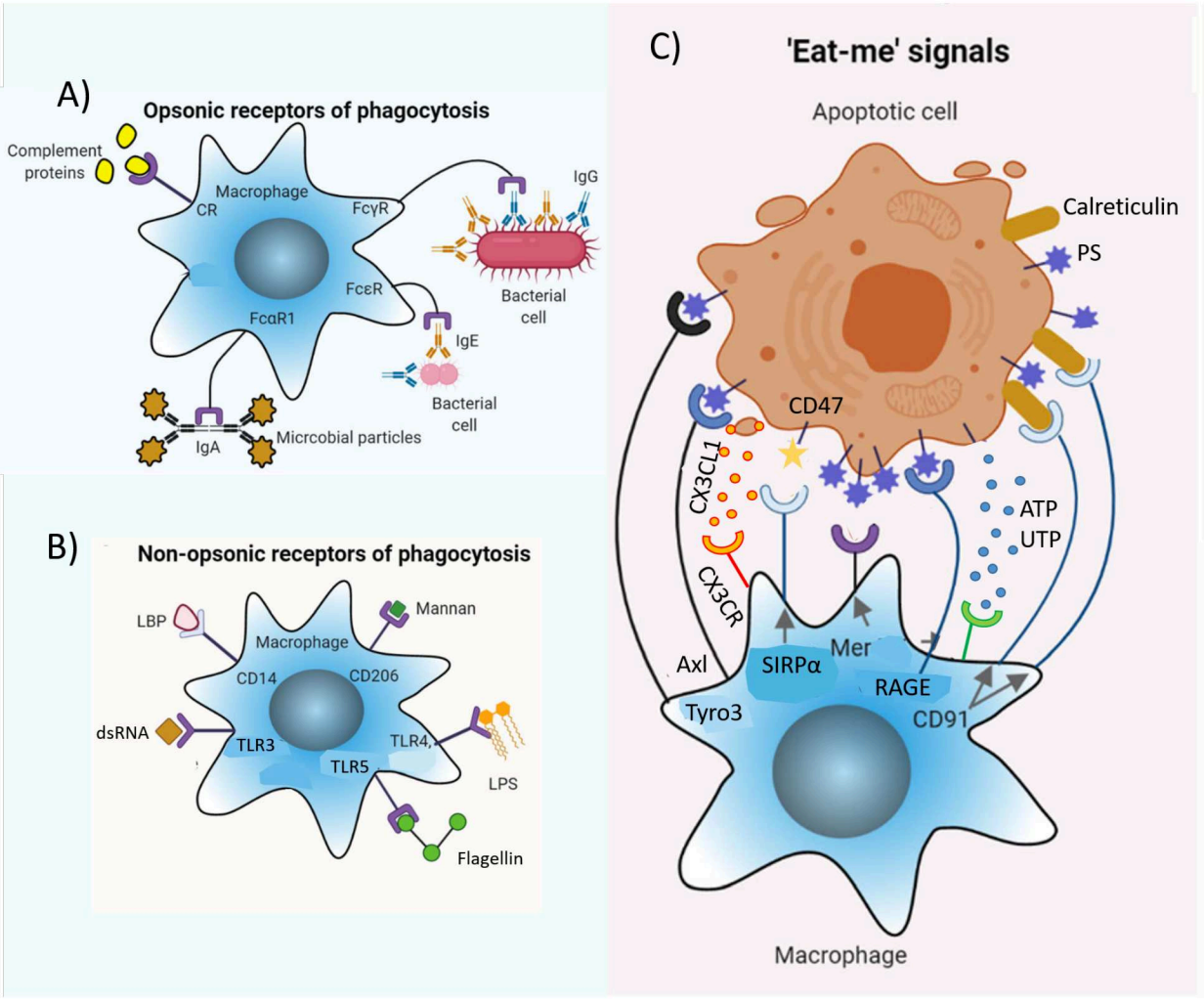

Figure 1.3.1. Diversity of macrophage phagocytic receptors.
This figure illustrates the various receptors employed by macrophages for the recognition and phagocytosis of particles. A) Opsonic receptors such as those in the CR family, and Fc receptors (FcγR, FcεR, FcαR1), engage with targets that have been opsonised, or coated, with antibodies or complement proteins, facilitating their recognition and phagocytosis. B) Macrophages utilise a spectrum of receptors for the direct recognition of cellular or microbial entities. These receptors are classified as "non-opsonic" because they bind to their targets without needing opsonisation by antibodies or complement proteins. These are TLR4 and CD14, which bind to LPS and LBP; TLR5, which recognises flagellin; and TLR3, targeting dsRNA. CD206 is a scavenging receptor that binds to mannan. C) Apoptotic cells release signalling molecules including nucleotides (ATP or UTP) and CX3CL1 on phagocytes, which are detected by specific receptors (P2Y2 and CX3CR), directing them towards dying cells. Cells undergoing apoptosis exhibit "eat-me" signals such as phosphatidylserine (PS) and calreticulin on their surface, which are recognised by phagocytic cells Healthy cells express CD47 as "don't eat me" signals, which target SIRPα to prevent phagocytosis. This figure has been adapted from (Das et al., 2020).

counters this by steering macrophages towards the M2-like phenotype, associated with healing and anti-inflammatory functions (Kloc, 2017; Ley et al., 2016).

The engagement of IL4, IL5, and IL13 receptors on macrophages reinforces the M2-like phenotype, indicating that M2-like polarisation may serve as the default state aimed at tissue repair. This is further supported by the action of Transforming Growth Factor Beta (TGF-β) receptors,

which signal macrophages about the health of surrounding tissues, especially signals originating from epithelial cells, thus promoting M2-like polarisation (Kloc, 2017; Ley et al., 2016).

1.4 Macrophage Signalling

The binding of cytokines or growth factors to these receptors often leads to the dimerisation or trimerisation of receptor subunits. This conformational change triggers the rapid activation of associated kinases, typically from the Janus kinase (JAK) family.

Activated JAKs phosphorylate specific tyrosine residues on the receptor, creating docking sites for signalling molecules with Src Homology 2 (SH2) domains. Among these signalling molecules are the Signal Transducers And Activators Of Transcription (STAT), a family of transcription factors. Once recruited to the receptor, STATs are phosphorylated by JAKs, allowing them to dimerise. These STAT dimers can then translocate to the nucleus, where they initiate the transcription of target genes.

The balance between the activation of STAT1 and STAT3/STAT6 is central to macrophage polarisation (Liu et al., 2021; Wang et al., 2014) (Figure 1.4.1). M1 polarisation, which is associated with pro-inflammatory responses, is promoted by a predominance of NF-κB and STAT1 activation. These factors are typically activated by IFN-γ and LPS, and cause expression of inflammatory cytokines and antimicrobial effector mechanisms (Kloc, 2017; Platanitis & Decker, 2018).

In contrast, M2 polarisation is driven by a predominance of STAT3 and STAT6 activation, primarily in response to IL-4/13 and IL-10. These cytokines promote the anti-inflammatory and tissue repair functions of M2 macrophages. Kruppel-like factor 4 (KLF4), which is downstream of STAT6, promotes M2 macrophage function by suppressing NF-κB/hypoxia-inducible factor 1-alpha (HIF-1α)-dependent transcription (Kerneur et al., 2022; Liu et al., 2021) (Figure 1.4.1).

NF-κB stands as a pivotal transcription factor orchestrating M1 macrophage activation, overseeing the regulation of numerous inflammation related genes, such as Tumor Necrosis Factor alpha (TNF-α) and IL1B. The modulation of NF-κB activity is intricately controlled through the activation of the inhibitor of kappa B kinase (IKK) complex, composed of two kinase proteins (IKKα and IKKβ) along with a regulatory unit (IKKγ). The convergence of upstream signalling pathways on this trimeric complex typically initiates with the phosphorylation and activation of IKKβ. Subsequently, activated IKKβ phosphorylates the inhibitor of kappa B (I-κB), leading to its recognition and degradation by the proteasome system. This degradation process liberates the NF-κB p65/p50 heterodimer from its inhibited state within the NF-κB/I-κB complex, allowing its translocation into the nucleus. Once in the nucleus, the NF-κB p65/p50 heterodimer binds to the promoter regions of target genes to initiate the transcription of inflammatory mediators, thereby amplifying the inflammatory response characteristic of M1 macrophages (Mussbacher et al., 2023).

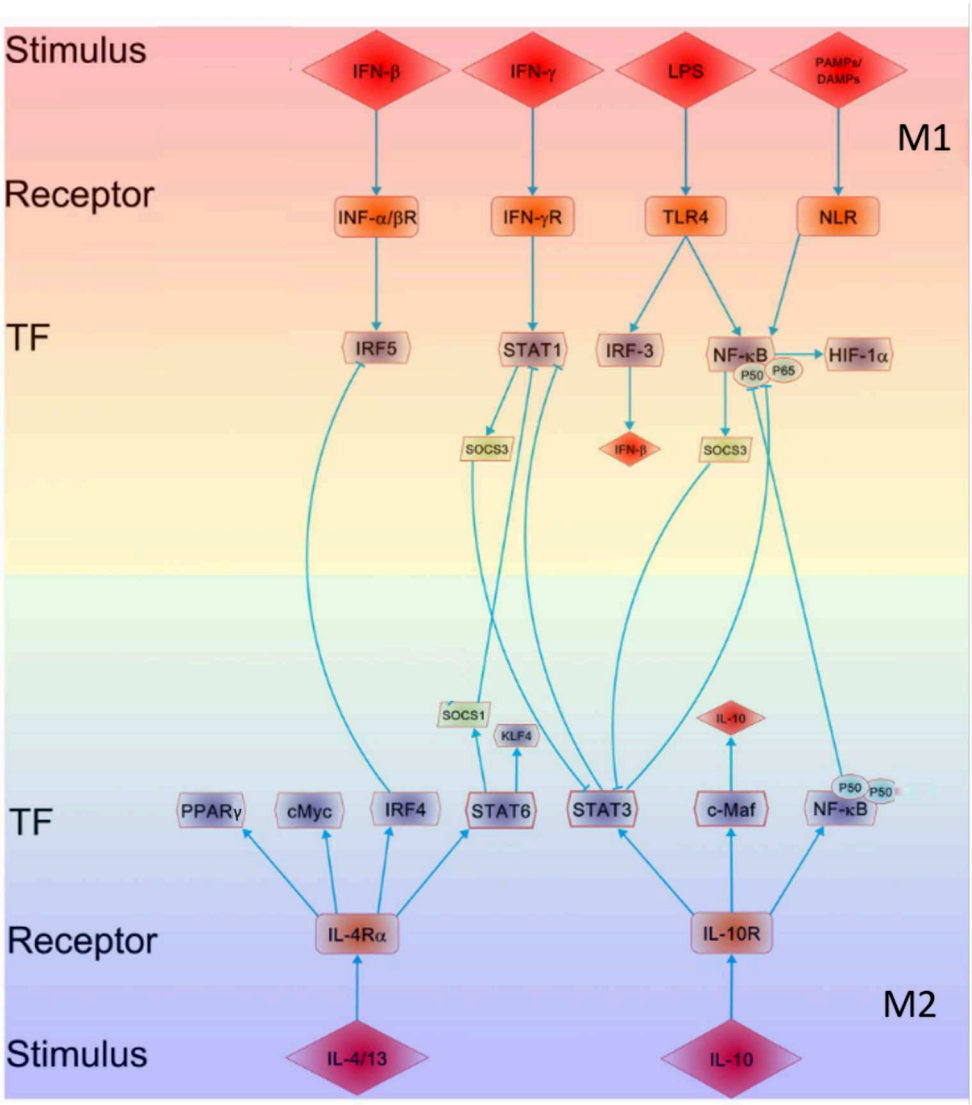

Figure 1.4.1. Regulatory pathways in macrophage M1–M2 polarisation.
This figure delineates the critical signalling pathways influencing the polarisation of macrophages into pro-inflammatory M1 or anti-inflammatory M2 phenotypes. The interplay between these pathways, especially the balance between STAT1 and STAT3/STAT6 signalling, is fundamental in controlling macrophage polarisation and their subsequent functions. Through the binding of LPS to TLR4 and IFN-γ to IFN-γR, NF-κB and STAT1 are activated. This is key to driving M1 macrophage polarisation. Other signals, such as PAMPs and DAMPs, can activate NF-κB through NLRs, while IFN-β can influence the M1 phenotype through IFN-α/βR and IRF5. Conversely, activation of STAT3 and STAT6, primarily through cytokines IL-4/13 and IL-10, favours M2 macrophage polarisation. KLF-4 is activated downstream of STAT6. Additionally, IL-4 activates c-Myc and PPARγ and the IRF4 axis, which respectively regulate M2-associated gene expression and suppress IRF5-mediated M1 polarisation. IL-10 further encourages M2 polarisation by inducing activities of p50 NF-κB homodimer, c-Maf, and STAT3. Adapted from (Wang et al., 2014).

Hypoxia conditions, often present at sites of inflammation, lead to the upregulation of hypoxia-inducible factors (HIFs) in macrophages. HIFs are transcription factors that respond to low oxygen levels and regulate the expression of genes involved in adaptation to hypoxia, including those affecting the inflammatory response of macrophages (McGettrick & O'Neill, 2020).

IL-4 induces the expression of Cellular Myelo-Cytomatosis Proto-Oncogene (c-Myc), a transcription factor that controls the expression of genes associated with the M2 phenotype (Pello, 2016). Additionally, IL-4 activates the interferon regulatory factor (IRF)4 pathway, which plays a role in promoting M2 polarisation while inhibiting the IRF5-mediated M1 polarisation pathway (Günthner & Anders, 2013; Liu et al., 2017) (Figure 1.4.1).

IL-10 further supports M2 polarisation through the induction of the p50 NF-κB homodimer, proto-oncogene c-Maf (c-Maf), and STAT3 activities. These factors contribute to the anti-inflammatory and tissue repair functions characteristic of M2 macrophages (Xia et al., 2023).

The Peroxisome Proliferator-Activated Receptor (PPAR), specifically PPARγ, is a nuclear receptor that control various aspects of M2 macrophage activation and oxidative metabolism. Their activation is associated with the promotion of anti-inflammatory responses and the regulation of lipid metabolism in macrophages (Szanto et al., 2010).

1.5 M1 and M2 macrophages

The original conceptualisation of M1 and M2 macrophages is rooted in the cytokine milieu associated with Th1 and Th2 immune responses, reflecting the metabolic pathways these cells utilise for arginine metabolism. This dichotomy emerges from the observation that macrophages activated with IFN-γ or LPS (linked with Th1 responses) or in a Th2 context exhibit distinct metabolic profiles: M1 macrophages employ inducible nitric oxide synthase (iNOS) to convert L-arginine into L-citrulline and nitric oxide (NO), a process critical for their antimicrobial and pro-inflammatory activities. In contrast, M2 macrophages use arginase to convert L-arginine into L-ornithine, a precursor for polyamines and proline, which are essential for tissue repair and anti-inflammatory functions (Mills et al., 2000).

Classical (M1) activation can be triggered by IFN-γ, bacterial components, and other pro-inflammatory signals, leading to the production of pro-inflammatory cytokines and reactive intermediates. Among these cytokines, TNF-α emerges as a key player, driving the inflammatory process by acting as an endogenous pyrogen. TNF-α's effects, including the induction of fever, vasodilation, and increased vascular permeability, are crucial for mobilising immune cells to the sites of infection or injury, thereby orchestrating a coordinated defence mechanism (Parameswaran & Patial, 2010).

In parallel, IL-1, which includes both IL-1α and IL-1β subtypes, plays a foundational role in the early stages of the immune response. This cytokine family acts on a wide array of cells, such

as monocytes, macrophages, DCs, and even non-immune cells like epithelial cells, to propagate the inflammatory signal. Specifically, IL-1β is instrumental in recruiting and activating granulocytes and T cells, further amplifying the body's ability to counteract invading pathogens and mitigate damage (Arango Duque & Descoteaux, 2014; Kaneko et al., 2019).

Complementing the actions of TNF-α and IL-1, IL-12 is instrumental in tailoring the immune system's adaptive arm, especially by directing T cell differentiation towards the Th1 phenotype. This cytokine not only boosts the effector functions of natural killer (NK) cells and CD8+ T cells, essential for eradicating intracellular adversaries and tumours but also promotes IFN-ɣ production, reinforcing the immune assault on infections (Arango Duque & Descoteaux, 2014; Murphy & Weaver, 2016).

Within the arsenal of M1 macrophages, alongside cytokines, a suite of chemokines including CCL5, C-X-C Motif Chemokine Ligand (CXCL)9, and CXCL10 play pivotal roles in coordinating the immune response to inflammation. CCL5, recognised for its capacity to mobilise T cells, basophils, eosinophils, and dendritic cells, serves as an essential chemo-attractant, guiding these cells to the sites of inflammation to bolster the immune defence. Similarly, CXCL10 (IP-10) attracts T cells, NK cells, and DCs, while CXCL9 (MIG), acts as a powerful chemo-attractant specifically for T cells, directing them to the heart of inflammatory sites (Arango Duque & Descoteaux, 2014; Kloc, 2017; Mantovani et al., 2004).

CD80 and CD86, known as B7-1 and B7-2 respectively, are critical costimulatory molecules expressed on the surface of antigen-presenting cells (APCs), including M1 macrophages (Kloc, 2017). Their primary function is to provide the necessary second signal for T cell activation, a process that is crucial for an effective immune response. For a T cell to be fully activated, it requires two signals. The first signal is antigen-specific, provided through the interaction between the T cell receptor (TCR) and the MHC presenting an antigen peptide on the surface of APCs. However, this signal alone is not sufficient to activate T cells fully. CD80 and CD86 provide the second, costimulatory signal by binding to CD28 on the surface of naive T cells. The interaction between CD80/CD86 and CD28 is essential for T cell activation, proliferation, and survival (Murphy & Weaver, 2016). On the other hand, they also bind to cytotoxic T-lymphocyte-associated protein 4 (CTLA-4) on T cells, which transmits an inhibitory signal to T cells. This interaction plays a crucial role in regulating the immune response, preventing autoimmunity, and maintaining peripheral tolerance. The differential binding affinities and temporal expression patterns of CD80 and CD86 to CD28 and CTLA-4 are thought to modulate the balance between T cell activation and inhibition (Vandenborre et al., 1999)(Figure 1.5.1).

M2 activation, originally defined by IL-4 stimulation, encompasses a broader set of triggers in recent findings, including IL-13, fungal pathogens, immune complexes, and IL-10 (Ross et al., 2021). M2 macrophages are characterised by their phagocytic nature, production of immunosuppressive cytokines, and roles in tissue remodelling and resolution of inflammation.

These cells are distinguished by their expression of specific receptors that further define their phenotype and function, such as CD163, CD206, CD209, resistin like alpha or Fizz1 (Retnl1), and chitinase-like 3 or Ym1 (Chil3) (Rőszer, 2015). These scavenger receptors facilitate the clearance of cellular debris, contributing to the anti-inflammatory milieu.

TGF-β is an immunosuppressive cytokine secreted by M2 macrophages. It promotes the expansion of regulatory T cells (Tregs) and simultaneously inhibits the generation and function of effector T cells, antigen-presenting DCs and NK cells (Batlle & Massagué, 2019). In parallel, IL-10 inhibits the development of Th1 cells. Furthermore, IL-10 has an autocrine inhibitory effect on macrophages, limiting their activation and production of pro-inflammatory cytokines.

Beyond the secretion of TGF-β and IL-10, M2 macrophages are known for their production of a range of chemokines such as CCL1, CCL17, and CCL22. These chemokines play a crucial role in attracting Th2 cells, thereby amplifying Th2 polarisation and facilitating immunoregulatory processes. The ability of M2 macrophages to secrete vascular endothelial growth factor vascular endothelial growth factor (VEGF) underscores their vital role in promoting angiogenesis and tissue regeneration. This secretion not only aids in the formation of new blood vessels but also supports the healing process, further delineating the multifunctional nature of M2 macrophages in maintaining and restoring tissue homeostasis (Figure 1.5.1).

The M1/M2 paradigm has undergone significant refinement to account for the functional diversity and heterogeneity among macrophage populations (Figure 1.5.2). This includes recognising a spectrum of activation states beyond the binary M1/M2 classification and proposing a more nuanced terminology that considers both the source of macrophages and their stimuli. Subtypes such as M2a, M2b, and M2c have been identified, each with specific inducers and functions, highlighting the adaptability and complexity of macrophage responses (Murray, 2017; Ross et al., 2021) (Figure 1.5.2).

Despite the utility of the M1/M2 framework for studying macrophage biology, it represents a simplification of the vast spectrum of macrophage activation states observed *in vivo*. This model is further complicated by species-specific differences in macrophage markers and functions between humans and mice, underscoring the need for caution in extrapolating findings across species (Mantovani et al., 2004).

The understanding of macrophage differentiation has undergone a significant evolution, moving away from the traditional bipolar model that categorised macrophages into either pro-inflammatory M1 or anti-inflammatory M2 phenotypes. This shift is largely attributed to advancements in technology, particularly in the realm of single-cell analysis and multiparametric technologies, which have facilitated a deeper exploration of macrophage diversity, such as multicolor flow cytometry, Cytometry by time of flight (CyTOF) (Roussel et al., 2017) and single cell RNA-sequencing (scRNA-seq) (Hume et al., 2023). These technological advances have unveiled a spectrum of macrophage phenotypes that transcend the simple M1 versus M2 classification, highlighting the influence of tissue imprinting and microenvironmental factors.

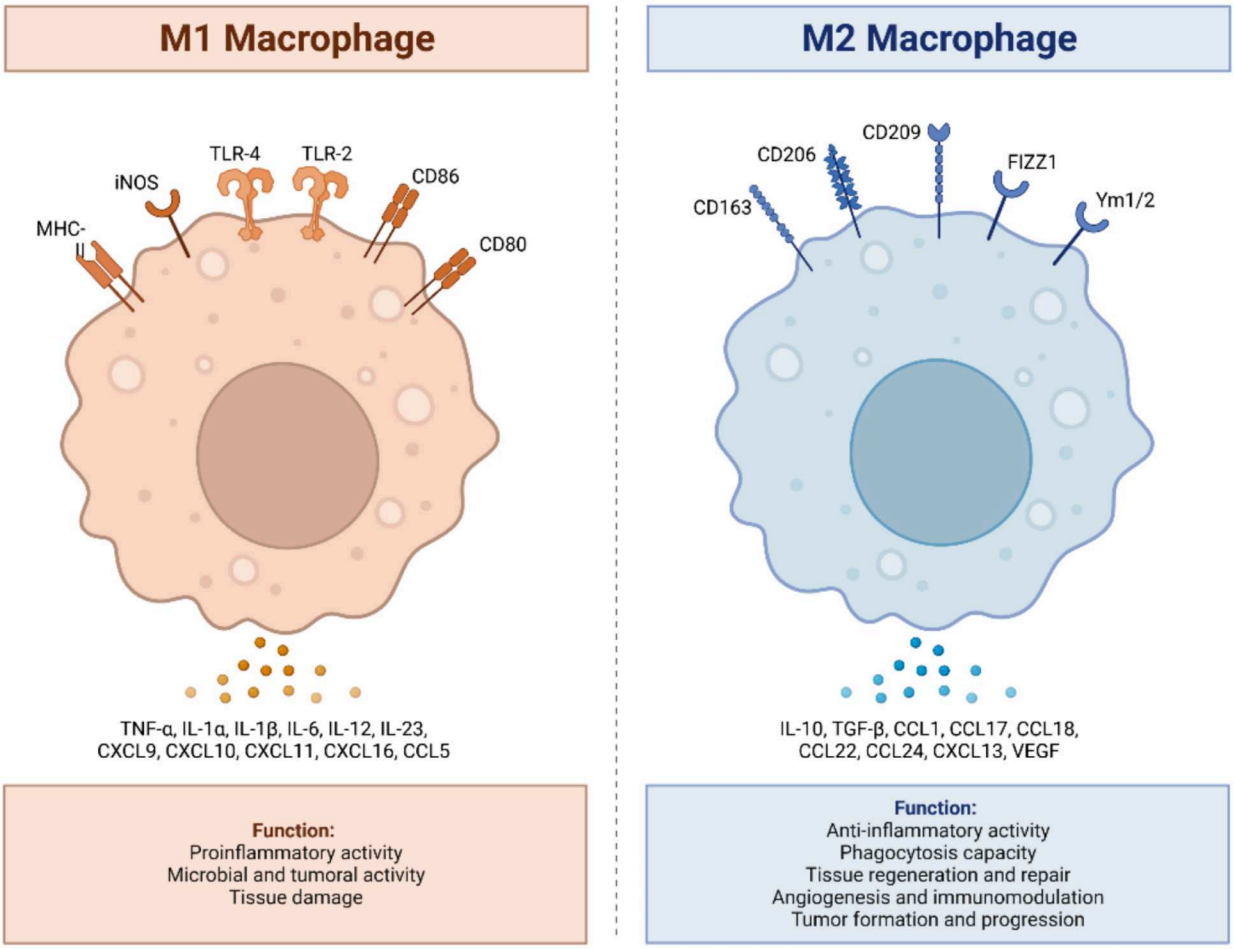

Figure 1.5.1. Distinct functional profiles of M1 and M2 macrophages in immune regulation. M1 macrophages are classically activated and essential for pro-inflammatory reactions, expressing MHC-II, TLR-2, TLR-4, CD86, and CD80. They release pro-inflammatory cytokines (TNF-α, IL-1α, IL-1β, IL-6, IL-12, IL-23, CXCL9, CXCL10, CXCL11, CXCL16, and CCL5), generate ROS and NO via iNOS, and encourage Th1 responses On the other hand, M2 macrophages are alternatively activated, focusing on anti-inflammatory actions and tissue repair, expressing CD163, CD206, CD209, Retnl, and Chil3. They emit anti-inflammatory cytokines (IL-10, TGF-β, CCL1, CCL17, CCL18, CCL22, CCL24, CXCL13, and VEGF), boost phagocytosis, and facilitate Th2 responses. Adapted from (Roa-Vidal et al., 2023).

Macrophages in different organs and tissues exhibit unique features and functions, demonstrating the complexity of their roles in the immune system, as do macrophages from different ontogenies. Furthermore, single-cell and multidimensional analyses have provided insights into the functional, transcriptional, and epigenetic landscapes of macrophages, offering a more comprehensive understanding of their roles in health and disease. These advancements have led to the integration of macrophage profiles into maps of trajectory, illustrating the dynamic nature of macrophage differentiation and function (Kloc, 2017) (Figure 1.5.2).

Therefore, in this thesis, I will adopt the terminology that refers to classically activated, pro-inflammatory macrophages as M1-like, emphasising their role in initiating and sustaining inflammatory responses. Conversely, the term M2-like will be used to describe alternatively ac-

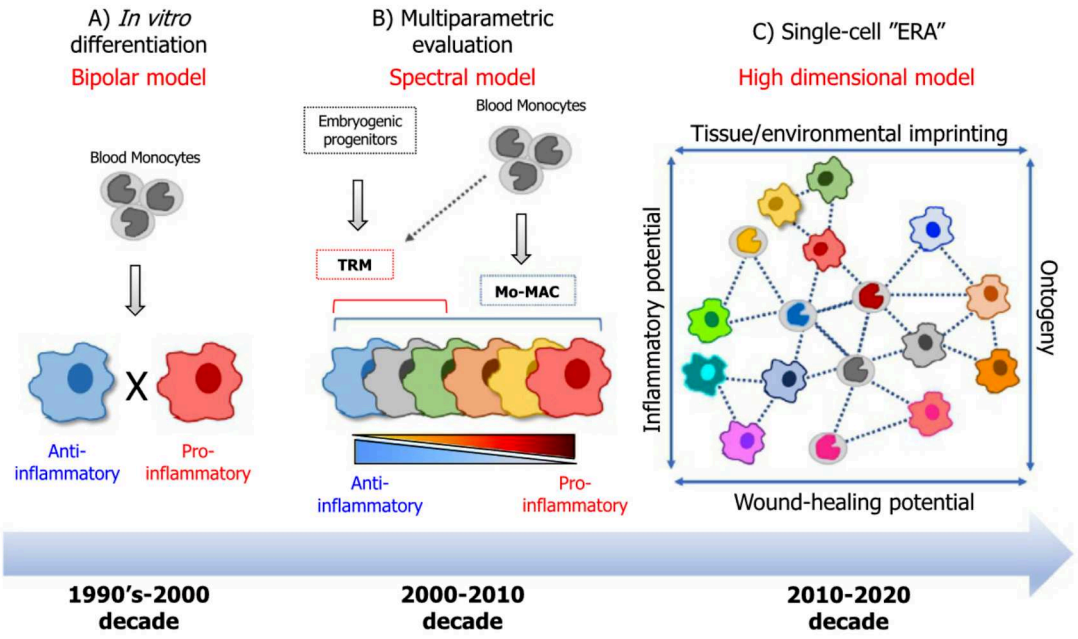

Figure 1.5.2. Evolution of macrophage polarisation concepts.
A) Initial *in vitro* studies introduced a binary classification of macrophage differentiation, identifying M1 macrophages with pro-inflammatory actions and M2 macrophages with anti-inflammatory effects, both originating from circulating monocytes. B) Subsequent advancements in analytical technologies and experimental methodologies broadened the scope of macrophage phenotyping, uncovering a continuum of phenotypes ranging from anti-inflammatory to pro-inflammatory traits. This expansion included the identification of tissue-resident macrophages (TRM), originating from embryonic progenitors and involved in tissue homeostasis, and monocyte-derived macrophages (Mo-MACs), which are pivotal in responding to pathological stimuli. C) The advent of single-cell sequencing and multidimensional analysis techniques has exposed an intricate array of macrophage diversity, revealing numerous distinct functional states, transcriptional profiles, and epigenetic landscapes. This comprehensive characterisation considers factors such as ontogeny and tissue-specific influences, illustrating dynamic developmental paths and the nuanced spectrum of macrophage biology. Image from (Kloc, 2017).

tivated, immunosuppressive macrophages that assist in tumour progression and tissue repair. This nomenclature acknowledges the complexity and heterogeneity of macrophage activation states beyond the traditional M1/M2 binary classification.

1.6 miRNAs and Macrophages

miRNAs are emerging regulators in the intricate network of macrophage polarisation, acting as modulators of gene expression at the post-transcriptional level (Essandoh et al., 2016). These small, 20–24 nucleotide-long, non-coding RNAs influence macrophage behavior by binding to the 3' untranslated regions (UTRs) of messenger RNAs (mRNAs), impacting the production of proteins either by inhibiting translation or promoting mRNA degradation.

The journey of miRNAs from genesis to action begins with the transcription of primary miRNAs (pri-miRNAs) from miRNA genes or intronic regions of protein-coding genes. These pri-miRNAs are processed in the cell nucleus by the Drosha microprocessor complex into precursor miRNAs (pre-miRNAs), which are then exported to the cytoplasm, by exportins. Here, the enzyme Dicer further cleaves them, yielding miRNA duplexes. One strand of this duplex, guided by an Argonaute (Ago) protein within the miRNA-induced silencing complex (miRISC), directs the complex to target mRNAs, leading to their silencing. Conversely, the passenger strand, often termed the miRNA* strand, is typically degraded (Liu et al., 2022) (Figure 1.6.1).

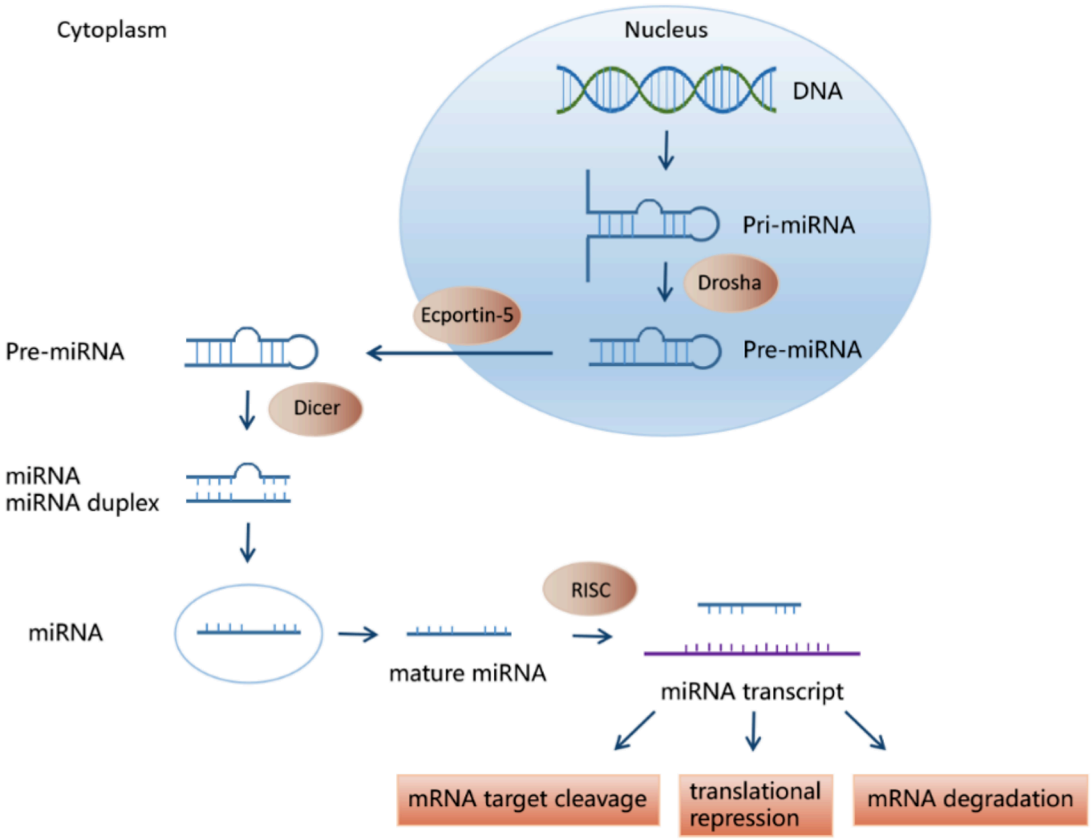

Figure 1.6.1. Overview of miRNA biogenesis pathway.
This figure outlines the steps involved in the production of miRNAs, starting with transcription, which generates pri-miRNAs. These pri-miRNAs are then processed by the Drosha microprocessor complex into pre-miRNAs. Next, pre-miRNAs are transported from the nucleus into the cytoplasm via exportins. In the cytoplasm, Dicer cleaves pre-miRNAs into double-stranded miRNA molecules. These molecules are then loaded onto the RISC, where the Ago protein separates the strands. The guide strand, or mature miRNA, remains associated with RISC to participate in gene regulation by targeting specific mRNA sequences, leading to repression or degradation of the target mRNA. From (Liu et al., 2022).

Several investigations have explored the expression patterns of miRNAs in macrophages under various polarisation states, shedding light on the dynamic regulatory roles these molecules play in both human and murine models. The role of miRNAs in influencing macrophage activation patterns is increasingly recognised, especially in the context of an imbalanced inflammatory

response. Evidence suggests that the dysregulation of miRNAs is closely associated with aberrant macrophage responses, where miRNAs such as miR-146, miR-125b, miR-155, and miR-9, induced by inflammatory signals, play pivotal roles in dampening TLR4/IL-1R signalling pathways in both monocytes and macrophages (Geiß et al., 2022). This regulatory mechanism involves a spectrum of miRNAs that orchestrate the inflammatory landscape of macrophages, categorising them into those associated with pro-inflammatory M1 activation and those linked to anti-inflammatory M2 activation. Particularly, the role of miR-155-5p in macrophage polarisation is underscored by its ability to drive macrophages towards M1 or M2 phenotypes upon overexpression or depletion, respectively (Cai et al., 2012). This demonstrates miR-155-5p's central role in regulating the inflammatory response. However, discrepancies in miRNA expression profiles between human and murine macrophages in specific polarised conditions suggest variations attributable to the macrophages' origin, highlighting the complexity of translating findings across species and the need for a nuanced understanding of miRNA-mediated regulation in macrophage polarisation.

1.7 Macrophages and Disease

The imbalance between macrophage activation states plays a crucial role in the pathogenesis of various diseases, highlighting the dual nature of macrophage function in health and disease. When M1-like activation is unregulated or prolonged, it can contribute to chronic inflammation and tissue damage, underlying the pathogenesis of autoimmune disorders like MS and RA (Funes et al., 2018; Ma et al., 2019).

MS is characterised by an autoimmune attack on the CNS, leading to demyelination and neurodegeneration. M1-like macrophages and microglia contribute to this process by releasing pro-inflammatory mediators that exacerbate inflammation and tissue damage (Wang et al., 2019). In RA, the chronic activation of M1-like macrophages within the joint synovium promotes inflammation, leading to joint destruction and systemic manifestations of the disease (Siouti & Andreakos, 2019). On the other hand excessive or dysregulated M2-like activation can lead to pathological outcomes, such as fibrosis and airway hyperreactivity. In diseases like idiopathic pulmonary fibrosis, M2-like macrophages contribute to the excessive deposition of extracellular matrix components, leading to tissue scarring (fibrosis) and compromised organ function (Shapouri-Moghaddam et al., 2018). In asthma, M2-like macrophages are implicated in promoting airway inflammation and hyperresponsiveness, contributing to the chronic nature of the disease (Shapouri-Moghaddam et al., 2018).

1.7.1 Macrophages and cancer

Cancer is a complex group of diseases characterised by the uncontrolled growth and spread of abnormal cells. It can develop almost anywhere in the body, forming solid tumours in organs and tissues or, in the case of leukemias, proliferating in the blood and bone marrow. The fundamental trait of cancer cells is their ability to evade the body's regulatory mechanisms that usually control cell proliferation, growth, and death (Hanahan & Weinberg, 2011).

At the heart of cancer's development are mutations and changes in the DNA within cells. These genetic alterations can be inherited, but more often they occur during a person's lifetime due to a variety of factors, including exposure to carcinogens (such as those found in tobacco smoke and certain chemicals), ultraviolet radiation from the sun, viruses like human papillomavirus (HPV) and hepatitis B and C, and lifestyle factors like diet, physical activity, and obesity. Some cancers also have a hormonal component to their growth.

Cancer progression involves not just the proliferation of cancer cells but also the creation of a microenvironment that supports the growth and spread of these cells. This includes inducing blood vessel growth (angiogenesis) to nourish the tumour, evading the immune system's attempts to destroy abnormal cells, and eventually metastasising, or spreading to other parts of the body through the lymphatic system or bloodstream (Hanahan & Weinberg, 2011).

In the context of cancer, macrophages, referred to as TAMs, are implicated in supporting tumour growth, progression, and metastasis (Boutilier & Elsawa, 2021). In solid tumours, macrophages represent the main immune population constituting up to 50% of the tumour mass. These macrophages are recruited to the tumour site where they are conditioned by the tumour microenvironment (TME), adopting an M2-like phenotype that promotes tissue repair and wound healing but, in the context of cancer, facilitates tumour survival and expansion.

Monocyte recruitment to tumours is mediated by various cytokines, chemokines, and growth factors, with the Macrophage colony-stimulating factor (M-CSF)-CSF1R, CCL2-CCR2, and CX3CL1-CX3CR1 ligand-receptor interactions being among the most prominent pathways (Richards et al., 2013). M-CSF is crucial for both the recruitment and M2-like polarisation of monocytes and self-renewal of tissue-resident macrophages (Laoui et al., 2011). TGF-β, produced by multiple cell types within the TME, including the tumour cells themselves, is a key regulator that polarises macrophages toward the M2-like phenotype (Gratchev, 2017).

M2-like TAMs are particularly adept at promoting tumour growth, angiogenesis, extracellular matrix modification, and the inhibition of anti-tumour immunity. They also play roles in metastasis, chemoresistance, and recurrence, severely disrupting effector cell functions required for tumour clearance (Hourani et al., 2021).

TAMs are capable of expressing an array of growth factors that actively promote tumour cell proliferation and survival, such as epithelial growth factor epithelial growth factor (EGF) and platelet-derived growth factor (PDGF) (Kielbassa et al., 2019). Several strategies by which TAMs mediate immune evasion include upregulating checkpoint inhibitors like Programmed

death-ligand (PD-L)1 and PD-L2, which deactivate effector Cytotoxic T lymphocytes (CTLs) (Li et al., 2022a), and producing immunosuppressive cytokines like IL-10 and TGF-β that dampen immune cell activity. IL-10 and TGF-β promote an anti-inflammatory phenotype among macrophages and simultaneously suppress the proliferation and cytokine production of CTLs (Thomas & Massagué, 2005), while inducing Tregs and inhibiting Th1 polarisation and DC maturation (Thepmalee et al., 2018) (Figure 1.7.1).

Under hypoxic conditions, TAMs upregulate HIF-1α/2α, which induces the production of angiogenic molecules such as VEGF and IL-8 (McGettrick & O'Neill, 2020). TAM phenotypes also play distinct roles in tumour metastasis, with certain TAMs promoting epithelial-to-mesenchymal transition (EMT) and the development of cancer stem cells in various cancers, thereby facilitating metastatic spread (Li et al., 2022b).

TAMs also produce proteolytic enzymes like Matrix metalloproteinases (MMPs) and factors involved in neovascular formation to enhance metastasis. For example, MMP9 derived from TAMs has been linked to enhanced invasion and migration in several cancers (Chen et al., 2019) (Figure 1.7.1).

TAM infiltration within the TME has been extensively studied for its role in cancer progression, and a growing body of evidence suggests that high levels of TAM infiltration is often associated with a poor prognosis in various types of cancer (Bingle et al., 2002).

In breast cancer, high infiltration of M2-like TAMs has been linked to enhanced tumour cell proliferation, angiogenesis, and metastasis, thereby correlating with poor prognosis (Lindsten et al., 2017; Tommasi et al., 2022). Similarly, in hepatocellular carcinoma (HCC), the presence of M2-like TAMs is associated with increased tumour aggressiveness and diminished overall survival rates (Zheng et al., 2023). Glioblastoma (GBM) patients also exhibit worse outcomes when the TME is rich in M2-like TAMs (Khan et al., 2023), underscoring their role in fostering tumour growth and therapeutic resistance.

1.8 Cancer Immunotherapy

Immunotherapy has emerged as a pivotal advancement in cancer treatment, representing a significant addition to conventional therapies such as chemotherapy and radiotherapy. By harnessing the body's immune system to combat cancer, immunotherapy introduces a novel and targeted approach to oncological care.

Checkpoint inhibitors have become a cornerstone of modern cancer therapy. These agents target the molecular brakes on the immune system, such as the PD-1-PD-L1 axis and CTLA-4, that prevent T-cell activation. By blocking these checkpoints, inhibitors lift the restraints on T cells, empowering them to more effectively identify and destroy cancer cells. This method has yielded remarkable outcomes in the treatment of various cancers, including melanoma and non-small cell lung cancer, underscoring its potential as a game-changer in cancer care (Seidel

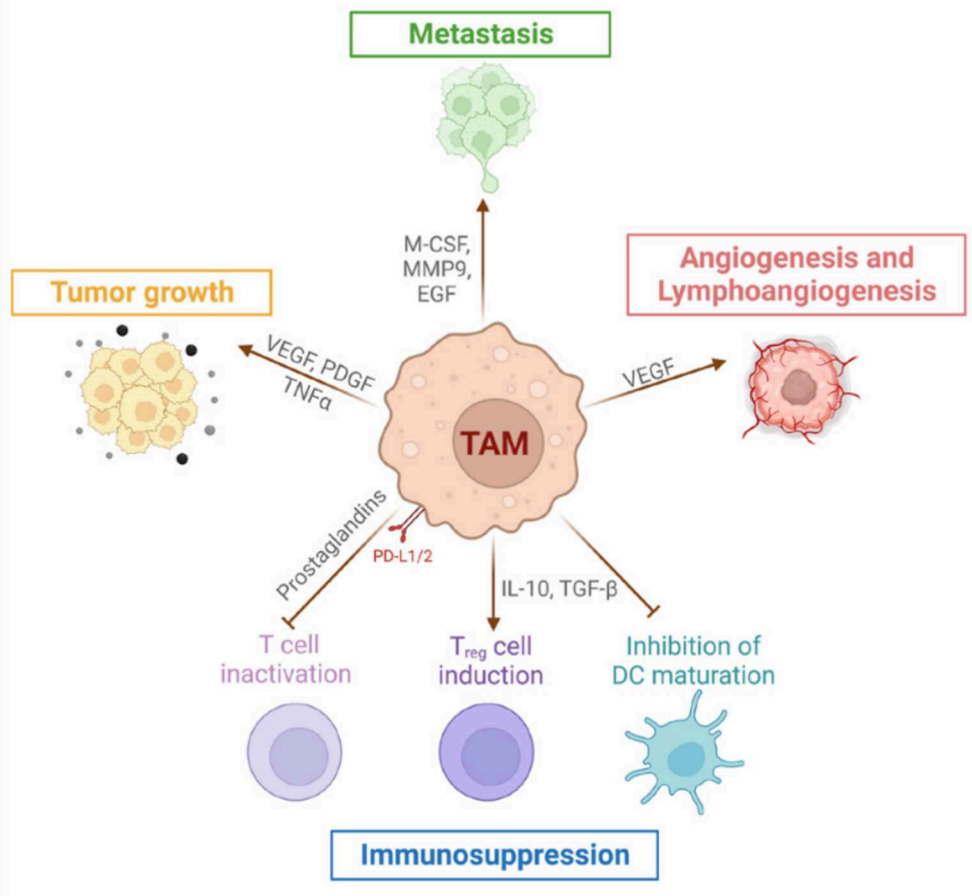

Figure 1.7.1. Pro-tumorigenic functions of tumour-associated macrophages (TAMs).
This figure illustrates the multifaceted role of TAMs within the tumour microenvironment, highlighting their contribution to cancer progression. By secreting various factors and presenting surface molecules, TAMs support tumorigenesis through enhancing tumour cell proliferation, promoting both angiogenesis and lymphangiogenesis, facilitating metastasis, and exerting immunosuppressive effects. TAMs contribute to immune evasion by promoting Treg development, impairing effector T cell activity, and hindering DC maturation. Key secreted molecules include EGF, interleukins, M-CSF, MMPs, PDGF, TGF-β, and VEGF. Modified from (Monnier et al., 2022).

et al., 2018). Despite their success in treating various tumours, these therapies have shown limited efficacy in or poorly immunogenic tumours. These tumours are characterised by a lack of T-cell infiltration, due to several factors, including the tumour's ability to produce an immunosuppressive microenvironment, the expression of fewer neoantigens that T cells can recognise, or physical barriers that prevent T-cell penetration. Because immune checkpoint inhibitors rely on the presence of active T cells within the tumour to exert their therapeutic effect, their efficacy is significantly reduced in the treatment of poorly immunogenic tumours (Appleton et al., 2021).

CAR T-cell therapy represents a breakthrough in cancer treatment, involving the genetic modification of a patient's T cells to express a chimeric antigen receptor (CAR) that specifically targets cancer cell antigens. While this therapy has achieved remarkable success in treating certain haematologic malignancies, particularly those expressing CD19, it faces significant obstacles when applied to solid tumours.

One major challenge is antigen heterogeneity within solid tumours, where the expression of target antigens varies significantly among cancer cells. This diversity can result in the incomplete eradication of tumour cells, as CAR T cells may only eliminate those expressing the targeted antigen, potentially leaving other cancer cells unaddressed.

Additionally, the selection of targets for CAR T-cell therapy in solid tumours poses risks of on-target, off-tumour toxicity. Often, the antigens targeted by CAR T cells are also present on healthy tissues, leading to significant collateral damage and limiting the therapy's safety and applicability.

The TME in solid tumours presents a hostile and complex landscape for CAR T cells. It is characterised by suppressive elements such as Tregs, TAMs, and various inhibitory cytokines (e.g., TGF-β, IL-10) that can significantly impair CAR T-cell function and survival. Furthermore, the dense extracellular matrix and other physical barriers within the TME can hinder CAR T-cell infiltration and access to cancer cells.

CAR T-cell exhaustion, driven by the harsh conditions of the TME, leads to a loss of effector functions and diminished persistence over time. This exhaustion, exacerbated by chronic antigen exposure and inhibitory signals, undermines the long-term effectiveness of CAR T-cell therapy in solid tumours (Cappell & Kochenderfer, 2023).

1.9 Targeting tumour-associated macrophages in cancer

Targeting TAMs has emerged as a promising strategy for cancer therapy due to their significant role in promoting tumour growth and suppressing the anti-tumour immune response. Therapeutic interventions aimed at TAMs generally fall into three categories: inhibiting the recruitment of monocytes to the TME, depleting of TAMs, and reprogramming TAMs from a pro-tumorigenic M2-like phenotype to an anti-tumorigenic M1-like phenotype (Hourani et al., 2021).

1.9.1 Macrophage recruitment blockade

Key signalling pathways, including M-CSF-CSF-1R, CCL2-CCR2, CCL5-CCR5, and CX3CL1-CX3CR1, are pivotal targets in the blockade of macrophage recruitment, with ongoing research and clinical trials focused on disrupting these pathways to combat tumour growth.

The development and approval of small molecule inhibitors (SMIs) and monoclonal antibodies targeting the CSF-1R pathway represent a significant advancement in cancer therapy. These therapeutic agents, designed to inhibit the activity of CSF-1R, have shown promise in both monotherapy settings and in combination with other treatments. Among these, Pexidartinib (PLX-3397), an FDA-approved inhibitor for tenosynovial giant cell tumour, has been explored for its efficacy in treating solid tumours. Pre-clinical studies highlight its efficacy in depleting TAMs, while in a recent trial in a clinical setting combining PLX-3397 with paclitaxel, there was

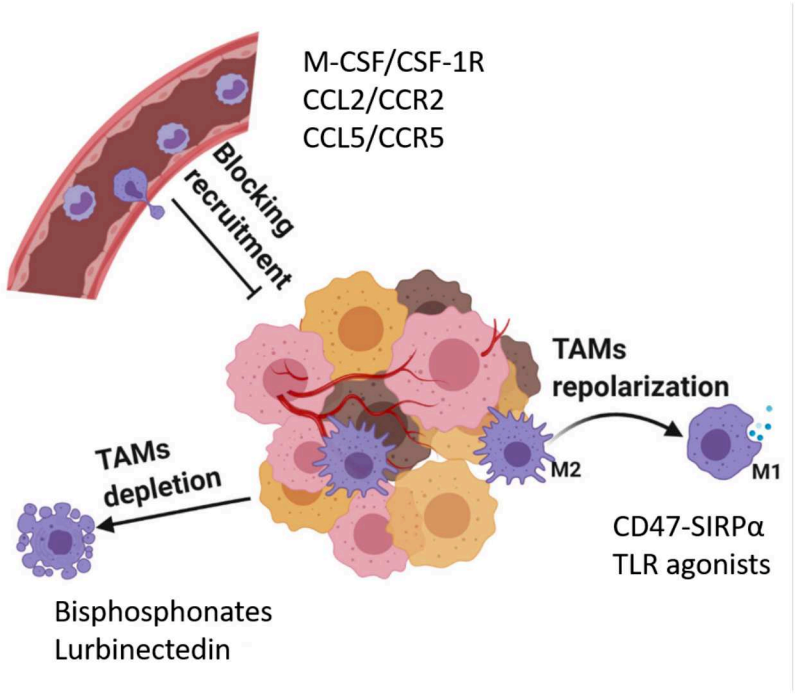

Figure 1.9.1. Targeting tumour associated macrophages in cancer.
Therapeutic interventions aimed at TAMs generally fall into three categories: blocking the recruitment of monocytes to the TME, through targeting pathways such as M-CSF-CSF-1R, CCL2-CCR2, CCL5-CCR5, and CX3CL1-CX3CR1, depleting of TAMs with Bisphosphonates and Lurbinectedin, and repolarisation of TAMs from a pro-tumorigenic M2-like phenotype to an anti-tumorigenic M1-like phenotype with inhibitors of CD47-SIRPα interaction and TLR agonists (Hourani et al., 2021).

a decline in peripheral blood monocytes and an increase in CSF1 levels, indicating effective CSF-1R blockade. Despite these promising results, the treatment has been associated with significant side effects, including haematological toxicities and hepatotoxicity (Lamb, 2019).

Utilising CCR5 and CCL1 inhibitors, including blocking antibodies and CCR5 antagonists such as Maraviroc, TAK-779, Anibamine, and GSK706769, has yielded promising anti-tumour responses (Hourani et al., 2021). Notably, Maraviroc's effectiveness was explored in a human colorectal cancer explant model and further validated in a pilot clinical trial for patients with advanced metastatic colorectal cancer, achieving a tumour control rate of 80%. Additionally, pre-clinical studies indicate that Maraviroc can significantly reduce TAM numbers and impede tumour growth in metastatic breast cancer models (Halama et al., 2016).

1.9.2 Macrophage depletion

Bisphosphonates, such as clodronate and zoledronic acid, are widely utilised for managing bone metastases in various cancers, including breast and prostate cancer (Hourani et al., 2021). Beyond their direct tumour cell-killing capabilities, they are acknowledged for their macrophage-depleting effects. However, their clinical utility is hampered by challenges such as low bioavailability, rapid systemic clearance, and the risk of severe side effects. To address these issues,

nanotechnology-based delivery systems for bisphosphonates have been investigated. *In vivo* studies have demonstrated that treatment with liposomal clodronate effectively reduces primary tumour size and the formation of secondary nodules. This treatment approach is associated with a significant decrease in TAMs and angiogenic cytokines, indicating its potential for enhancing therapeutic outcomes in cancer treatment (Piaggio et al., 2016).

Lurbinectedin also possesses macrophage-depleting properties. It has shown efficacy in depleting TAMs in various cancer models, including pancreatic ductal adenocarcinoma (PDAC) and ovarian cancer (Hourani et al., 2021). Moreover, when combined with gemcitabine, lurbinectedin exhibits synergistic effects in tumour reduction, highlighting its potential for combination therapy. This combination has been well-tolerated in phase I clinical trials, suggesting a promising therapeutic strategy for advanced solid tumours (Paz-Ares et al., 2017).

While these studies underscore the potential of TAM depletion as a cancer treatment strategy, the systemic reduction of macrophages poses a risk to the body's innate immune defence. Thus, the development of nanotargeted approaches to specifically deplete TAMs while sparing systemic macrophage populations is a critical area of research.

1.9.3 Macrophage repolarisation

Pre-clinical and clinical research highlights the potential of enhancing phagocytosis by TAMs to promote tumour cell clearance and improve antigen presentation. Tumour cells often evade immune detection and destruction by expressing CD47. The CD47-SIRPα interaction is a critical mechanism by which tumour cells achieve immune evasion across a wide range of haematological and solid tumour (Hourani et al., 2021).

Several therapeutic agents, including anti-CD47 antibodies, anti-SIRPα antibodies, and recombinant SIRPα proteins, are currently in pre-clinical and clinical development. One such agent, Hu5F9-G4, a humanised anti-CD47 antibody, has shown promise in a Phase I clinical trial involving patients with advanced solid tumours and lymphomas (Patnaik et al., 2020).

TLRs agonists have been researched, aiming to shift the macrophage phenotype towards a more pro-inflammatory M1-like state, thereby amplifying the anti-tumour response of the body. Pre-clinical studies leveraging TLR agonists TLR3, TLR7/8, and TLR9 have shown promise in polarising macrophages to this desired phenotype which, in turn, contributes to a reduction in tumour progression (Kumar et al., 2020). For instance, polyinosinic-polycytidylic acid, a double stranded RNA, binds TLR3 and is in Phase 1/2 clinical studies for its potential to treat various solid tumours (Saenger et al., 2014). This study demonstrates the potential of TLR targeting in not only modulating the immune response but also directly influencing tumour regression.

This strategic focus on TLRs, particularly in macrophages, underscores a novel method in cancer therapy. By reprogramming immune cells to adopt an anti-tumorigenic phenotype, researchers are exploring avenues that not only inhibit tumour growth but also potentially harness the body's natural immune response for more effective cancer treatment outcomes.

1.10 Objectives of this thesis

Recognising the therapeutic potential of reprogramming or repolarising TAMs towards an anti-tumour M1-like phenotype, my research aims to unlock and manipulate the underlying mechanisms of macrophage activation. By focusing on inhibiting key transcription factors and leveraging the regulatory action of miRNAs, this work seeks to shift the balance towards a phenotype that supports disease resolution. These objectives are driven by the hypothesis that targeted manipulation of macrophage polarisation can herald a new era of treatments, transforming the landscape of immunotherapy and offering novel, effective strategies against diseases that currently elude conventional therapies.

The objectives of this thesis encompass:

1. **Identification of Polarisation Regulators**: The primary objective is to screen for and identify key regulators, including transcription factors and miRNAs, that can induce a shift in macrophage polarisation towards a pro-inflammatory (M1-like) phenotype. This will involve techniques such as upstream regulator analysis and miRNA sequencing to uncover potential candidates capable of modulating macrophage polarisation.

2. **Validation of Identified Regulators:** Following the identification of potential regulators, the thesis will focus on validating the impact of these candidates on macrophage polarisation. This includes evaluating the influence of selected transcription factor inhibitors and miRNAs on shifting macrophages towards an M1-like state, examining changes at both gene and protein expression levels, and assessing alterations in macrophage functionality.

3. **Cross-Species Analysis and Translational Potential:** A critical component of this research is to compare the mechanisms of polarisation and the effectiveness of the identified repolarising agents between murine and human macrophages. This comparison aims to bridge the gap between pre-clinical findings and potential clinical applications, highlighting the translational relevance of the research.

4. **Assessment of Repolarisation Outcomes:** This objective seeks to understand the functional consequences of macrophage repolarisation on the immune response to tumours, specifically focusing on interactions with tumour cells and the activation of CTLs. Evaluations will include the effects of repolarised macrophages on tumour cell phagocytosis, proliferation, and the enhancement of CTL-mediated tumour cytotoxicity.

These objectives comprise the overall goal of this thesis, which is to contribute to a deeper understanding of macrophage polarisation mechanisms, identify potential therapeutic targets for modulating macrophage activity, and enhance the translational relevance of macrophage-based therapies for cancer and other diseases involving the immune system.

Chapter 2

Results

2.1 Screen for Regulators of Macrophage Polarisation

2.1.1 Characterisation of M2-like and M1-like Murine BMDMs

In this study, I employed murine BMDMs as an *in vitro* model system to investigate the repolarisation potential of specific candidates, aiming to induce phenotypic changes indicative of a shift towards the M1-like activation state. To achieve this, I conducted a detailed characterisation of murine macrophages in response to IL4 and IFN-γ plus LPS activation.

After a 48-hour exposure to these cytokines, I analysed the expression of genes associated with M1-like (IFN-γ+LPS) and M2-like (IL4) activation states by quantitative real time polymerase chain reaction (qRT-PCR) (Figure 2.1.1). In M1-like BMDMs, compared to their M2-like counterparts, I found substantial down-regulation of Mannose Receptor C-Type 1 or CD206 (*Mrc1*) ($\log_2$FC $= -4.614, n = 6, p = 0.0007$) and Triggering Receptor Expressed On Myeloid Cells 2 (*Trem2*) ($\log_2$FC $= -3.728, n = 6, p = 0.0007$) expression. Alongside this, I observed up-regulation of *Cxcl10* ($\log_2$FC $= 7.249, n = 6, p = 0.0012$), *Il1b* ($\log_2$FC $= 7.612, n = 3, p = 0.0357$), and Tumor Necrosis Factor (*Tnf*) ($\log_2$FC $= 5.375, n = 5, p = 0.0159$).

Subsequently, I examined the protein expression of these macrophages after 72 hours of treatment. TNF-α secretion and NO production, assessed through enzyme-linked immunosorbent assay (ELISA) and the Griess assay, respectively, were significantly higher in M1-like macrophages (TNF-α: 83.50pg/mL, $n = 7, p = 0.0006$; NO: 9.952μM, $n = 4, p = 0.0286$) compared to M2-like macrophages (Figure 2.1.1 upper panel).

Leveraging FACS, I analysed the protein expression of additional M1-like markers by gating on single events, live cells, and macrophages. M1-like BMDMs displayed heightened positivity for Nitric oxide synthase 2 (Nos2) ($92.10\%, n = 4, p = 0.0286$), CD38 ($69.85\%, n = 4, p = 0.0286$), CD86 ($91.20\%, n = 4, p = 0.0286$), and MHC Class II Allele IAb (IA^b) ($45.07\%, n = 4, p = 0.0286$), providing further insights into their pro-inflammatory and classically activated phenotype (Figure 2.1.1 lower panel).

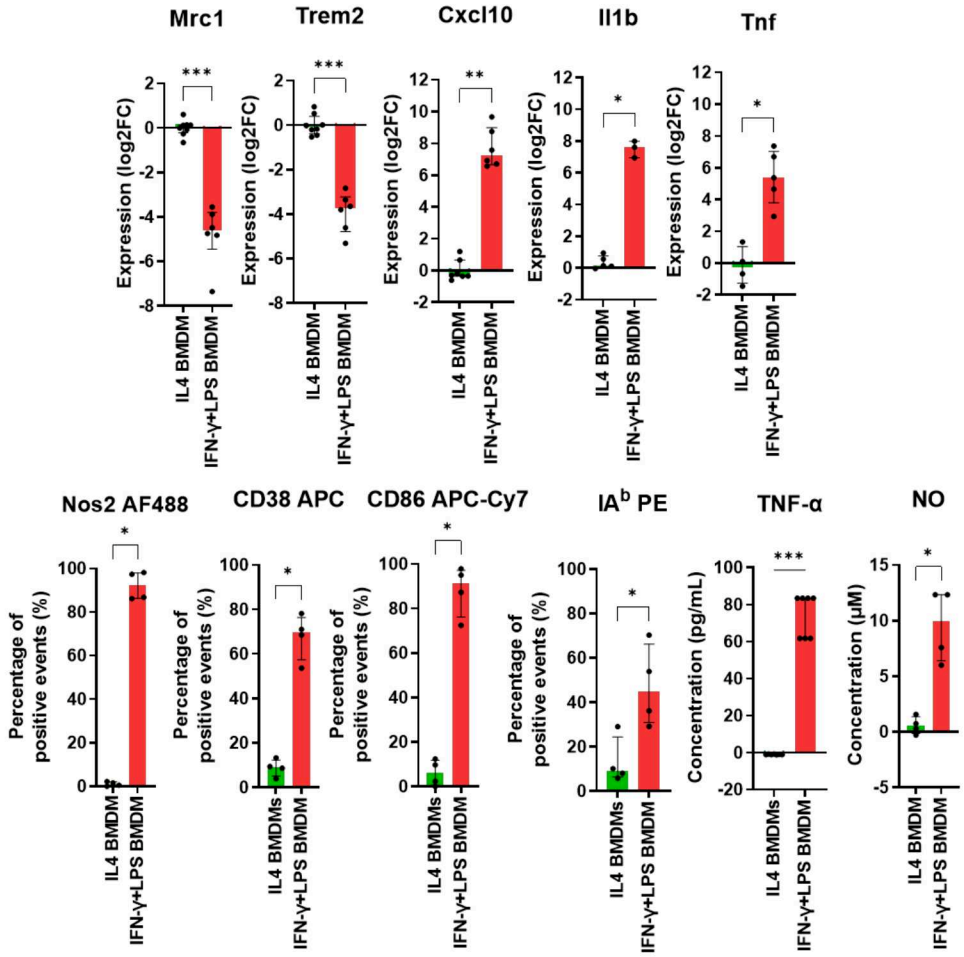

Figure 2.1.1. Characterisation of gene and protein expression in murine BMDMs after treatment with IL4 or IFN-γ+LPS.
Murine BMDMs were cultured for 48h for gene expression analysis through qRT-PCR (top row) and 72h for protein expression analysis through FACS (NOS2, CD38, CD86 and IA^b) and ELISA (TNF-α and NO) (bottom row). The qRT-PCR bar graphs show $\log_2$ of the fold change (log2FC) compared to IL4-treated BMDMs. The housekeeping gene was *Ribosomal Protein L19 (Rpl19)*. FACS bar graphs show the percentage of expression of markers among the viable macrophages (LIVE/DEAD Fixable Yellow Dead Cell dye$^-$, CD11b$^+$ and F4/80$^+$). ELISA graphs show concentration in pg/ml of TNF-α and in μM of NO. Median with interquartile range. P-values assessed by the Mann-Whitney test. n=4-8; * p<0.05; ** p<0.01; *** p<0.001; log2FC: $\log_2$ of the Fold Change; BMDM: Bone marrow derived macrophages; FACS: Fluorescence-activated cell sorting; ELISA: Enzyme-linked immunosorbent assay.

2.1.2 Characterisation of M2-like and M1-like Human MdMs

After elucidating the activation states of the murine macrophages, I sought to characterise the response of human MdMs to a similar stimulus involving IL4 and IFN-γ with LPS. This approach aimed to unravel cross-species conserved biological mechanisms and differences.

Conducting this comparative analysis allowed me to better grasp the strengths and limitations of my murine model, thereby contributing to more informed result interpretations and bolstering the translational relevance of my findings. This exploration also provided valuable insights into the potential efficacy of my repolarising candidates across species, offering a cru-

cial step in refining them. Moreover, it enabled the discernment of whether observed effects were conserved across species, or if there were species-specific nuances that warranted careful consideration. Therefore, in parallel to the characterisation of BMDMs, I assessed the expression of various markers of M1-like (IFN-γ+LPS) and M2-like (IL4) activation in human macrophages following treatment with these stimuli.

Gene expression analysis 48 hours post-stimulation revealed a consistent down-regulation of *MRC1* ($\log_2$FC $= -1.841, n = 10, p = 0.0017$) and *TREM2* ($\log_2$FC $= -2.004, n = 10, p = 0.0017$), coupled with up-regulation of *CXCL10* ($\log_2$FC $= 5.686, n = 10, p < 0.0001$) and *TNF* ($\log_2$FC $= 2.009, n = 6, p = 0.0043$) in human IFN-γ+LPS-treated MdMs, mirroring patterns observed in BMDMs. Noteworthy was the up-regulation of *CCL5* ($\log_2$FC $= 4.479, n = 6, p = 0.0303$) in these human macrophages, adding an additional layer to the observed responses (Figure 2.1.2).

Subsequently, I assessed protein expression 72 hours post-stimulus. I found significantly heightened secretion of CXCL10 ($27.96 pg/mL, n = 12, p < 0.0001$) and TNF-α ($230.8, n = 13, p < 0.0001$) by IFN-γ+LPS MdMs compared to IL4 MdMs, while NO levels remained undetectable (data not shown). FACS analysis further demonstrated that M1-like MdMs exhibited a higher percentage cells expressing the M1-like markers CD80 ($23.15\%, n = 4, p = 0.0286$) or CD38 ($59.65\%, n = 4, p = 0.0286$), and a lower percentage of CD209 expressing cells ($19.10\%, n = 4, p = 0.0159$) compared to M2-like MdMs (Figure 2.1.2).

With these comprehensive characterizations, I established an *in vitro* setup facilitating the differentiation of murine and human M1-like and M2-like macrophages. Subsequently, my focus shifted to a comparative analysis through RNA sequencing and miRNA sequencing to unveil common pathways of transcriptional regulation between murine and human, aiming to identify targets for repolarisation.

2.1.3 Candidate upstream regulators of macrophage polarisation

To elucidate the upstream regulators of macrophage polarisation, I conducted a comprehensive analysis using RNA and miRNA sequencing. This analysis involved treating monocyte-derived macrophages (MdMs) and BMDMs with IL4 and IFN-γ+LPS, followed by sequencing of biological triplicate samples.

The approach I adopted for differential gene expression analysis was to compare M1-like and M2-like macrophages, focusing on genes that exhibited a $\log_2$ fold change greater than 1 or less than -1, coupled with an adjusted p-value below 0.05. These were categorised as differentially-expressed genes (DEGs) (Figure 2.1.3A). To validate the reliability of this sequencing data, I aligned it with previously acquired qRT-PCR data. This comparison revealed that markers such as MRC1, TREM2, CXCL10, TNF, and CD38 held significant relevance in both murine and human macrophages, which was consistent across qRT-PCR, FACS, and sequencing data (Figure 2.1.3C).

Further analysis revealed a substantial number of DEGs in murine and human macrophages. In murine M1-like BMDMs, there were 2751 up-regulated and 2875 down-regulated DEGs in

comparison to M2-like BMDMs. In a similar pattern, human M1-like MdMs exhibited 1773 up-regulated and 1638 down-regulated DEGs when compared with their M2-like counterparts. Notably, the study identified 523 DEGs that were commonly up-regulated in human and murine M1-like macrophages, and 371 DEGs that were common in M2-like macrophages (Figure 2.1.3B).

I subsequently analysed the enriched biological process gene ontology (GO:BP) pathways in M1-like macrophages from both murine and human samples. In this analysis, I discovered that 1388 GO:BP pathways were enriched in murine M1-like macrophages, while 817 were en-

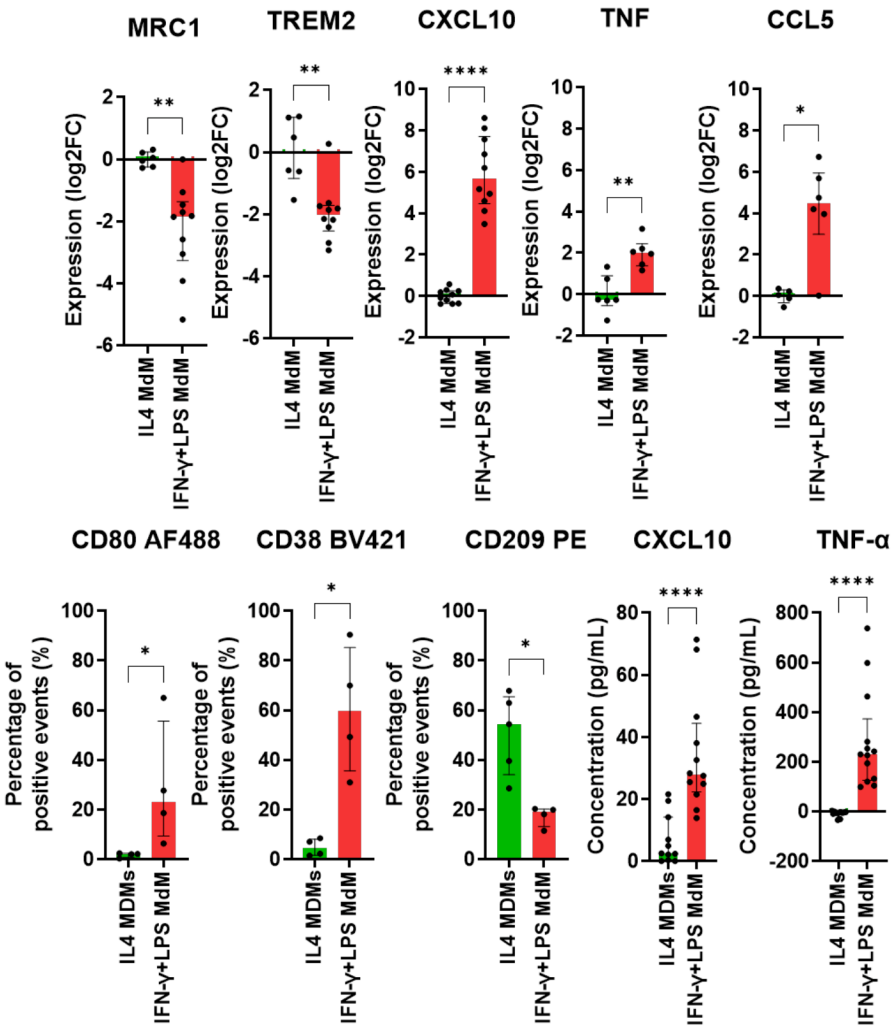

Figure 2.1.2. Characterisation of gene and protein expression in human MdMs after activation with IL4 or IFN-γ+LPS.
Human MdMs were cultured for 48h for gene expression analysis through qRT-PCR (upper graphs) and 72h for protein expression analysis through FACS and ELISA (lower graphs). qRT-PCR bar graphs show log_2 of the fold change compared to IL4-treated MdM, the housekeeping gene was *RPL19*. FACS bar graphs show % of the expression of markers in the Live macrophage population (LIVE/DEAD Fixable Yellow Dead Cell dye(-)CD11b(+)CD14(+)). Protein secretion graphs show concentration in pg/ml. Median with interquartile range. P-values assessed by the Mann-Whitney test. n=4-15; * p<0.05; ** p<0.01; *** p<0.001; **** p<0.0001; log2FC: log_2 of the Fold Change; MDMs: monocyte derived macrophages; FACS: Fluorescence-activated cell sorting; ELISA: Enzyme-linked immunosorbent assay.

riched in human M1-like macrophages. Remarkably, 734 of these pathways were common to both species, indicating a notable degree of compatibility in their macrophage activation processes. Among these shared pathways, the most significantly enriched were those related to the immune response, including processes such as the 'immune system process' and 'defence response', as detailed in Figure 2.1.3D. This overlap highlights key similarities in the immune functionalities of murine and human macrophages at the molecular level.

This comprehensive gene expression profiling not only yielded a rich dataset for understanding macrophage polarisation but also laid the groundwork for exploring the shared and distinct regulatory mechanisms operative in human and murine macrophages.

In the pursuit of identifying key transcription factors that were up-regulated in M2-like macrophages as compared to their M1-like counterparts, my focus was on those genes that could potentially be targeted for down-regulation, aiming to repolarise the macrophages towards a more pro-inflammatory phenotype. In this endeavour, I discovered a significant up-regulation of 200 transcription factors in M2-like murine macrophages and 80 in their human counterparts (Figure 2.1.4A).

Interestingly, 17 of these transcription factors were common to both human and murine M2-like macrophages, highlighting a cross-species similarity in macrophage polarisation. Notably, PPARG and Myelo-Cytomatosis Proto-Oncogene (MYC) emerged as commonly up-regulated transcription factors in M2-like activation across both species (Figure 2.1.4B).

Shifting the focus to M1-like activation, my analysis revealed 177 up-regulated transcription factors in murine M1-like macrophages and 114 in humans, with 46 being common to both. This set included members of the IRF family—IRF1, IRF7, and IRF9—as well as STAT1, underscoring their importance in the M1-like activation state (Figure 2.1.4A right).

To deepen my understanding of these regulatory networks, I utilised Ingenuity Pathway Analysis (IPA) software to analyse RNA sequencing data from murine macrophages. I analysed the upstream regulators calculated by the IPA software, taking into account only transcription regulators predicted to be activated in the M2-like macrophages, with the p-value of the overlap at $p<0.05$. This analysis identified Tripartite Motif Containing 24 (Trim24) and Stat6 as the most prominently activated transcription regulators in IL4-stimulated BMDMs (Figure 2.1.4C). Furthermore, I found a correlation between the activation of Stat6 and the up-regulation of Myc and Pparg, both well-recognised as being activated by IL4 signalling (Liu et al., 2021). In contrast, Stat1 emerged as a crucial factor in M1-like activation, primarily influenced by TNF-α signalling and acting upstream of IRF1.

Corroborating these findings through an extensive literature review, I confirmed a pathway crosstalk between Stat6 and Trim24, where the loss of Trim24 inhibits Stat6 acetylation and consequently promotes M2-like polarisation in both murine and human macrophages (Yu et al., 2019). As such, Trim24 would not be a viable candidate for down-regulation. Also, research has shown that STAT6 acts as an upregulator of PPARɣ in macrophages, particularly in response to

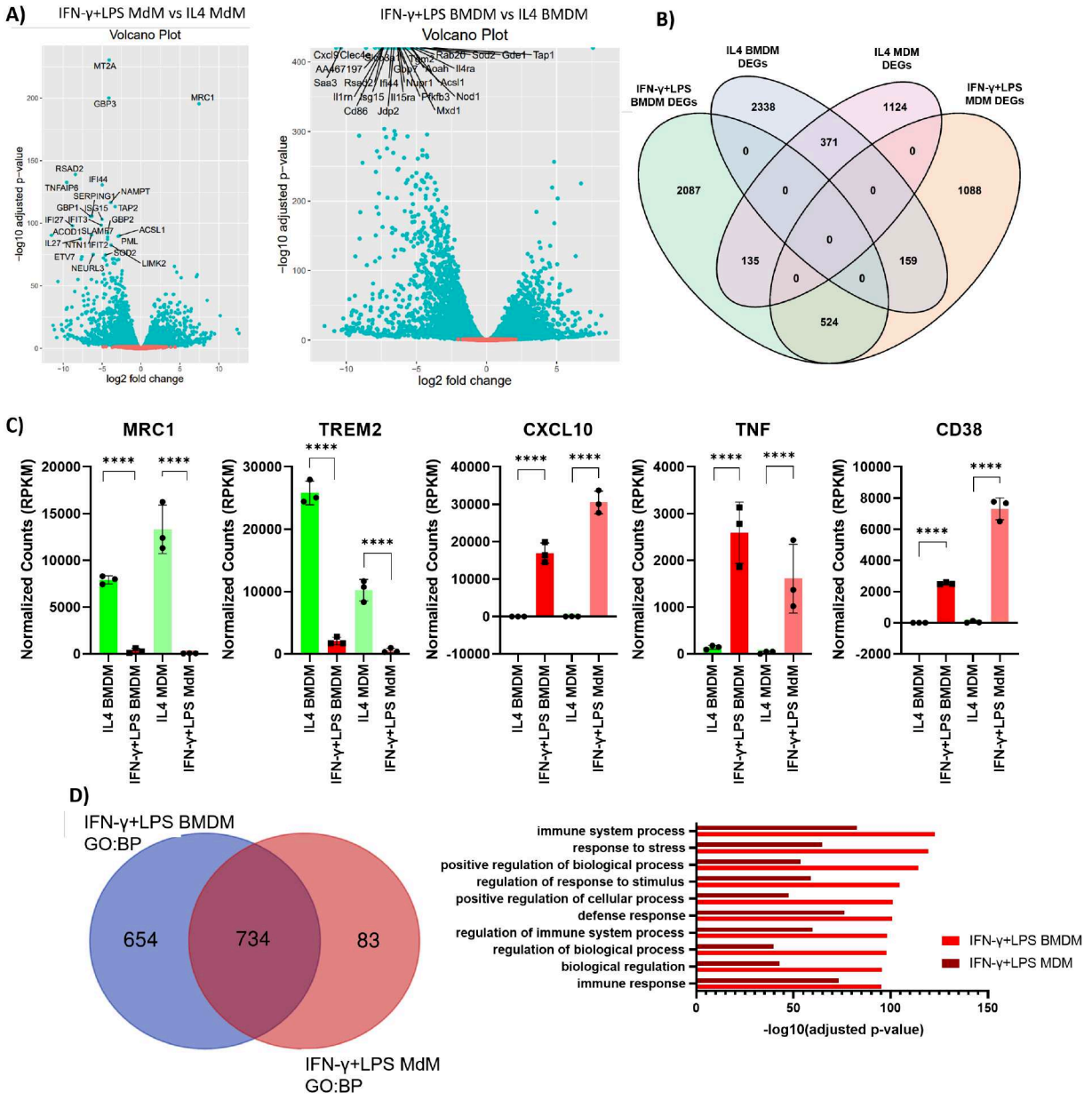

Figure 2.1.3. Transcriptomics analysis of murine BMDMs and human MdMs.
A) Volcano plots of DEGs in MdMs (left) and BMDMs (right), with the 20 most significant DEGs labelled.
B) A Venn diagram details the overlap and distinct DEGs between human and murine M1-like and M2-like macrophages, demonstrating shared and unique gene expression patterns.
C) Bar graphs with normalised expression levels of selected M2-like and M1-like markers in human and murine macrophages. Statistical significance indicated by adjusted p-values (**** p<0.0001; n=3).
D) A Venn diagram reveals the number of enriched Gene Ontology:Biological Process (GO:BP) pathways in M1-like macrophages from both species, with their intersections signifying common pathways.
The bar graph on the right represents the 10 most enriched pathways shared by murine and human macrophages, measured by the negative log10 of the adjusted p-values, highlighting significant pathways in the immune response. BMDM: bone marrow derived macrophages; MdM: monocyte derived macrophages; DEGs: differently expressed genes; GO:BP: Gene Ontology:Biological Process.

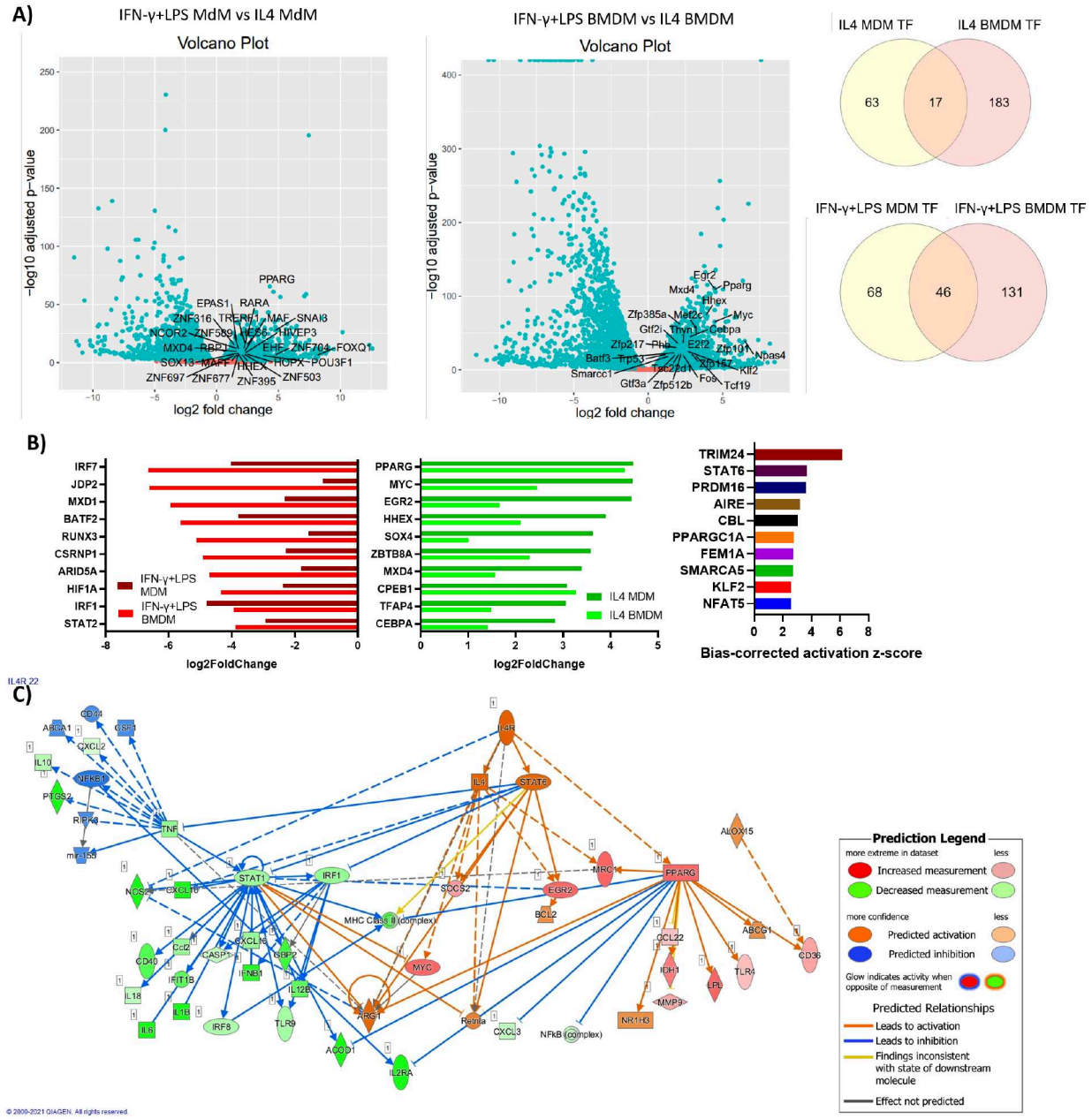

Figure 2.1.4. Transcriptional regulation in M2-like macrophages.
A) Volcano plots display RNA sequencing data, highlighting the most significant transcription factors on M2-like macrophages from both human and murine macrophages. The Venn diagram in the right illustrate the up-regulated transcription factors in M2-like and M1-like macrophages, detailing common factors between the two species.
B) Bar graphs denote the normalised expression of the most highly expressed transcription factors in M2-like and M1-like murine and human macrophages, showcasing the differential expression. The bar graph to the right displays the Bias-corrected activation z-score of the upstream regulators identified by IPA software as activated transcription regulators in M2-like macrophages.
C) Network pathway analysis conducted using IPA software, visualising activated upstream regulators in M2-like macrophages upon IL4 stimulation, indicating potential targets for modulating macrophage polarisation.
TF: transcription factor; BMDM: Bone marrow derived macrophages.

IL-4 signalling, suggesting a synergistic role in promoting M2-like polarisation (Liu et al., 2021). Therefore, we focused on Stat6 inhibition, as it acts upstream of Pparg. Stat6 and Myc have been identified as pivotal regulators of the M2-like phenotype (Liu et al., 2021).

Additional candidates for potential downregulation include Stat3, which is recognised for its role as a negative regulator of Stat1 and an enhancer of the anti-inflammatory macrophage phenotype (Liu et al., 2021; Xia et al., 2023). Intriguingly, the inhibition of Histone deacetylases (HDACs) in macrophages has also been shown to induce repolarisation towards an M1-like phenotype, adding another dimension to the regulatory mechanisms under consideration (Hu et al., 2021).

Given these insights, I determined that the principal transcription regulator candidates for down-regulation using SMIs include Stat6, Myc, Stat3, and various genes from the Hdac family. This selection was also influenced by the availability of commercially obtainable inhibitors, ensuring the practical applicability of these findings in future experimental endeavours.

2.1.4 miRNAs regulating macrophage polarisation

In my parallel analysis of miRNA sequencing data, I identified miRNAs that were up-regulated in M1-like macrophages, theorising they could drive repolarisation by down-regulating M2-like genes and therefore enhancing M1-like features. In murine BMDMs, 22 miRNAs were up-regulated in the M1-like state, and 18 in the M2-like state, with a p-value threshold of 0.05 and $\log_2$ fold change threshold ranging from -1 to 1. Human macrophages showed a similar trend, with 19 miRNAs up-regulated in M1-like macrophages and 19 in M2-like (Figure 2.1.5).

A notable intersection of four miRNAs was found between human and murine IFN-γ+LPS-treated macrophages. Of these, miR-155-5p emerged as the miRNA with the highest expression commonality between the two, accompanied by two variants of miRNA-9-5p, miR-9-1 and miR-9-3. Finally, miR-147b, known from literature as a negative inflammation regulator in macrophages (Liu et al., 2009), was also identified.

No miRNAs were commonly up-regulated in human and murine IL4-treated macrophages. Based on these findings, we proceeded to explore whether the transfection of miR-155-5p and miR-9-5p into M2-like macrophages could induce a phenotypic shift towards the M1-like state.

In an effort to identify miRNA candidates for the M1-like polarisation of macrophages, I employed *in silico* methods to predict miRNA binding to key transcriptional regulators. This analysis involved querying several databases known for miRNA-target gene interaction predictions, including MicroCosm, mirDB, miRNAMAP, PITA, and TargetScan. The aim was to determine which miRNAs are likely to bind to and potentially down-regulate transcription factors that promote an M2-like phenotype, therefore encouraging a shift towards an M1-like state. The miRNAs were scored based on the number of databases that predicted their binding affinity to the transcription regulators in question. A higher cumulative score across these databases was

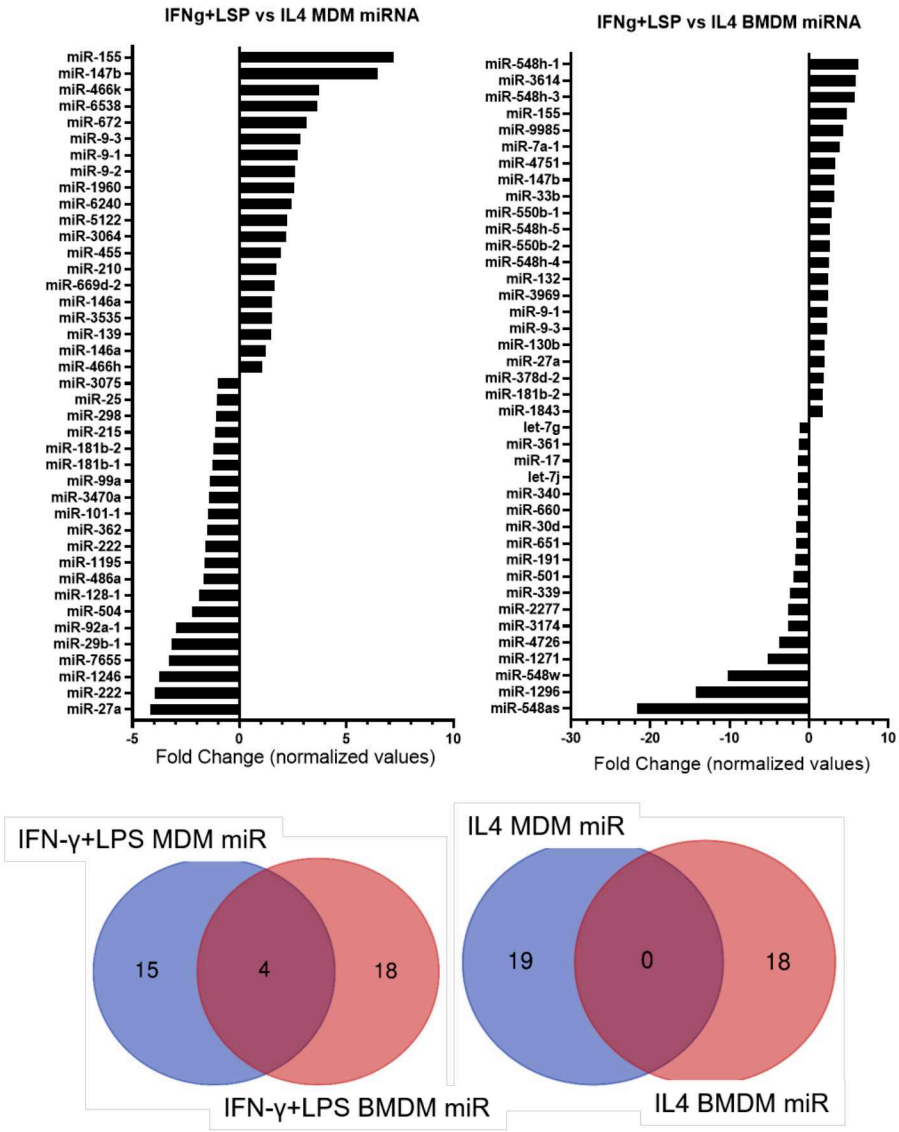

Figure 2.1.5. Comparative miRNA expression profiles in human and murine macrophages. The bar graphs illustrate the differential expression of miRNAs in M1-like versus M2-like macrophages, with human data presented on the left and murine data on the right. These graphs display the fold change in normalised miRNA expression levels. Accompanying Venn diagrams (bottom) detail the count of miRNAs up-regulated in M1-like compared to M2-like macrophages for both humans and mice, highlighting the shared and species-specific regulatory miRNAs. BMDM: bone marrow derived macrophages; MdM: monocyte derived macrophages.

interpreted as a stronger indication of the miRNA's regulatory potential. Selected miRNAs with high scores were prioritised for further experimental validation.

The table below presents the summarised predictions, where the sum column indicates the total predictive score for each miRNA, followed by individual scores for their potential interaction with Hdac1, Hdac3, Myc, Stat6, and Stat3. The selection of miRNAs for transfection into M2-like macrophages was based on the hypothesis that these miRNAs could effectively down-regulate the associated transcription factors and thereby influence the macrophage phenotype towards M1-like polarisation. These miRNAs are written in the table below.

miRNA	Sum	*Hdac1*	*Hdac3*	*Myc*	*Stat6*	*Pparg*	*Stat3*
mmu-miR-709	10	0	1	5	2	0	2
mmu-miR-694	10	5	0	4	0	0	1
mmu-miR-144-3p	9	0	5	0	3	4	1
mmu-miR-125a-5p	9	0	4	0	1	0	4
mmu-miR-125b-5p	9	0	4	0	1	0	4
mmu-miR-155-5p	0	0	0	0	0	0	0
mmu-miR-9-5p	7	1	1	1	2	0	2

Table 2.1.1. *In silico* predictive binding scores of candidate miRNAs to key transcriptional regulators in macrophage polarisation.

It is important to note that mmu-miR-155-5p, despite its potential relevance, did not score in this predictive model, while mmu-miR-9-5p had at least one database score to most of the down-regulation candidates, with a sum score of 7. The miRNAs selected for further analysis were then miR-155-5p, miR-9-5p, observed in murine and human M1-like macrophages, and miR-709, miR-694, miR-144-3p, miR-125a-5p and miR-125b-5p, identified through *in silico* analysis.

Transfection of miRNAs into Bone Marrow Derived Macrophages

To test the aforementioned miRNAs as potential candidates for the repolarisation of M2-like murine macrophages, I employed the transfection method. First, I conducted a comparative analysis of several transfection reagents for the optimisation of transfection into M2-like BMDMs. Utilising 20nM of a Cyanine3 (Cy3)-coupled control small RNA following the manufacturer's guidelines of each transfection reagent, I evaluated the cells 24 hours post-transfection for both viability, marked by the absence of LIVE/DEAD Fixable Yellow Dead Cell dye staining and Cy3 incorporation to assess transfection efficiency.

The analysis revealed varied transfection efficiencies: HiPerFect achieved 48.2% Cy3 positive cells, RNAiMax reached 59.9%, while DharmaFect4 and Lipofectamine 3000 displayed approximately 70% (70.2% and 72.2%, respectively). Metafectene exhibited the highest transfection efficiency at 80.4%, although it also resulted in the lowest cell viability (85.1% LIVE/DEAD Fixable Yellow Dead Cell dye negative) (Figure 2.1.6A).

Further investigation into the impact of these reagents on macrophage phenotype showed a substantial increase in IA^b expression with Metafectene (91.1%). In comparison, HiPerFect and Lipofectamine 3000 showed moderate effects (38.9% and 42.2%, respectively), while the impact of DharmaFect4's (28.7%) was comparable to the non-transfected control (26.9%) (Figure 2.1.6A).

Given these results, DharmaFect4 was selected for subsequent BMDM transfections due to its balance of high efficiency, low effect on viability and minimal phenotypic alteration. Initially, transfection efficiency was high (80% Cy3), but it decreased to 65% Cy3 at 48 hours and further to 47.1% Cy3 at 72 hours post-transfection. To address this, I established a regimen of daily re-transfection, which maintained a stable intracellular RNA level (96% Cy3 at 48 hours and 99.8% Cy3 at 72 hours) without affecting cell viability (Figure 2.1.6B and C).

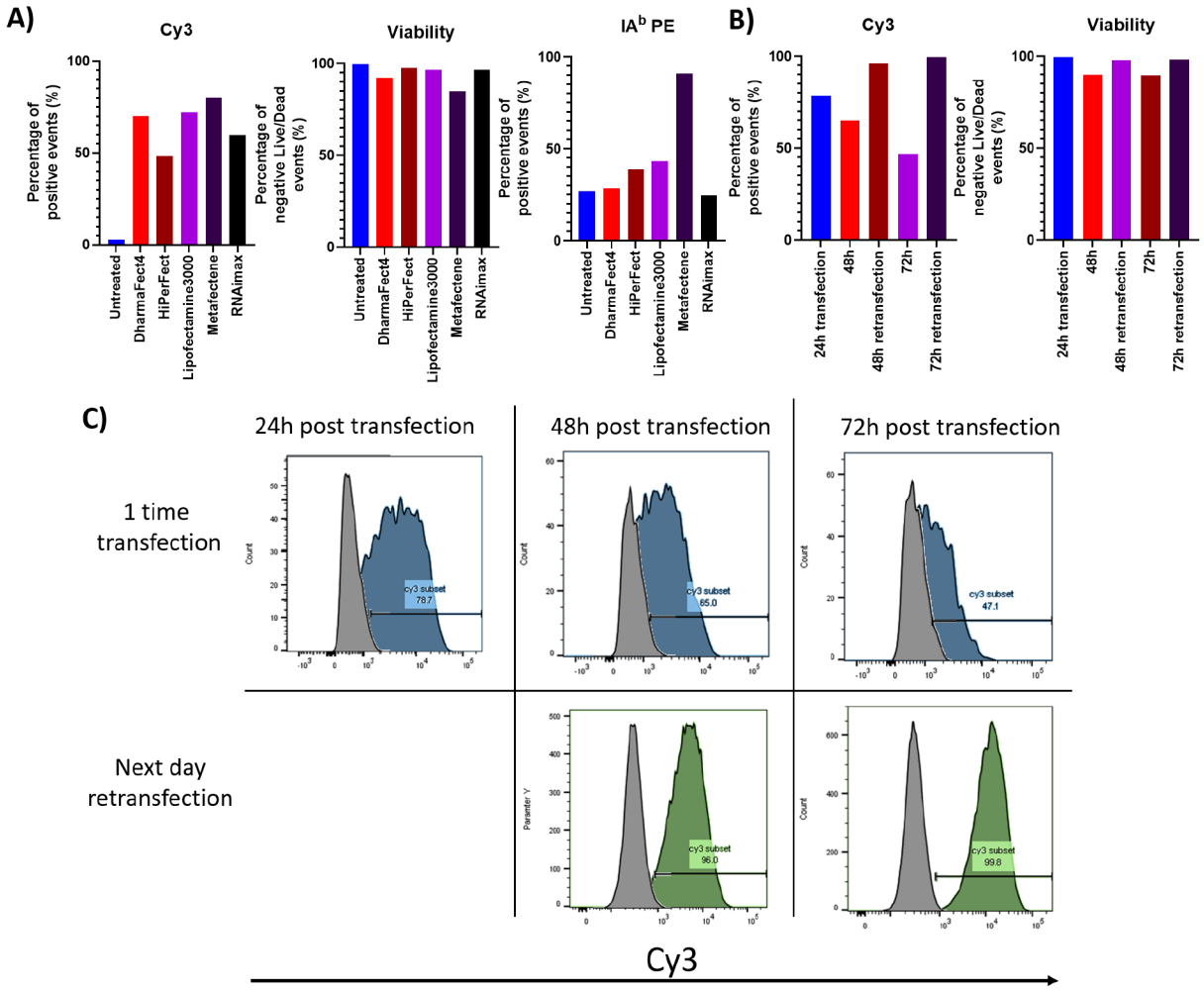

Figure 2.1.6. Transfection efficiency, cell viability, and macrophage phenotype post-transfection.
A) The series of bar graphs quantifies transfection efficiency, depicted as the percentage of Cy3-positive macrophages 24 hours post-transfection. The middle graph assesses cell viability by displaying the percentage of LIVE/DEAD Fixable Yellow Dead Cell dye-negative events. The final graph on the right evaluates the impact of various transfection reagents on macrophage phenotype, specifically measuring the percentage of IA^b-positive events following treatment.
B) This set of bar graphs details the impact of retransfection on BMDMs by comparing transfection efficiency (Cy3 percentage) and cell viability (LIVE/DEAD Fixable Yellow Dead Cell dye-negative percentage) at 24, 48, and 72 hours after initial transfection or with subsequent retransfections.
C) Histograms display the transfection efficiency (Cy3) in BMDMs following a single transfection event versus the efficiency after subsequent retransfections.

Evaluation of Candidate miRNAs for Macrophage Repolarisation

In a series of independent experiments, candidate miRNAs were transfected into BMDMs to evaluate their potential to repolarise macrophages from an M2-like to an M1-like state. qRT-PCR was used to measure the changes in gene expression, with ath-miR-416 serving as the normalisation control.

The standout result was the performance of miR-155-5p, which consistently influenced key genes associated with macrophage polarisation. Specifically, it significantly down-regulated *Mrc1* ($\log_2$FC $-$ 0.8596, p = 0.0359, n = 14) and up-regulated *Cxcl10* ($\log_2$FC = 2.143, p = 0.0069, n = 10), *Il1b* ($\log_2$FC = 2.475, p = 0.0006, n = 9), and *Tnf* ($\log_2$FC = 2.303, p = 0.0002, n = 13), suggesting a robust shift towards an M1-like phenotype (Figure 2.1.7A).

Other candidate miRNAs (Table 2.1.1), such as mmu-miR-694 ($\log_2$FC = 3.391, p = 0.0051, n = 5), mmu-miR-144-3p ($\log_2$FC = 1.871, p = 0.0197, n = 6), and mmu-miR-125a-5p ($\log_2$FC = 2.298, p = 0.0296, n = 5), also showed significant effects in modulating *Tnf* expression.

However, contrary to *in silico* predictions, these miRNAs did not down-regulate *Myc*, *Stat6*, or *Pparg*, indicating a disconnect between predictive binding and actual gene regulation (Figure 2.1.7B). This highlights the complex nature of miRNA-mediated regulatory mechanisms and the importance of experimental confirmation of computational forecasts. The absence of any significant impact on Trem2 by the tested miRNAs further accentuates these complexities (Figure 2.1.7A).

Overall, miR-155-5p emerged as a prime candidate for driving an M1-like phenotype in BMDMs, showcasing the therapeutic potential of miRNAs in modulating immune cell function.

2.1.5 Small molecules regulating macrophage polarisation

In the quest to modulate macrophage polarisation, I assessed a spectrum of inhibitors against transcription regulators Myc, Stat6, Stat3, and members of the Hdac family—key transcriptional regulators implicated in the M2-like phenotype. The goal was to find optimal inhibitor concentrations that effectively disrupt these targets, thereby facilitating a polarisation shift while concurrently minimising cell toxicity.

For Myc inhibition, 10074-G5 was selected for its capacity to impede c-Myc-Max dimerisation, a crucial interaction for Myc's transcriptional activity (Clausen et al., 2010). An optimal concentration of 10 µM was determined, informed by the compound's IC50 and its documented efficacy in Daudi and HL-60 cell lines(Chauhan et al., 2014; Clausen et al., 2010; Yap et al., 2013).

Stat3 activity was countered using Stattic at 5 µM, chosen for its potent inhibition of Stat3 phosphorylation and selectivity, as evidenced by its negligible impact on STAT1 and other signalling molecules (Schust et al., 2006). It disrupts the binding to Stat3's SH2 domain, reducing Stat3's nuclear presence and surviving levels, ultimately impeding cell growth and inducing apoptosis in cancer cell lines (Lin et al., 2016; Schust et al., 2006).

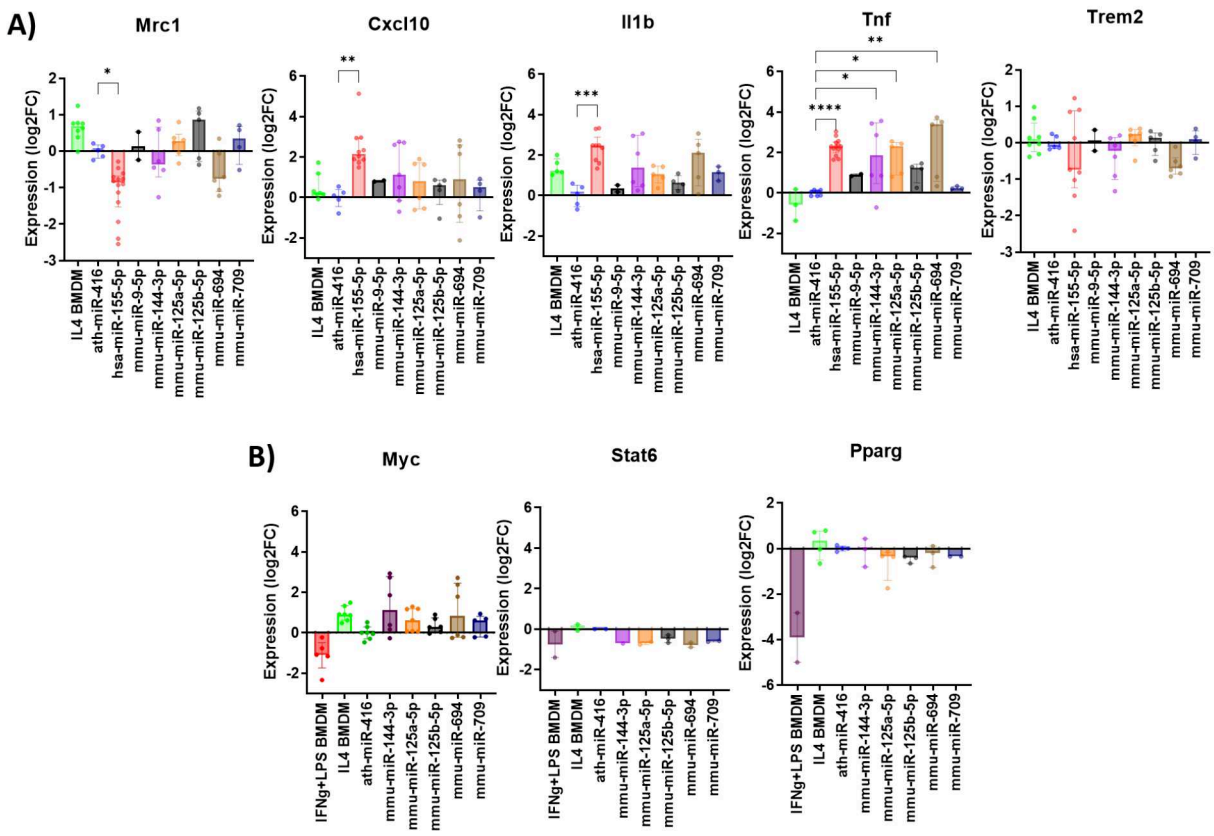

Figure 2.1.7. Differential gene expression in BMDMs post-miRNA transfection.
A) This panel displays bar graphs representing the expression changes of M2-like and M1-like markers in BMDMs, as determined by qRT-PCR following treatment with various miRNAs. The data is presented as $\log_2$ fold change ($\log_2$FC).
B) The expression levels of transcription factors regulating M2-like genes are depicted in bar graphs. Data is shown as median with interquartile range.
Statistical significance was evaluated using the Kruskal-Wallis test followed by Dunn's multiple comparisons test. The housekeeping gene was Rpl19. Sample sizes ranged from n=2 to n=14. Significance levels are indicated as * for p<0.05, ** for p<0.01, *** for p<0.001, and **** for p<0.0001.

AS1517499, administered at 1 µM, was used to inhibit Stat6 phosphorylation. It is recognised for its potent and selective inhibition of Stat6, effectively blocking IL-4-induced Th2 differentiation without affecting Th1 differentiation, thereby providing a more tailored approach to macrophage repolarisation (Chiba et al., 2009; Kim et al., 2018; Nagashima et al., 2007).

Mocetinostat, an Hdac inhibitor, was applied at 2 µM due to its specific activity against Hdac classes I and IV (Fournel et al., 2008). It inhibits Hdac1-3 and Hdac11 at nanomolar to low micromolar concentrations without affecting class II Hdacs, as demonstrated in cell-free assays and *in vitro* (El-Khoury et al., 2010; Fournel et al., 2008).

The impact of these inhibitors on gene expression was significant. Mocetinostat alone downregulated *Mrc1* expression ($\log_2\text{FC} = -2.923, p = 0.0171, n = 6$). A cocktail of the aforementioned inhibitors markedly suppressed *Mrc1* expression ($\log_2\text{FC} = -3.848, p = 0.0003, n = 9$)

while up-regulating inflammatory markers like *Cxcl10* ($\log_2$FC $= 4.244, p = 0.0356, n = 6$) and *Il1b* ($\log_2$FC $= 5.250, p = 0.0310, n = 7$) (Figure 2.1.8A).

Although these inhibitors did not universally achieve complete macrophage polarisation, Mocetinostat's selective down-regulation of Mrc1 was noteworthy. The combined inhibitor pool elicited the strongest repolarisation effects, albeit with associated cytotoxicity (data not shown). This suggests that the complex interplay of signalling pathways may require a nuanced, multi-targeted inhibition strategy.

In addressing the high cytotoxicity of Stattic, our search for alternative Stat3 inhibitors led us to Niclosamide and FLLL32, both targeting Stat3 phosphorylation. We used Niclosamide at a concentration of 500 nM, notable for its precise inhibition of Stat3 phosphorylation while sparingly affecting similar molecules like Stat1 and Stat5. Its functionality as an anticancer agent further added to its appeal (Ren et al., 2010). FLLL32, on the other hand, was administered at 1 µM (Bill et al., 2010; Lin et al., 2010).

In our Hdac inhibition strategy, we utilised known inhibitors whose selectivity has been well-documented in the literature. Entinostat, which selectively targets Hdac1, Hdac2, and Hdac3, was employed at a concentration of 1 µM (Lauffer et al., 2013; Rosato et al., 2003). This choice was based on its established efficacy in selectively inhibiting these specific Hdacs without markedly impacting other members of the Hdac family. RGFP966, another inhibitor with a well-characterised profile, was used at 100 nM. It is recognised for its targeted inhibition of Hdac3, offering high selectivity with minimal effects on Hdacs 1, 2, and 8. These concentrations were carefully chosen to leverage their known inhibitory properties and cytotoxicity (Malvaez et al., 2013; Wells et al., 2013)

Subsequently, I formulated various inhibitor pools by combining these alternative Stat3 and Hdac inhibitors with Myc and Stat6 inhibitors. The aim was to enhance macrophage repolarisation while maintaining cell viability. These combinations were methodically compared, focusing on their effects on cell viability and the expression of M1-like and M2-like markers (Figure 2.1.8B).

The cell viability following treatment with these inhibitor pools varied, with some combinations like MS275+FLLL32 showing lower viability (45.5%) and others like RGFP966+Niclosamide demonstrating higher viability (67.5%), compared to untreated controls. Despite the challenges of cytotoxicity, it was imperative to identify a combination that effectively promoted repolarisation without excessively compromising cell survival.

The combination of Entinostat and Niclosamide, along with Myc and Stat6 inhibitors, emerged as notably effective. It showed significant down-regulation of *Mrc1* ($\log_2$FC-0.6666, $p = 0.0225$) and up-regulation of *Cxcl10* ($\log_2$FC1.488, $p = 0.0005$) and *Il1b* ($\log_2$FC1.906, $p = 0.0005$), indicative of a shift towards an M1-like phenotype. Moreover, this was achieved with a more favourable cytotoxicity profile than other combinations. The results highlighted the need to inhibit a range of Hdacs, beyond just Hdac3, to achieve the desired repolarisation effect (Figure 2.1.8B).

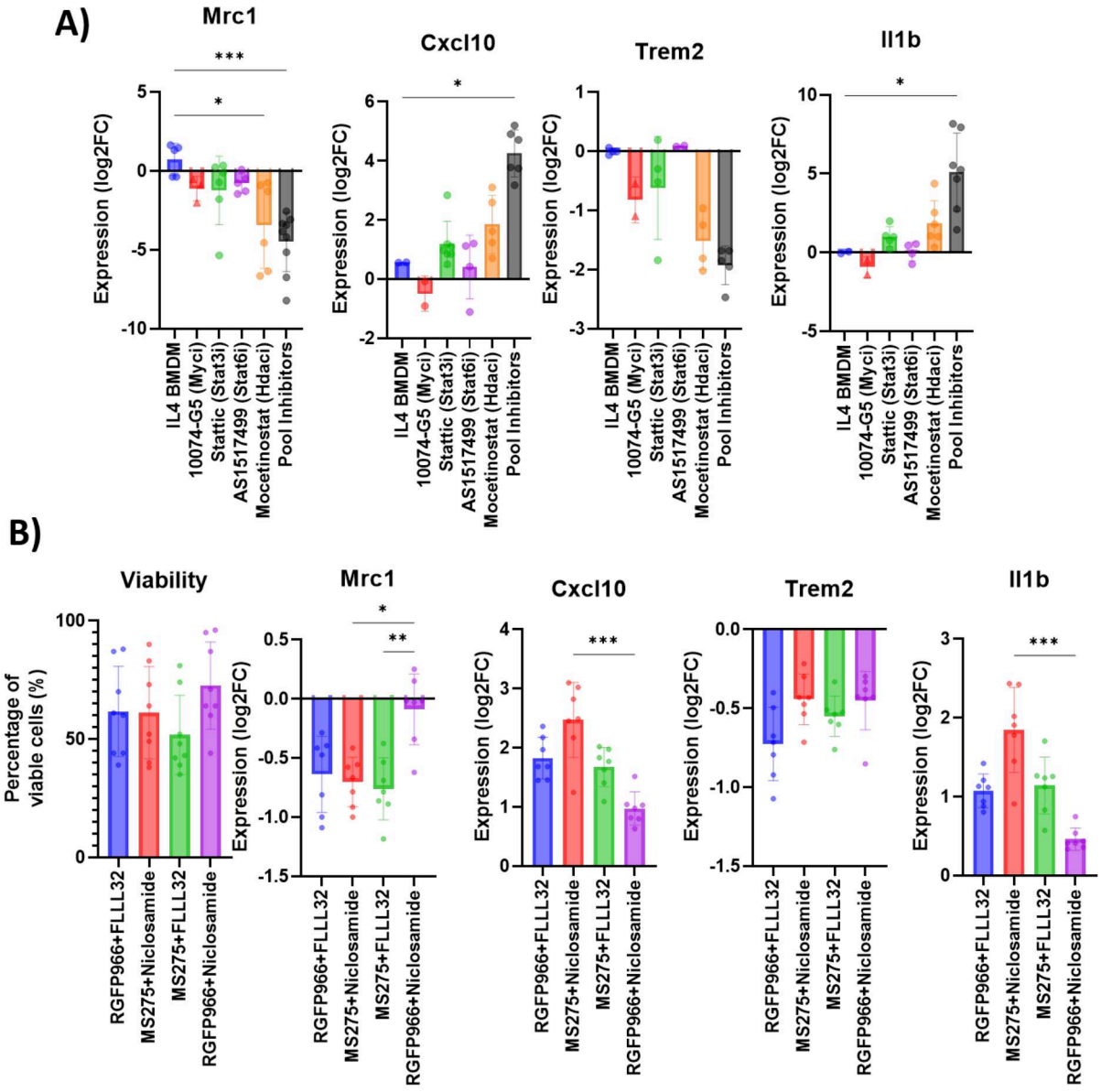

Figure 2.1.8. Impact of small molecule inhibitors on gene expression in BMDMs.
A) This section features bar graphs illustrating the changes in the expression of M2-like and M1-like markers in bone marrow-derived macrophages (BMDMs) following treatment with various small molecule inhibitors, including individual inhibitors and their combined pool. These changes, measured in $\log_2$ fold change ($\log_2$FC), were assessed via qRT-PCR.
B) Additional bar graphs present the viability of BMDMs as a percentage relative to untreated controls, alongside the expression of M2-like (*Mrc1* and *Trem2*) and M1-like (*Cxcl10* and *Il1b*) markers post-treatment. These treatments involved multiple inhibitor pools, each containing 10074-G5 (Myc inhibitor), AS1617499 (Stat6 inhibitor), and different combinations of Stat3 (FLL32 and Niclosamide) and Hdac family (RGFP966 and MS275) inhibitors.
The data is represented as a median with an interquartile range, and statistical significance was determined using the Kruskal-Wallis test, followed by Dunn's multiple comparisons test. Housekeeping gene was *Rpl19*. The number of samples varied from n=2 to n=14. Significance levels are denoted as * for $p<0.05$, ** for $p<0.01$, and *** for $p<0.001$.

In summary, the most effective inhibitor pool for macrophage repolarisation consisted of Niclosamide for Stat3, AS1517499 for Stat6, 10074-G5 for Myc, and Entinostat for Hdac. This combination struck a balance between facilitating effective polarisation and maintaining manageable cytotoxicity, offering a promising approach for therapeutic interventions in scenarios where macrophage polarisation plays a crucial role.

2.2 Validation of repolarisation candidates for murine BMDM

2.2.1 Protein expression changes after repolarisation

In our subsequent analysis, we focused on the protein expression in macrophages 72 hours after treatment with our most promising miRNA, miR-155-5p, and inhibitor pool, consisting of Niclosamide for Stat3, AS1517499 for Stat6, 10074-G5 for Myc, and Entinostat for Hdac inhibition. Using FACS, we evaluated the expression of several M1-like macrophage markers, IA^b, CD38, and CD86. In this assessment, miR-155-5p -treated cells were compared against the ath-miR-416 control, and cells treated with the inhibitor pool were evaluated against untreated M2-like BMDMs.

The treatment with miR-155-5p resulted in a significant increase in CD38 expression by 25.08% ($p = 0.0286, n = 4$), suggesting a shift towards an M1-like phenotype. Additionally, there was a moderate rise in IA^b expression (31.33%, $n = 4$), although this change did not reach statistical significance. In contrast, the cells treated with the inhibitor pool did not exhibit a similar up-regulation in these M1-like surface markers, indicating a differential impact on macrophage polarisation (Figure 2.2.1).

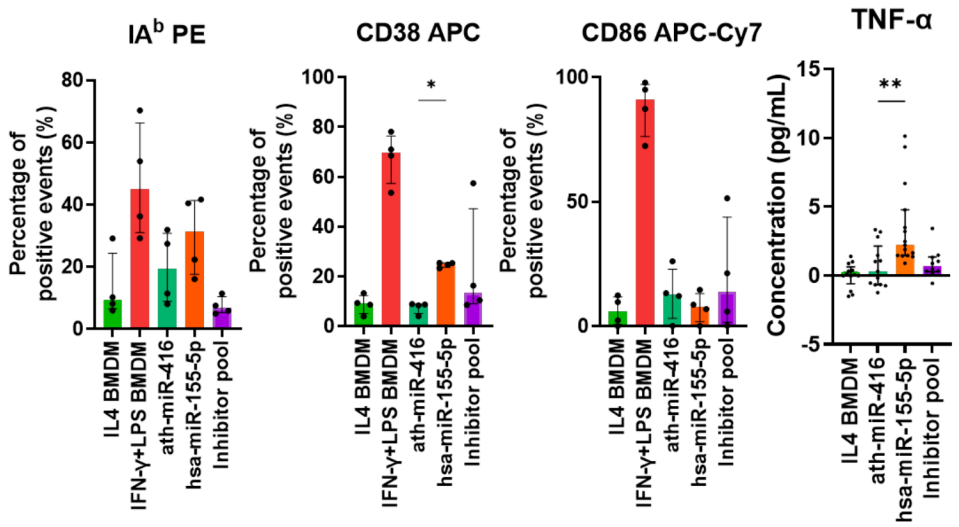

Figure 2.2.1. Expression of M1-like marker proteins in BMDMs after treatment with miR-155-5p and inhibitor pool.
This figure displays the results of FACS analysis, showing the percentage of positive cells for IA^b, CD38, and CD86 within the live macrophages gate, identified as LIVE/DEAD Fixable Yellow Dead Cell dye(–) F4/80(+) CD11b(+). Additionally, TNF-α secretion levels were quantified using ELISA. The expression impact of miR-155-5p was evaluated against the ath-miR-416 control, and the effects of the inhibitor pool were compared with those of untreated controls (IL4 BMDMs).
Data are presented as median values with interquartile ranges, and statistical significance was assessed using the Mann-Whitney test. Sample sizes included n=4 for FACS and n=10-15 for ELISA. Statistical significance is indicated with * for p<0.05, ** for p<0.01, and *** for p<0.001.

Moreover, the TNF-α secretion, measured via ELISA, displayed a slight but significant increase in the miR-155-5p treated group (2.204 pg/mL, $p = 0.0026, n = 15$), reinforcing the potential of miR-155-5p as an effective agent for macrophage repolarisation (Figure 2.2.1).

These outcomes underscore the efficacy of miR-155-5p in promoting a pro-inflammatory M1-like state, contrasting with the less pronounced effect of the inhibitor pool.

In summary, these results reinforce the potential of miR-155-5p as a promising agent for macrophage repolarisation, specifically toward an M1-like, pro-inflammatory state. The differential impact observed between miRNA treatment and the inhibitor pool underscores the complexity of macrophage polarisation mechanisms and highlights the importance of selecting appropriate agents for targeted therapeutic interventions.

2.2.2 Gene expression changes after murine macrophage repolarisation

Our study utilised microarray analysis to gain a deeper understanding of the pathways involved in macrophage polarisation by miR-155-5p and the inhibitor pool, comprising Niclosamide, Entinostat, AS1517499, and 10074-G5. 48 hours after treatment with these repolarisation candidates, biological replicates of the BMDMs were harvested and set for microarray analysis. The criteria set for identifying DEGs included a p-value of 0.05 and a $\log_2$ fold change of 1 or -1. This approach led to identifying 1308 DEGs up-regulated and 1381 down-regulated in IFN-γ+LPS treated BMDMs compared to IL4-treated BMDMs.

Specifically focusing on the effects of miR-155-5p, we observed 39 DEGs up-regulated, of which 15 intersected with M1-like BMDM DEGs (Figure 2.2.2). For down-regulated genes, miR-155-5p showed 55 DEGs, with 7 in common with M1-like BMDMs, highlighting the influence of miR-155-5p in macrophage polarisation.

In the case of the inhibitor pool treatment, there were 741 DEGs up-regulated, with 264 intersecting with M1-like BMDMs, and 933 DEGs down-regulated, with 249 intersecting with M1-like BMDMs (Figure 2.2.2, upper part). This result suggests a broad impact of the inhibitor pool on gene expression related to macrophage polarisation.

It's noteworthy that the low yield of BMDM miR-155-5p RNA could explain the relatively small number of significantly DEGs observed in the miR-155-5p treatment group.

Further, the GO:BP pathway analysis revealed 1250 enriched pathways for M1-like BMDMs. In the miR-155-5p treated BMDMs, 17 pathways were enriched, with 14 of them intersecting with the miR-155-5p group, thereby demonstrating the polarisation aspect of these macrophages. The inhibitor pool showed enrichment in 352 pathways, with 337 intersecting with M1-like BMDMs (Figure 2.2.2).

Of particular interest were the 11 pathways that intersected between M1-like BMDMs and both miR-155-5p and inhibitor-treated BMDMs. These pathways were predominantly associated with immune defence responses and inflammation, encompassing processes like the 'immune system process', 'defence response', 'response to stress', and 'immune response' (Figure 2.2.2, bottom). These findings provide a crucial insight into the molecular mechanisms underlying macrophage polarisation and the potential therapeutic applications of miR-155-5p and specific inhibitor pools in modulating immune responses.

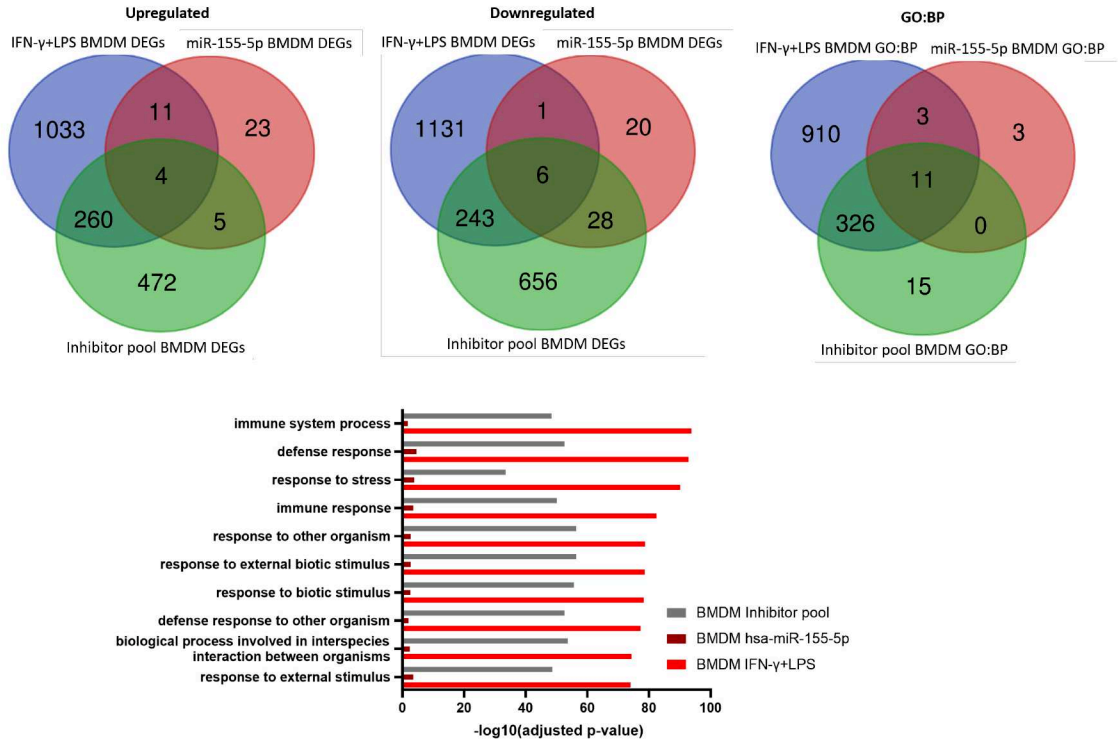

Figure 2.2.2. Gene expression and pathway analysis in murine macrophage repolarisation. The first two Venn diagrams display the overlap of up-regulated (left) and down-regulated (right) differentially-expressed genes (DEGs) among IFN-γ+LPS treated BMDMs, miR-155-5p treated BMDMs, and BMDMs treated with the inhibitor pool. The third Venn diagram illustrates the intersections of Gene Ontology Biological Process (GO:BP) pathways enriched in the three treatment groups. Below these diagrams, the bar graph details the -log10 of the adjusted p-values for the top ten most significant GO:BP pathways across IFN-γ+LPS treated BMDMs, miR-155-5p treated BMDMs, and inhibitor-treated BMDMs.

2.2.3 Functional changes after repolarisation

To investigate whether changes in gene and protein expression in murine BMDMs induced by repolarisation agents translated to functional outcomes, I conducted a co-culture experiment. First, IL4 macrophages were treated with IFN-γ+LPS or the most promising repolarising candidates miR-155-5p (compared to the ath-miR-416 control-treated macrophages) or the inhibitor pool (compared to the untreated control) to steer them towards an M1-like phenotype.

Following this, EO771 cancer cells, engineered to express Ovalbumin (OVA), were tagged with the fluorescent dye Carboxyfluorescein succinimidyl ester (CFSE), and OVA-specific CTLs were similarly labeled with CellTrace Violet (CTV). These labelled cells were then added to the treated macrophages in various combinations. The co-culture experiment set out to test the functional implications of macrophage repolarisation on the interaction between BMDMs, EO771-OVA cancer cells, and OVA-CTLs. This experiment was structured to evaluate three distinct interactions (Figure 2.2.3):

1. The direct impact of macrophages on tumour cell viability by co-culturing macrophages with EO771-OVA cells.

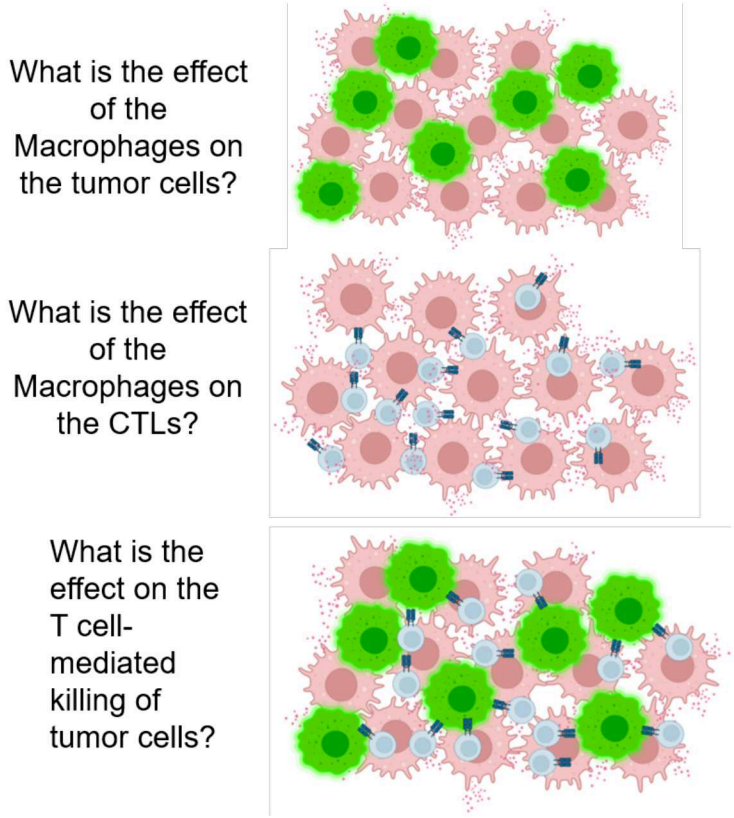

Figure 2.2.3. Co-culture experimental strategy for evaluating macrophage function.
This figure outlines the experimental design of the co-culture study, where repolarised macrophages, labelled EO771-OVA cells, and CTLs are cultured together to understand their interplay. The study focused on the direct and indirect effects these cells exert on one another following treatments aimed at repolarising macrophages towards an M1-like state. Created with BioRender.com.

2. The influence of macrophages on the activation state of CTLs by co-culturing macrophages with OVA-specific CTLs.

3. The combined effect of macrophages on both CTL-mediated cytotoxicity and the subsequent killing of tumour cells by creating a tri-culture of macrophages, OVA-specific CTLs, and EO771-OVA cells.

After a 24-hour incubation, the supernatant was collected for cytokine analysis via ELISA, and the cells were prepared and analysed by flow cytometry. Two distinct FACS panels were employed to accurately quantify the EO771-OVA tumour cells and to characterise the activation markers on CTLs, providing a comprehensive profile of the cellular interactions and functional outcomes of the repolarisation treatments.

FACS Panel 1

Panel 1 incorporated absolute cell counting beads to quantify the CFSE+ EO771-OVA tumour cells. These beads are easily identified by their high side scatter side scatter (SSC) and low forward scatter forward scatter (FSC) properties, as well as their distinct fluorescence. Alongside

this, we utilised specific macrophage markers, F4/80 and CD11b, to observe macrophage phagocytosis of tumour cells or tumour debris. This was achieved by tracking the uptake of CFSE+ events within the macrophage population, characterised as F4/80+CD11b+ (Figure 2.2.4A).

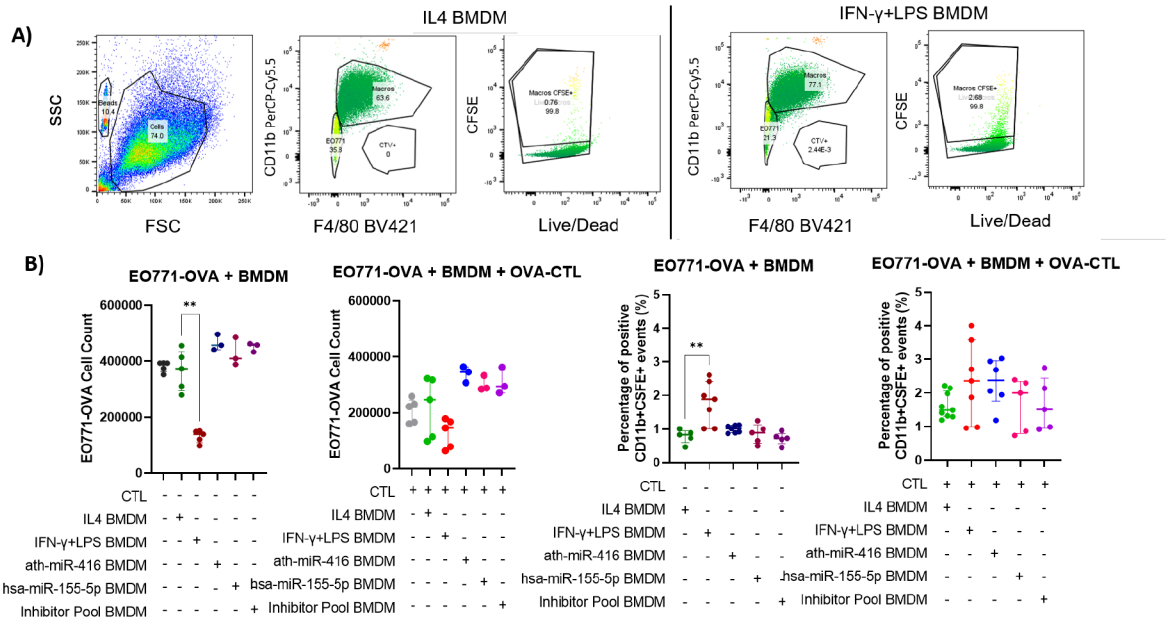

Figure 2.2.4. Functional dynamics in co-culture of EO771-OVA tumour cells, murine BMDMs, and OVA-CTLs.
A) Flow cytometry dot plots illustrate the gating strategy for identifying and quantifying different cell populations. The gating strategy is demonstrated through SSCxFSC dot plots for counting beads (characterised by high SSC and low FSC) and other cell populations. Subsequent dot plots display CD11b PerCP-Cy5.5 and F4/80 BV421 staining, delineating macrophages (CD11b+F4/80+), CFSE+ EO771-OVA cells (CD11b-F4/80-CFSE+), and CTV+ CTLs (CD11b-CTV+). CFSE fluorescence intensity is indicated through a colour gradient from green (low CFSE) to red (high CFSE). The gating of live macrophages is further detailed, showing the selection of LIVE/DEAD Fixable Yellow Dead Cell dye negative cells and the assessment of phagocytosis based on the CFSE+ gate within the live macrophage (CD11b+F4/80+LIVE/DEAD Fixable Yellow Dead Cell dye-) population. B) Graphs depict the quantitative analysis of EO771-OVA cell numbers and macrophage phagocytosis. The first graph presents EO771-OVA cell counts in co-cultures with differently-treated macrophages. The second graph illustrates cell counts in a triple culture setup, including OVA-CTLs. The third graph quantifies the percentage of tumour cell phagocytosis by macrophages (CD11b+F4/80+CFSE+) in co-cultures with EO771-OVA cells, and the fourth graph details phagocytosis in the presence of OVA-CTLs. Data are presented as median values with interquartile ranges, and statistical significance was assessed using the Kruskal-Wallis test, followed by Dunn's multiple comparisons test. Sample sizes ranged from n=3 to n=9, and statistical significance is denoted by * ($p<0.05$) and ** ($p<0.01$).

FACS Panel 2

Panel 2 was intended for phenotypic analysis of CTL activation, using antibodies against CD25 and CD69 to gauge the activation state of T cells following interaction with treated macrophages and EO771-OVA tumour cells (Figure 2.2.4C). This dual-panel approach allowed for a granular analysis of the repolarisation treatment's impact on both the innate and adaptive immune responses in the tumour microenvironment (Table 2).

Fluorescence Channel	Panel 1	Panel 2
BL530/30	CFSE	CFSE
BL670LP	CD11b PerCP-Cy5.5	CD25 PerCP-Cy5.5
BL780/60	–	CD69 PE-Cy7
VL450/50	F4/80 BV421 and CTV	CTV
VL510/50	Live/Dead	Live/Dead
N/A	Cell Counting Beads	–

Table 2.2.1. FACS panels for co-culture analysis

The results from the co-culture experiments were revealing. Macrophages repolarised with IFN-ɣ+LPS demonstrated a remarkable decrease in EO771-OVA cell counts (139,184 EO771-OVA cell count, n=5, p=0.0079), reduced to just 37.28% compared to IL4 BMDMs (373,319 EO771-OVA cell count, n=5) (Figure 2.2.4B). Furthermore, IFN-ɣ+LPS-repolarised BMDMs showcased an enhanced ability to phagocytose CFSE+ tumour cells (1.890%, n=7, p=0.0100), surpassing that of BMDMs treated with IL4 (0.8329%, n=5) (Figure 2.2.4B) and secreted higher levels of TNF-α (174.6 pg/mL, n=5, p=0.0015) and NO (10.95 μM, n=3, p=0.0571) (Figure 2.2.5E). Such findings were indicative of their potentiated anti-tumour activity and heightened pro-inflammatory response. Conversely, miR-155-5p (409,529 EO771-OVA cell count, n=3; 0.893% CFSE+ phagocytosis, n=5) and the inhibitor pool (458,442 EO771-OVA cell count, n=3; 0.725% CFSE+ phagocytosis, n=5) treatments did not manifest a similar degree of anti-tumour effects.

2.2.4 Evaluation of repolarised macrophages impact on OVA-specific CTLs

Evaluating the influence of macrophages on OVA-specific CTLs in the absence of OVA antigen, we observed that CTLs co-cultured with IFN-ɣ+LPS-repolarised macrophages expressed increased levels of activation markers CD69 (1518 PE-Cy7 Median Fluorescence Intensity (MFI), n=8, p=0.0216) and CD25 (827.5 PerCP-Cy5.5 MFI, n=8, p=0.0039) (Figure 2.2.5D). This contrasted with CTLs incubated with IL4 BMDMs (365 PE-Cy7 MFI and 5 PerCP-Cy5.5 MFI, n=9), as analysed through flow cytometry, indicating the potential of IFN-ɣ+LPS-repolarised macrophages to modulate CTL activation. Macrophages repolarised with miR-155-5p (250 PE-Cy7 MFI and 10 PerCP-Cy5.5 MFI, n=5) and inhibitor pool (413 PE-Cy7 MFI and 345 PerCP-Cy5.5 MFI, n=5) did not exhibit a significant functional effect of CTL activation.

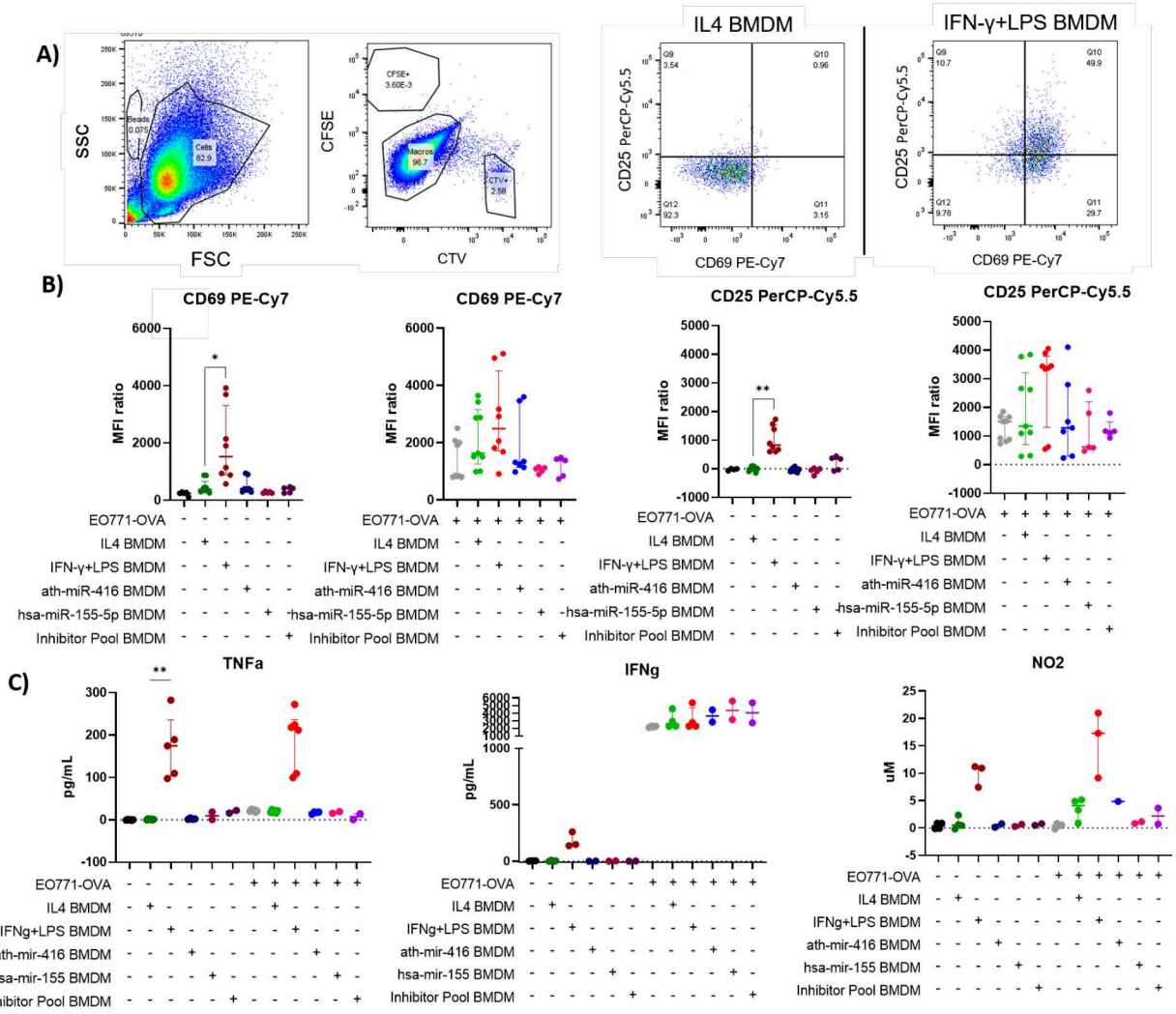

Figure 2.2.5. Functional dynamics in co-culture of EO771-OVA tumour cells, murine BMDMs, and OVA-CTLs (cont.).
A) Additional FACS dot plots delineate the second panel's gating strategy for T-cell phenotype assessment. The CTLs (CFSE-CTV+) are identified and analysed for activation markers CD25 PerCP-Cy5.5 and CD69 Pecy7, with live CTLs (CTV+LIVE/DEAD Fixable Yellow Dead Cell dye-) specifically targeted.
B) The graphical representation of CTL activation markers includes the MFI ratio of CD69 PEcy7 and CD25 PerCP-Cy5.5 against the isotype control. The first and second graphs display CD69 expression levels in CTLs co-cultured with treated macrophages alone and in the triple culture. The third and fourth graphs illustrate CD25 expression under similar experimental conditions.
C) The final set of graphs reveals secretion profiles (TNF-α, IFN-γ, and NO) in the media of various co-culture configurations, as measured by ELISA. These configurations include CTLs co-cultured with or without EO771-OVA cells and various BMDM treatments.
Data are presented as median values with interquartile ranges, and statistical significance was assessed using the Kruskal-Wallis test, followed by Dunn's multiple comparisons test. Sample sizes ranged from n=3 to n=9, and statistical significance is denoted by * ($p<0.05$) and ** ($p<0.01$).

2.2.5 OVA-CTL cellular function during EO771-OVA co-culture

The functionality of OVA-CTLs in the presence of EO771-OVA tumour cells was then assessed both in the absence and the presence of differently-treated BMDMs. Initially, the impact of OVA-CTLs on EO771-OVA tumour cells alone was assessed. Remarkably, the presence of OVA-CTLs

led to a significant reduction in tumour cell count, with the number of EO771-OVA cells dropping to 56.66% (222,918 EO771-OVA cell count, n=5, p=0.0079) of the control group without CTLs (393,380 EO771-OVA cells count, n=5) (Figure 2.2.4B). This pronounced decrease highlighted the potent cytotoxic ability of the activated CTLs. Furthermore, these CTLs demonstrated a heightened state of activation, secreting substantial amounts of IFN-ɣ (2253 pg/mL, n=4, p=0.0286) and TNF-α (20.93 pg/mL, n=6, p=0.0022) (Figure 2.2.5E). This was corroborated by elevated expression levels of activation markers CD69 (855.0 PE-Cy7 MFI, n=9, p=0.0010) and CD25 (1505 PerCP-Cy5.5 MFI, n=9, p=0.0028) (Figure 2.2.5D), as measured by ELISA and flow cytometry, respectively.

2.2.6 Tri-culture analysis

When CTLs were introduced into cultures containing both BMDMs and EO771-OVA cells, a reduction in EO771-OVA cell count was observed, along with an increased phagocytosis activity by the macrophages. Notably, this effect was consistent across all macrophage treatment groups, indicating that the presence of CTLs enhanced the macrophage's tumour cell phagocytic ability, independent of their repolarisation status (Figure 2.2.4B). Moreover, CTLs in these co-cultures maintained their activated state, with no discernible differences in activation or cytotoxicity towards EO771-OVA cells attributable to the type of macrophage repolarisation treatment (Figure 2.2.5D). This suggests that the macrophage treatment modalities did not significantly influence CTL functionality in this context.

In summary, macrophages repolarised with IFN-ɣ+LPS displayed the most pronounced effects regarding tumour cell killing, phagocytosis, and T-cell activation. This underscores the functionality of M1-like macrophages in the tumour microenvironment. The results suggest that while miRNAs and SMIs can influence macrophage phenotype, the functional consequences, particularly in the context of *in vitro* cancer cell interaction and CTL activation, are more complex and may require specific repolarisation signals, like those provided by IFN-ɣ+LPS, for effective therapeutic response.

2.2.7 Longitudinal effects of macrophage repolarisation

Building on these findings, we utilised the Incucyte system to monitor the confluence of cultures over multiple time points during the co-culture of BMDMs with EO771-OVA cells. This approach allowed us to observe the dynamic effects of treated BMDMs on tumour cell growth.

A notable reduction in tumour cell growth was observed when EO771 cells were co-cultured with IFN-ɣ+LPS-repolarised macrophages (75.1% normalised confluence at 24h and 62.9% at 48h, $p < 0.0001$) compared to IL4 BMDMs (109.7% confluence at 24h, 82.6% at 48h), as evidenced by a decrease in phase confluence, normalised to the starting point of the culture (hour 0) (Figure 2.2.6A and B). Interestingly, a slight but significant decrease in confluence was also seen

with the inhibitor pool-treated BMDMs (92.8% confluence at 24h and 62.7% at 48h, $p < 0.0001$) (Figure 2.2.6B).

While this treatment did not result in the same level of tumour cell growth inhibition as IFN-ɣ+LPS repolarisation, it did produce a noticeable and statistically significant decrease in confluence, particularly in the later stages of the culture. This observation underscored the importance of longitudinal monitoring, as it captured a nuanced effect that was not readily apparent in the FACS analysis. It emphasised the necessity of tracking cellular interactions over extended periods to understand the treatment's impact comprehensively.

On the other hand, miR-155-5p-treated BMDMs (112.7% confluence at 24h and 85.8% at 48h) did not show a discernible difference in confluence compared to control (ath-miR-416) miRNA-treated BMDMs (114% confluence at 24h and 85.3% at 48h) (Figure 2.2.6B).

This data corroborated our FACS findings, where IFN-ɣ+LPS-repolarised BMDMs significantly reduced EO771-OVA cell numbers. The slight decrease in tumour cell growth observed in cultures with inhibitor pool-treated BMDMs, not captured in FACS analysis, emphasised the importance of monitoring cellular interactions over time to gain a comprehensive understanding of treatment effects.

2.2.8 Effects of cell-cell contact between macrophages and tumour cells

To assess if cell-cell contact was needed for this pronounced impact of repolarised macrophages on the EO771-OVA tumour cells, we co-cultured the tumour cells with supernatant taken from repolarised BMDMs.

We observed that the supernatant from the IFN-ɣ+LPS repolarised macrophages (38.7% confluence at 24h and 36.5% at 48h, $p < 0.0001$) alone could reduce tumour cell growth, even in the absence of direct cell-cell contact, as compared to untreated EO771-OVA cells (67.5% confluence at 24h and 75.4% at 48h) (Figure 2.2.6C). The secreted cytokines TNF-α and NO from these macrophages likely played a pivotal role in inhibiting tumour cell growth, providing additional insights into the mechanisms of macrophage-mediated tumour suppression. On the other hand, the treatment with inhibitor pool BMDM supernatant gave no difference in EO771-OVA cell growth, showing this needs cell-cell contact (Figure 2.2.6C).

In summary, this study highlights the varying functional outcomes of different repolarisation agents on macrophages. While IFN-ɣ+LPS showed a strong capacity to induce functional M1-like characteristics in BMDMs, miR-155-5p, despite its molecular effects, did not translate to functional outcomes in the assays used. The inhibitor pool demonstrated a functional role in tumour cell proliferation, indicating its potential utility in specific contexts. These findings emphasise the importance of not only assessing molecular changes but also understanding the functional implications of macrophage repolarisation agents for effective therapeutic applications.

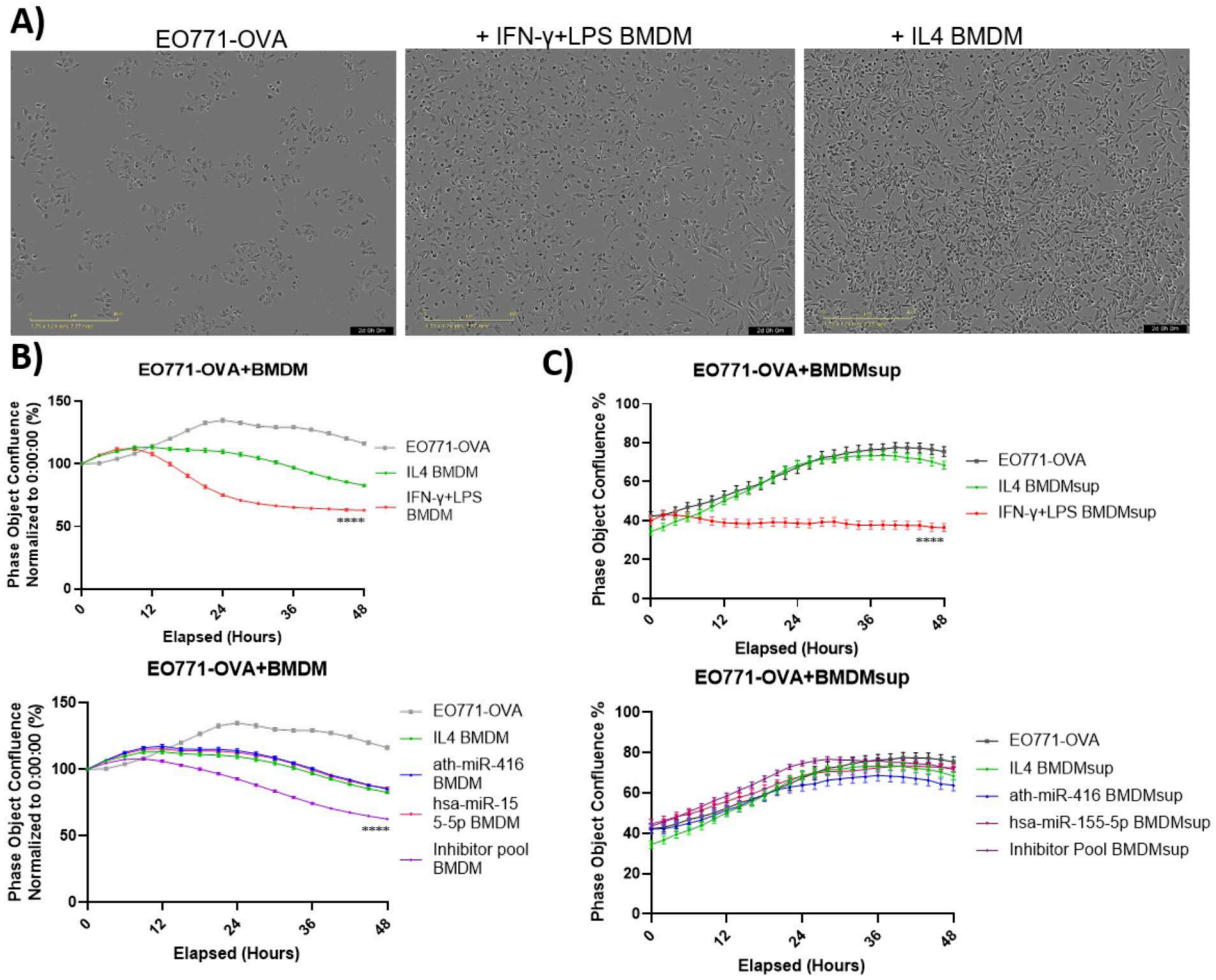

Figure 2.2.6. Effect of differently repolarised BMDMs on EO771-OVA tumour cells.
A) Incucyte Images on the 24h of culture of EO771-OVA cells, EO771-OVA cells cultured with IFN-γ+LPS repolarised BMDMs and cultured with IL4 BMDMs.
B) Graphs of Confluence normalised to the start of the culture (hour 0) x Elapsed time in hours of the co-cultures with EO771-OVA. The upper graph shows the effects of IL4 and IFN-γ+LPS repolarised BMDMs on the tumour cells; the graph below shows the co-culture with BMDMs treated with the inhibitor pool and miR-155-5p, and the ath-miR-416 control and IL4 BMDM control.
C) Graphs of Confluence x Elapsed time in hours of EO771-OVA cells treated with supernatant of differently polarised BMDMs. The upper graph shows the effect of the supernatant of IFN-γ+LPS repolarised macrophages compared to IL4 BMDMs and Untreated EO771-OVA cells. The lower graph shows the effect of other repolarised BMDM supernatants on the EO771-OVA cells.
n=6, **** $p<0.0001$. A non-linear regression model was applied to the growth curve to determine the kinetic parameters of cell growth. The goodness-of-fit for the non-linear model was assessed using an extra sum of squares F test.

2.3 Human MdM repolarisation candidate validation

Following the identification of promising repolarisation candidates in murine macrophages, notably miR-155-5p and an inhibitor pool targeting Stat3, Stat6, Myc, and members of the Hdac family, my focus shifted towards a comparative analysis between human and murine models. This phase centred on validating these candidates in human MdMs and comparing them with murine BMDMs. The primary objective of these experiments is to assess the translatability of repolarisation candidates identified in murine models to human cells. This comparison is crucial for confirming the viability and relevance of repolarisation strategies initially identified in murine models for human therapeutic applications. This approach also allows us to discern species-specific cellular mechanisms.

MdMs underwent treatment with candidate repolarising agents, specifically miR-155-5p and an inhibitor pool. The effectiveness and impact of these treatments were assessed through comparative analyses. MdMs transfected with miR-155-5p were compared against a control group transfected with a control miRNA (ath-miR-416), while those treated with the inhibitor pool were compared with an untreated control group. 48 hours post-treatment, the MdMs were harvested for gene expression analysis, through qRT-PCR. For protein expression analysis, MdMs were harvested 72 hours after the treatment. Protein expression was then analysed using FACS and ELISA.

The gene expression analysis in human MdMs post-transfection with miR-155-5p revealed a pattern of down-regulation and up-regulation of genes indicative of macrophage repolarisation. *MRC1* was down-regulated ($\log_2$FC $= -0.8690, n = 9, p = 0.0033$), while *CXCL10* ($\log_2$FC $= 9.651$, $n = 8, p < 0.0001$), *TNF* ($\log_2$FC $= 5.100$, $n = 4, p = 0.0286$), and *CCL5* ($\log_2$FC $= 4.270$, $n = 8, p = 0.0005$) were up-regulated. On the other hand, treatment with the inhibitor pool did not show an increased expression in M1-like markers and only decreased the expression of TREM2 ($\log_2$FC $= -1.114, n = 6, p = 0.0649$) (Figure 2.3.1A).

In terms of protein expression, after transfection with miR-155-5p, there was an increase in CD80 (15.68%, compared to control miR 5.4%, $n = 2$) and CD38 (28.16%, compared to control miR 13.02%, $n = 2$) percentages post miR-155-5p transfection, though not statistically significant. Additionally, the MFI ratio against miR control for CD206 (MFI ratio=0.5606, $n = 2$) further confirmed these findings. Complementing the FACS data, the ELISA results demonstrated significant increases in the concentrations of TNF-α (178.6 pg/mL, $n = 15, p < 0.0001$) and Cxcl10 (218.2 pg/mL, $n = 9, p < 0.0001$) in the cell culture media, highlighting the potent impact of miR-155-5p transfection on M1-like marker protein secretion in human MdMs (Figure 2.3.1B).

These results underscore the conserved function of miR-155-5p in macrophage repolarisation across both human and murine models. However, the lack of efficacy of the inhibitor pool in reversing the M2-like phenotype in human cells, as opposed to murine models, highlights the necessity of understanding species-specific transcription regulators. This differential response

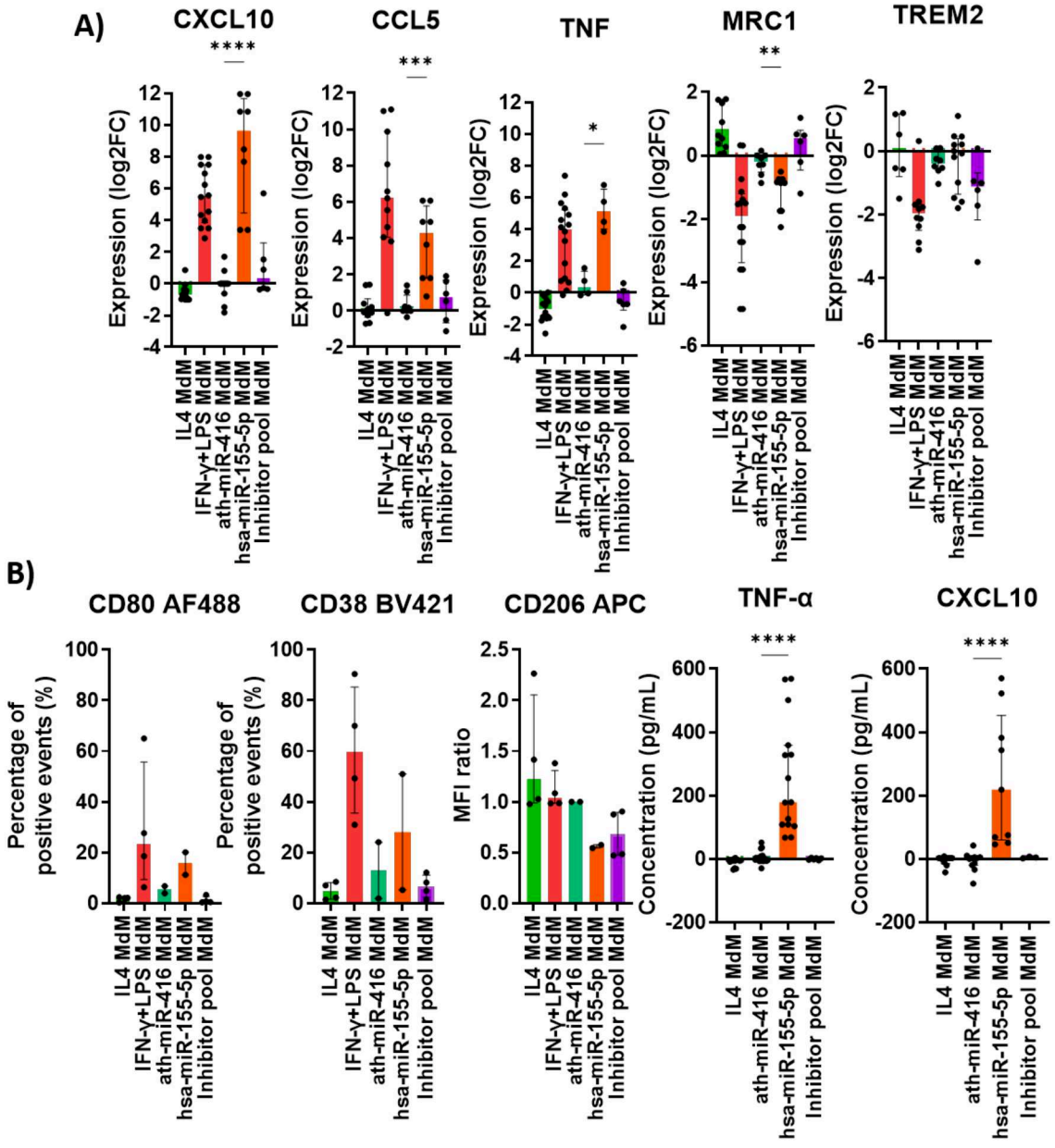

Figure 2.3.1. Differential gene and protein expression in human MdMs after transfection with miR-155-5p and treatment with inhibitor pool.

MdMs were cultured for 48h for gene expression analysis through qRT-PCR, where the housekeeping gene was RPL19 (A) and 72h for protein expression analysis through FACS and ELISA (B)

A) This panel displays bar graphs representing the gene expression changes of M2-like (*MRC1* and *TREM2*) and M1-like (*CXCL10*, *CCL5*, and *TNF*) markers in human MdM, as determined by qRT-PCR. The data is presented as $\log_2$ fold change ($\log_2$FC).

B) FACS bar graphs show % and MFI ratio of expression of markers M2-like (CD206) and M1-like (CD80 and CD38) markers in the Live macrophage population (LIVE/DEAD Fixable Yellow Dead Cell dye(-)CD11b(+)CD14(+)).

The last two graphs show concentration in pg/ml of M1-like (TNF-α and CXCL10), as analysed by ELISA. The Data is shown as a median with an interquartile range. Statistical significance was evaluated using the Mann-Whitney test. Sample sizes ranged from n=2 to n=14. Significance levels are indicated as * for $p<0.05$, ** for $p<0.01$, *** for $p<0.001$, and **** for $p<0.0001$; FACS: Fluorescence-activated cell sorting; ELISA: Enzyme-linked immunosorbent assay.

emphasises the complexity of the repolarisation process and the importance of developing targeted strategies for human macrophage modulation.

2.3.1 Gene expression changes after repolarisation

I utilised microarray analysis to understand the pathways involved in human macrophage repolarisation, focusing on the effects of miR-155-5p and the inhibitor pool consisting of Niclosamide, Etinostat, AS1517499, and 10074-G5. Forty-eight hours after treating MdMs with these repolarisation candidates, biological replicates were harvested for microarray analysis. The criteria for identifying DEGs were set at a p-value of 0.05 and a $\log_2$ fold change ($\log_2$FC) of 1 or -1, facilitating the identification of specific genes significantly up-regulated or down-regulated in MdMs treated with repolarisation candidates compared to the control.

Upon repolarisation of MdMs with IFN-γ+LPS, 175 DEGs were up-regulated compared to IL4-treated controls. In contrast, miR-155-5p transfection resulted in a notable increase in the number of up-regulated genes, totalling 562 DEGs compared to control miRNA (ath-miR-416). Among these, 49 DEGs overlapped with those up-regulated by IFN-γ+LPS treatment, indicating a common pathway of activation shared between the two treatments (Figure 2.3.2A). However, the inhibitor pool treatment up-regulated 57 DEGs, with only one overlap with IFN-γ+LPS-induced genes, suggesting a distinct set of genetic pathways (Figure 2.3.2A).

IFN-γ+LPS treatment led to 73 down-regulated DEGs, while miR-155-5p transfection resulted in 670 down-regulated genes, with only 7 DEGs common with IFN-γ+LPS treatment. The inhibitor pool treatment down-regulated 127 genes, with 6 intersecting with IFN-γ+LPS treatment (Figure 2.3.2A).

The analysis of enriched GO:BP pathways revealed 250 pathways enriched in IFN-γ+LPS-treated human MdMs, while miR-155-5p transfection enriched 425 pathways, with 182 pathways intersecting with those enriched by IFN-γ+LPS treatment (Figure 2.3.2B). These pathways predominantly involved immune response processes (Figure 2.3.2C).

The inhibitor pool-treated human MdMs did not exhibit a significant repolarisation profile, contrasting with results observed in murine macrophages. This outcome led to the conclusion that the inhibitor pool's effectiveness was limited to murine macrophages, and its use was discontinued for human macrophages in further studies.

2.3.2 Cross-species expression changes in repolarised macrophages

I then compared the human MdM microarray data with the murine BMDMs microarray data to check for common DEGs and GO:BPs between human and murine M1-like macrophages. Of the 175 up-regulated DEGs in human M1-like macrophages, 41 were common with murine M1 BMDMs, which had 1307 up-regulated DEGs. The comparative analysis of enriched GO:BP pathways in human and murine M1-like macrophages revealed 250 and 1035 enriched path-

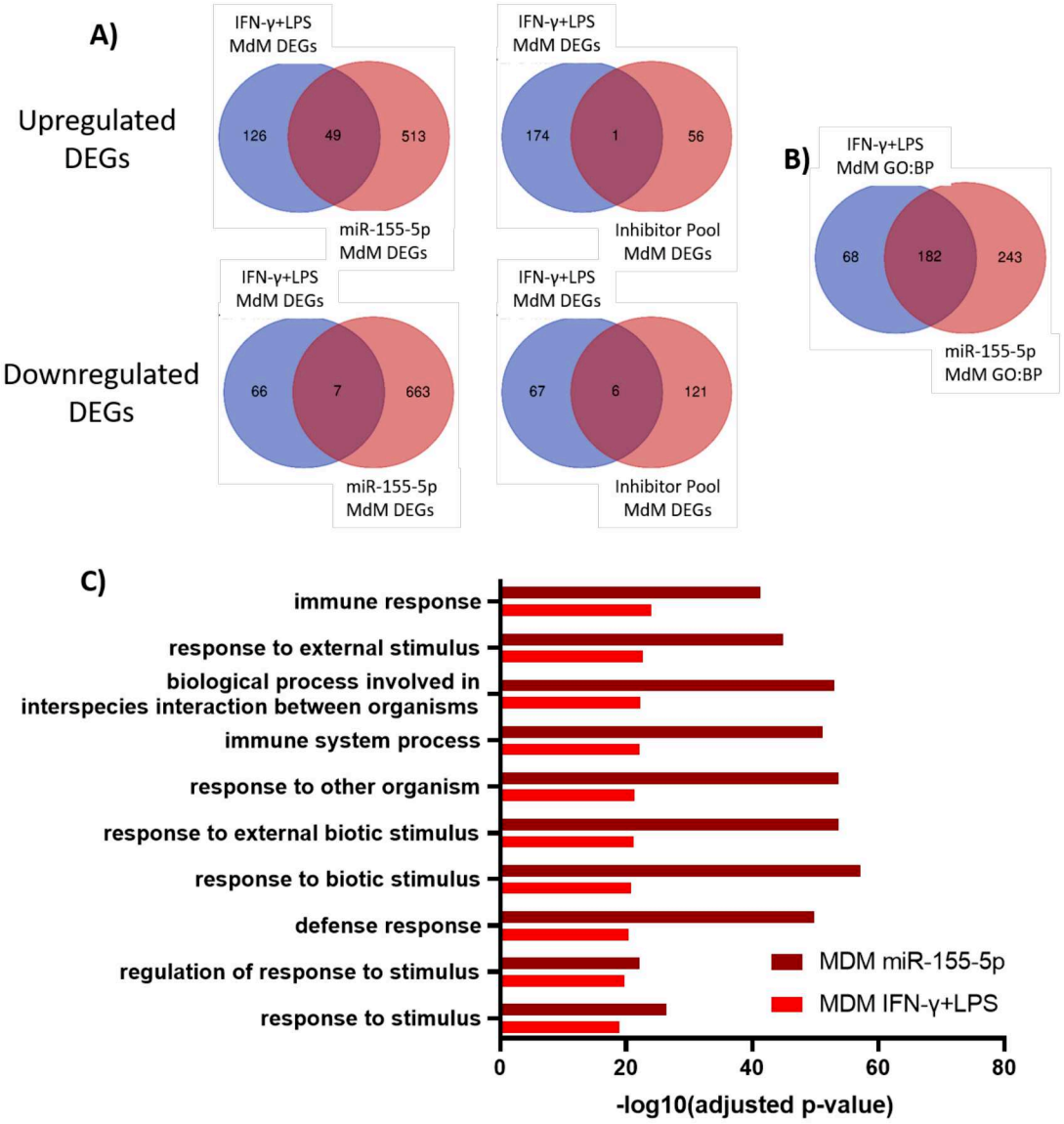

Figure 2.3.2. Gene expression and pathway analysis in human macrophage repolarisation.
A) The first two Venn diagrams display the overlap of up-regulated differentially-expressed genes (DEGs) among IFN-γ+LPS-treated MdMs and miR-155-5p-treated MdMs (left), and MdMs treated with the inhibitor pool (right), while the Venn diagrams below show the down-regulated DEGs in these treatments.
B) The Venn diagram illustrates the intersections of Gene Ontology Biological Process (GO:BP) pathways enriched in the miR-155-5p-treated MdMs compared to IFN-γ+LPS-treated MdMs.
C) The bar graph details the -log10 of the adjusted p-values for the top ten most significant GO:BP pathways across IFN-γ+LPS-treated MdMs and miR-155-5p-treated MdMs.

ways, respectively, with 232 intersecting between the two species (Figure 2.3.3A). Among the 41 common up-regulated DEGs, SOD2 superoxide dismutase 2 (Sod2) stood out for being uniquely up-regulated in both human and murine macrophages successfully repolarised with miR-155-5p and the inhibitor pool. Additionally, in both human and murine models, miR-155-5p led to the up-regulation of Phosphodiesterase 4B (PDE4B). The most effectively repolarised macrophages, miR-155-5p-treated human and inhibitor pool-treated murine macrophages, demonstrated a

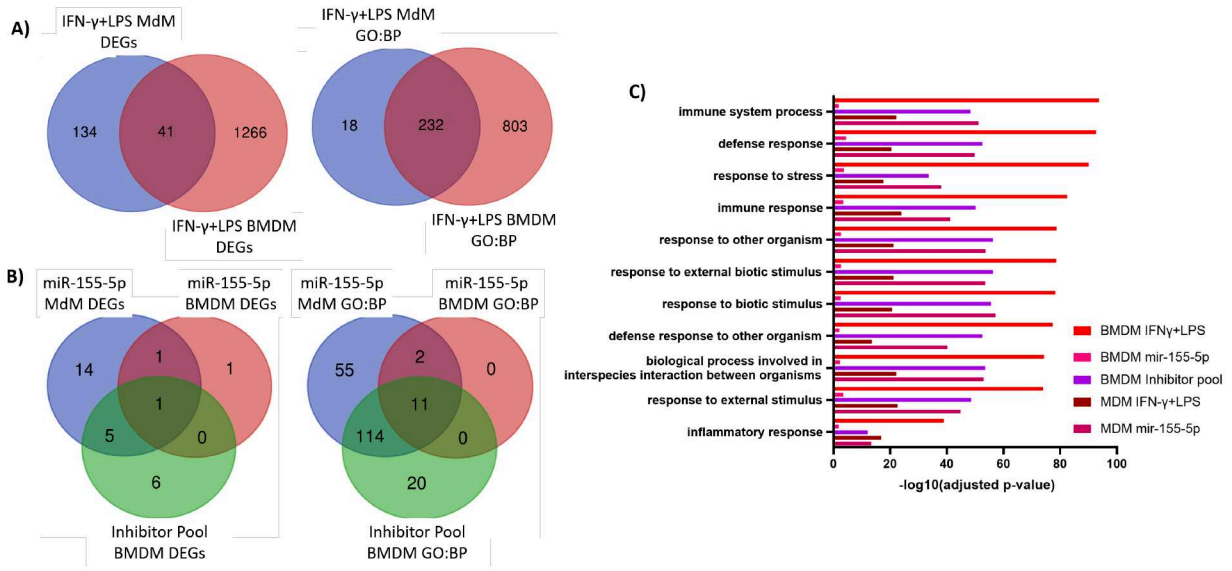

Figure 2.3.3. Gene expression and pathway analysis in human and murine macrophages.
A) The left Venn diagram displays the overlap of up-regulated differentially-expressed genes (DEGs) among IFN-γ+LPS-treated MdMs and BMDMs. The right Venn diagram illustrates the intersections of Gene Ontology Biological Process (GO:BP) pathways enriched in the IFN-γ+LPS-treated MdMs compared to BMDMs. B) The left Venn diagram displays the overlap of up-regulated DEGs, that were common between IFN-γ+LPS repolarised MdMs and BMDMs, in BMDMs repolarised with miR-155-5p, BMDMs repolarised with inhibitor pool and MdMs repolarised with miR-155-5p. The right Venn diagram illustrates the intersections of GO:BP pathways, which were commonly enriched in IFN-γ+LPS-treated MdMs and BMDMs, in BMDMs repolarised with miR-155-5p , BMDMs repolarised with inhibitor pool, and MdMs repolarised with miR-155-5p. C) The bar graph details the -log10 of the adjusted p-values for the eleven significant GO:BP pathways across IFN-γ+LPS-treated MdM, IFN-γ+LPS-treated BMDMs, miR-155-5p-treated MdM, miR-155-5p-treated BMDMs and inhibitor pool-treated BMDMs.

shared up-regulation in 5 genes: TNF receptor-associated factor 1 (TRAF1), Indoleamine 2,3-dioxygenase 1 (IDO1), Complement Factor B (CFB), Solute carrier family 2, facilitated glucose transporter member 6 (SLC2A6), and CD274 (Figure 2.3.3B).

From the 232 pathways commonly enriched in both human and murine M1-like macrophages, 11 were found to be enriched in human and murine macrophages repolarised with miR-155-5p and in murine macrophages treated with the inhibitor pool, underlining their involvement in immune response pathways (Figure 2.3.3B and C). Additionally, there were 114 common enriched pathways in murine macrophages that were effectively repolarised with the inhibitor pool and in human macrophages that were repolarised with miR-155-5p (Figure 2.3.3B).

The study's findings illustrate the complexity of macrophage repolarisation, highlighting the differences and similarities in the gene expression profiles and enriched pathways between human and murine macrophages and across different repolarisation treatments. This comprehensive understanding is crucial for developing targeted therapies for diseases involving macrophage-mediated immune responses. Particularly noteworthy is the strong repolarisation

effect observed with miR-155-5p in human macrophages, highlighting its potential as a key agent in therapeutic strategies mediated by macrophages.

2.3.3 Effect of MdMs on tumour cell lines and activation of CAR-T cells

To assess the functionality of repolarised human MdMs, experiments were conducted by culturing two different tumour cell lines, MDA-MB231-RFP and MaMel002-RFP, with human MdMs. The tumour cell lines expressed Red Fluorescent Protein (RFP), enabling quantification of tumour cells through the Orange channel in the Incucyte system. The objective was to observe any changes in tumour cell growth induced by the repolarised macrophages. Interestingly, neither IFN-γ+LPS nor miR-155-5p repolarised human MdMs resulted in a significant change in the growth of these tumour cell lines. Stable Orange Object Count (RFP+) was observed at multiple points in time using the Incucyte system (Figure 2.3.4A).

In a separate set of experiments, the impact of repolarised macrophages on T-cell activation, particularly focusing on activation of CAR-T cells activation, was assessed. For this, the Carcinoembryonic antigen (CEA)-expressing tumour cell line HT-29 was co-cultured with Jurkat cells modified to express an anti-CEA CAR and Venus Fluorescent Protein, which activates upon stimulation by the CAR construct. The activation of these Jurkat cells was monitored via the Incucyte green channel.

When HT-29 was co-cultured with IFN-γ+LPS-repolarised human MdMs, there was a noticeable increase in the green object count and integrated intensity, indicating enhanced T-cell activation. Specifically, at 96 hours, the green object count for IL4 MdMs was 2348.833, compared to 2740.792 for IFN-γ+LPS MdMs ($p<0.0001$). Similarly, the total green object integrated intensity was higher for IFN-γ+LPS MdMs (5267682, $p<0.0001$) compared to IL4 MdMs (4293554), suggesting a more robust activation of CAR T-cells in the presence of IFN-γ+LPS-repolarised MdMs (Figure 2.3.4B). However, this enhancement in T-cell activation was not observed in miR-155-5p repolarised macrophages (Figure 2.3.4C).

The results from these experiments indicate that human MdMs do not impact tumour cell growth in the same manner as murine macrophages. Furthermore, while IFN-γ+LPS repolarisation of human MdMs seems to enhance CAR T-cell activation, repolarisation with miR-155-5p did not result in noticeable functional changes. This highlights a distinct difference in the functionality of human macrophages compared to their murine counterparts and underlines the need for further investigation into the specific roles and mechanisms of repolarised human macrophages in cancer and immunotherapy contexts.

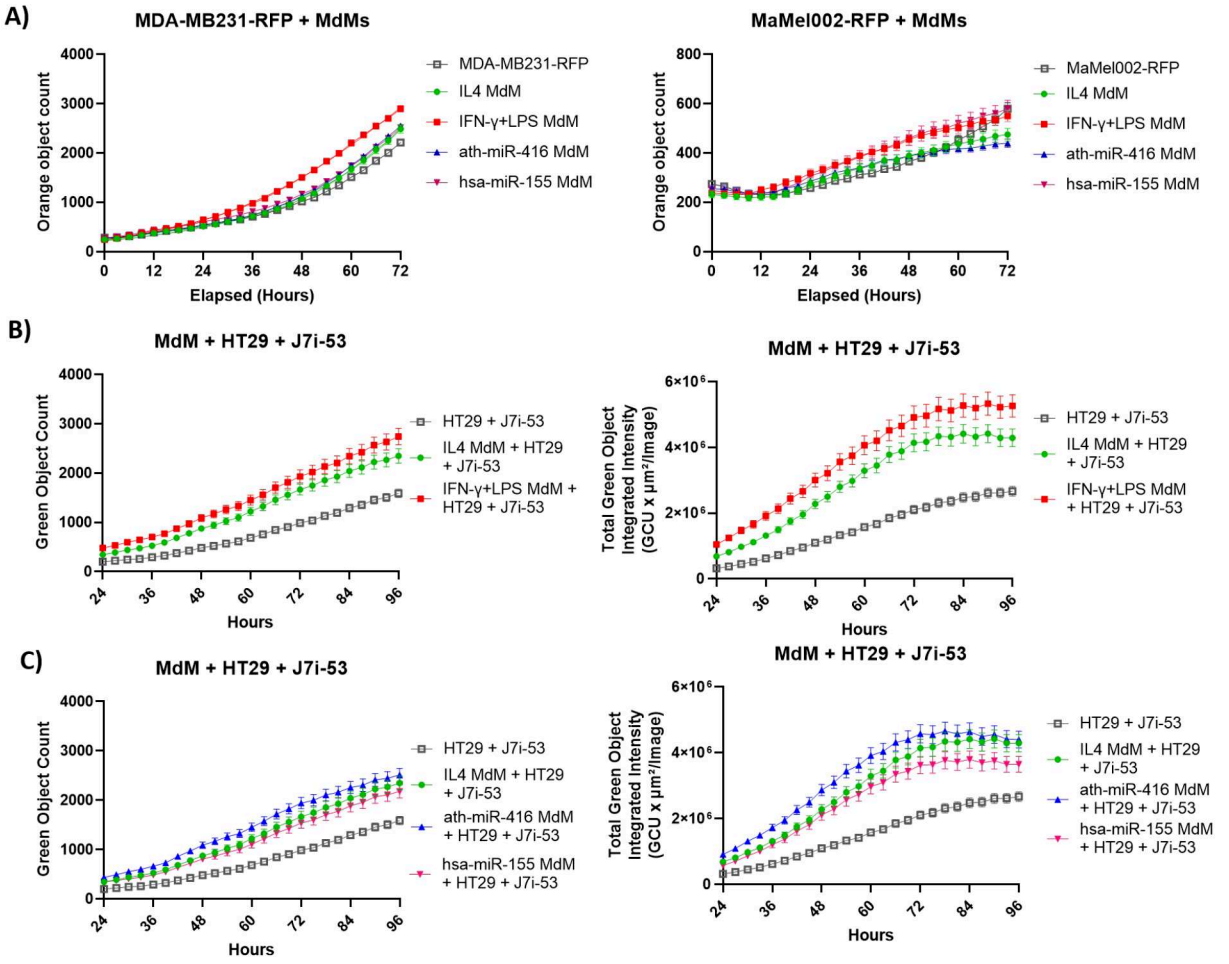

Figure 2.3.4. Effect of human macrophages on the proliferation of tumour cell lines and activation of CAR-T cells.

A) MDA-MB231-RFP and MaMel002-RFP were cultured with human MdMs for 72 h, and cell growth is shown by the Orange object count. B) HT-29 and modified Jurkat cells (J7i-53) were cultured with human MdMs for 96h. Jurkat activation is seen by green object count (B) and intensity (C). A non-linear regression model was applied to the growth curve to determine the kinetic parameters of cell growth. The goodness-of-fit for the non-linear model was assessed using an extra sum of squares F test.

Chapter 3

Discussion

The primary objective of this study was to explore the repolarisation potential of both murine and human macrophages, with a special emphasis on identifying and testing functional molecules that could induce shifts toward an M1-like activation state. The research delved deeply into the molecular mechanisms of macrophage activation, a crucial aspect in the realm of immunology and therapeutic interventions.

The study presented several key findings that contribute significantly to our understanding of macrophage polarisation and repolarisation, with potential implications for therapeutic interventions:

1. **Cross-Species Comparisons**: The study revealed shared pathways in gene expression across human and murine macrophages, indicating conserved mechanisms of activation, which is vital for the translational relevance of the research. I identified PPARG and MYC as key transcription factors that sustain M2 polarisation consistently across mouse and human macrophages.

2. **Identification of Repolarising Functional Molecules**: The study identified specific miRNAs and small molecule inhibitors with the potential to redirect macrophage polarisation towards an M1-like state. Notably, miR-155-5p stood out as a particularly potent miRNA in steering macrophages towards this phenotype. Furthermore, an optimal combination of small molecule inhibitors was identified to target transcription factors associated with M2-like polarisation effectively. This combination includes Niclosamide for Stat3, AS1517499 for Stat6, 10074-G5 for Myc, and Entinostat for Hdacs, proving to be the most effective regimen in promoting an M1 phenotype in murine BMDM.

3. **Functional Outcomes**: The study also assessed the functional outcomes of repolarisation, particularly focusing on anti-tumour activity and T-cell activation. In murine and human macrophages, IFNγ+LPS repolarisation enhanced these functional aspects. However, despite molecular changes observed with miR-155-5p and the inhibitor pool, these did not

translate into the expected functional outcomes in the assays used. This finding emphasises the importance of evaluating not just molecular changes but also the functional implications of repolarisation strategies to ensure their effectiveness in therapeutic applications.

3.1 Identification of functional molecules for repolarisation

Central to the study was establishing baseline conditions for macrophage activation using IL4 and IFN-γ with LPS to induce M2-like and M1-like states, respectively. This foundational step was pivotal in understanding the molecular underpinnings of macrophage polarisation and provided insights into the genetic shifts accompanying the transition to a pro-inflammatory state. The research utilised both murine BMDMs and human MdMs as models. This approach allowed for a comprehensive investigation of cross-species similarities and differences, thereby enhancing the study's applicability to human health.

Through RNA sequencing, the study identified common transcription factors in murine and human M2-like macrophages. This approach pinpointed targets for potential repolarisation strategies, highlighting transcription factors such as PPARG and MYC, which were upregulated in both human and murine M2-like macrophages. Further analysis, supplemented by extensive literature research, identified additional targets like STAT6, TRIM24, STAT3, and HDACs.

The literature review conducted as part of the study revealed a complex interplay between these factors in macrophage polarisation. Notably, a crosstalk between Stat6 and Trim24 was described (Yu et al., 2019), where the loss of Trim24 inhibits Stat6 acetylation, thus promoting M2 polarisation in both murine and human macrophages. Consequently, Trim24 was deemed unsuitable for downregulation. Further elucidating the role of Stat6, another study revealed its function as an upregulator of PPARγ in macrophages, particularly under the influence of IL4 signalling (Liu et al., 2021; Szanto et al., 2010). This suggests that Stat6 and PPARγ may work synergistically to promote M2-like polarisation; therefore, we focused on Stat6 inhibition, as it is upstream of Pparg. Other studies further highlighted the roles of Stat6, Myc, and Stat3 in macrophage polarisation, with Stat3 acting as a negative regulator of Stat1 and promoting an anti-inflammatory phenotype (Kerneur et al., 2022). Additionally, inhibiting Hdacs was shown to induce a shift toward an M1-like phenotype (Hu et al., 2021).

Given these insights, key transcription regulators for downregulation through SMIs were identified as Stat6, Myc, Stat3, and genes from the Hdac family.

3.2 Small molecule inhibitors

My research focused on evaluating the effects of various inhibitors on macrophage polarisation, specifically examining their influence on Stat3, Stat6, Myc, and Hdac family members, which are crucial for driving macrophages toward an M1-like inflammatory phenotype. Initial treatments

involved 10074-G5 to inhibit Myc, AS1517499 for Stat6, Stattic for Stat3, and Mocetinostat for Hdac family members. Of these, Mocetinostat stood out for its ability to significantly reduce *Mrc1* expression, highlighting its potential to induce an M1-like repolarisation. When these inhibitors were used in combination, they not only further reduced *Mrc1* expression but also elevated levels of inflammatory markers *Cxcl10* and *Il1b*, suggesting a more pronounced repolarisation effect, albeit with notable cytotoxicity.

To mitigate this cytotoxicity, the study sought alternative inhibitors with less harmful effects, identifying Niclosamide and FLLL32 as viable Stat3 inhibitors and Entinostat and RGFP966 for targeted Hdac inhibition. The efficacy and specificity of these inhibitors were thoroughly documented, prompting their selection for further testing in various combinations alongside Myc and Stat6 inhibitors. These tests aimed to optimise macrophage polarisation while preserving cell viability.

The most effective combination of inhibitors for macrophage repolarisation was determined to be Niclosamide (for Stat3 inhibition), AS1517499 (for Stat6), 10074-G5 (for Myc), and Entinostat (for Hdac). This regimen effectively diminished *Mrc1* levels while increasing *Cxcl10* and *Il1b*, indicating a shift towards the M1 phenotype with minimal cytotoxicity. These findings underscore the intricate interplay of signalling pathways in macrophage polarisation and illustrate the therapeutic potential of a multifaceted inhibition strategy to modulate macrophage function effectively.

3.2.1 Myc

We observed a significant upregulation of the transcription factor *Myc* in both mouse and human macrophages following treatment with IL4, a finding that is consistent with previous research indicating that IL4 and other M2-like stimuli can induce Myc expression (Jablonski et al., 2015; Pello et al., 2012b). This underscores the pivotal role of Myc in macrophage polarisation towards an M2-like phenotype, a process critical for understanding immune response modulation and the pathogenesis of various diseases.

Our findings are further supported by the detailed mechanisms uncovered in previous studies. Specifically, the transcription factor c-MYC has been identified as essential for the alternative polarisation of macrophages, with its expression and nuclear translocation being induced by IL4 and other M2-polarising stimuli. c-MYC is instrumental in regulating a significant fraction (45%) of the genes associated with alternative macrophage activation, as revealed by ChIP assays (Pello et al., 2012b). These include direct regulation of genes such as Scavenger receptor class B member 1 (SCARB1), arachidonate 15-lipoxygenase (ALOX15), and MRC1 and indirect regulation of others like CD209. Moreover, c-MYC is crucial in enhancing the expression of IL4 signalling mediators such as the Stat6 and the Pparg. This role extends to TAMs, where c-MYC's inhibition affects the expression of pro-tumoural genes, including VEGF, MMP9, HIF-1α, and TGF-β, high-

lighting its potential as a therapeutic target in macrophage-related diseases and tumourigenesis (Pello et al., 2012b).

In our study, we employed 10074-G5 to disrupt Myc functionality by obstructing the dimerisation between c-Myc and Max (Clausen et al., 2010) in BMDM. However, this intervention did not reverse the M2-like polarisation in the macrophages, indicating that Myc's role in polarisation is complex and may involve additional pathways or factors beyond the inhibition of its dimerisation.

Supporting this notion, research utilising the compound 10058-F4, another Myc inhibitor that also inhibits the c-Myc-Max interaction, has demonstrated its capability to inhibit the IL4–dependent induction of genes associated with the M2 macrophage phenotype, such as SCARB1, ALOX15, MRC1, and several others (Pello et al., 2012b). This indicates that Myc plays a significant role in regulating the expression of genes crucial for the M2-like activation of macrophages.

Additionally, experiments involving the transfection of BMDMs with siRNAs targeting c-Myc underscored the importance of Myc in macrophage polarisation. The efficient knockdown of c-Myc expression led to a significant decrease in the expression of M2-associated markers, such as Mrc1, arginase 1 (Arg1), and Chil3, upon IL4 stimulation (Yang et al., 2018).

The generation of c-Myc$^{fl/fl}$ LysM$^{cre/+}$ mice, which lack c-Myc expression in macrophages, provided further insight into the role of Myc in the macrophage-mediated immune response, especially in the context of cancer (Pello et al., 2012a). In a melanoma model, TAMs devoid of c-Myc exhibited delayed maturation, reduced expression of pro-tumoural factors such as VEGF, MMP9, and HIF1a, and consequently, impaired tumour growth. This highlights Myc's critical function as a regulator of TAMs' pro-tumoural activities and underscores its potential as a target for cancer therapy.

3.2.2 Stat6

In my research, I employed AS1517499 to inhibit Stat6 function, leveraging its capability to effectively inhibit Stat6 phosphorylation (Nagashima et al., 2007). Despite its potential, this approach did not yield any repolarisation effect in BMDM when used alone. Recent research highlights the outcomes of Stat6 inhibition on macrophage behavior across various models.

STAT6 inhibition using AS1517499 has been shown to disrupt the anti-inflammatory process typically promoted by STAT6, which involves the development of M2 macrophages. The study found that administration of AS1517499 following zymosan injection, a TLR ligand, suppressed STAT6 phosphorylation in peritoneal macrophages, which delayed the resolution of acute inflammation (Lee et al., 2022). This was evidenced by an increased secretion of pro-inflammatory cytokines, reduced secretion of anti-inflammatory cytokines, and exacerbated neutrophil infiltration. The use of AS1517499 demonstrated that inhibiting STAT6 delayed the recovery of PPARγ expression and activity, suggesting that STAT6 activation is crucial for resolving acute inflammation through mediating PPARγ expression and activity in macrophages.

In two distinct syngeneic mouse models of breast cancer brain metastasis, the employment of the STAT6 inhibitor AS1517499 was linked to a notable reduction in Arg1 expression among microglial cells, alongside significant diminution of brain tumour load (Economopoulos et al., 2022). These outcomes support the hypothesis that promoting a shift of macrophages and microglia toward pro-inflammatory phenotypes could represent a viable approach for treating brain metastases

Further research by Binnemars-Postma et al., 2018 targeted the Stat6 pathway in TAMs to counter their protumourigenic activities. Using AS1517499 and siRNA to inhibit Stat6 *in vitro* prevented RAW264.7 macrophages from differentiating into the M2 phenotype, indicated by decreased Arg1 and Mrc1 expression. *In vivo*, AS1517499 significantly reduced tumour growth and early liver metastasis in a 4T1 mammary carcinoma mouse model. Treatment with AS1517499 also led to a reduction in markers associated with M2 macrophages (Arg1 and Mrc1) and the metastatic niche in the liver. Another study focused on targeting M2 macrophages in the acidic TME with a micellar nanodrug. This nanodrug co-delivered siRNA targeting IKKβ, pivotal for NF-κB activation and AS1517499 (Xiao et al., 2020). The treatment effectively prompted M2-to-M1 repolarisation, diminishing tumour growth and metastasis. The nanodrug treatment notably reduced M2-like TAMs and increased M1-like TAMs. iNOS was upregulated, while Arg1, a M2-like marker, was downregulated, highlighting the therapeutic promise of modulating STAT6 activity in cancer.

Together, these studies elucidate the dual role of STAT6 in both promoting anti-inflammatory processes and its potential as a target for therapeutic intervention in cancer immunotherapy.

3.2.3 Stat3

In our study, we utilised Stattic at a 5 μM concentration for its effective inhibition of STAT3 phosphorylation, demonstrating selectivity by minimally impacting STAT1 and other signalling molecules (Schust et al., 2006). Stattic alone was not able to repolarise M2-like BMDM towards an M1-like phenotype. Due to concerns over Stattic's cytotoxicity, we explored alternative STAT3 inhibitors, including Niclosamide and FLLL32. Niclosamide was employed at 500 nM, targeting STAT3 phosphorylation with high specificity and minimal effects on STAT1 and STAT5 (Ren et al., 2010). FLLL32 was used at 1 μM, further diversifying our approach to targeting STAT3 phosphorylation (Bill et al., 2010).

The role of STAT3 in macrophage biology and its implications for cancer therapy have been highlighted in recent studies. provide For instance, STAT3 knockout in LPS-stimulated RAW264.7 macrophages leads to an increase in the expression of pro-inflammatory genes iNOS and Cyclooxygenase 2 (COX2), alongside early surges in cytokines like TNF-α, IL1β, IL6, and IFN-β (Ahuja et al., 2020). This evidence underscores the critical role of STAT3 in regulating the immune response of macrophages.

Further research by Solís-Martínez et al., 2018 reinforced the importance of STAT3 in the immunophenotypic modulation of macrophages in the context of cancer. Their findings revealed that the application of Stattic, a specific STAT3 inhibitor, to macrophages treated with the supernatant from PC3 prostate cancer cells led to the restoration of M1 profile cytokines, TNF-α, and IFN-γ. These cytokines had been diminished in macrophages exposed to the cancer cell-line supernatant, indicating a tumour-induced suppression of the M1 phenotype. Importantly, the inhibition of STAT3 phosphorylation through Stattic not only reversed this suppression but also suggested a mechanism for recovering the anti-tumour activity of macrophages.

Zhang et al., 2009 found that Stat3 inhibition in microglia and macrophages activated these cells and inhibited tumour growth in a murine glioma model. The significance of this effect lies in Stat3's capacity to suppress the anti-neoplastic functions of microglia. By inhibiting Stat3 *in vivo* within the glioma microenvironment, there was a notable reduction in the expression of immunosuppressive cytokines such as IL6 and IL10 while simultaneously enhancing the production of the pro-inflammatory cytokine TNF-α, which significantly curtailed tumour growth and extended survival rates in mice afflicted with gliomas.

Similarly, Shobaki et al., 2020 targeted TAMs in a human tumour xenograft model using siRNA-loaded lipid nanoparticles (LNPs) to silence STAT3 and HIF-1α. This strategy effectively reversed TAMs' pro-tumourous functions, notably angiogenesis and tumour cell activation, by decreasing angiogenesis markers and TGF-β expression. Moreover, it significantly increased macrophage infiltration into the TME and promoted a shift toward the M1 phenotype, increasing the expression of TNF-α.

These studies underscore the therapeutic potential of STAT3 inhibition in modulating immune cell function and the tumour microenvironment, offering insights into innovative cancer treatment strategies.

3.2.4 Hdac family

Our study employed various HDAC inhibitors to explore their effects on macrophage polarisation. Mocetinostat, applied at 2 μM, was chosen for its specificity against HDAC classes I and IV, effectively inhibiting HDAC1-3 and HDAC11 without affecting class II HDACs (Fournel et al., 2008). This inhibition led to a down-regulation of Mrc1 expression, indicating a potential shift in macrophage phenotype. Entinostat, used at 1 μM, preferentially targets HDAC1 but also affects HDACs 2 and 3, based on its efficacy in selectively inhibiting these HDACs without significant impact on other family members (Lauffer et al., 2013; Rosato et al., 2003). RGFP966, administered at 100 nM, offers targeted inhibition of HDAC3 with minimal effects on other class I HDACs (Malvaez et al., 2013).

Class I and II HDACs play crucial roles in regulating immunity and inflammation, impacting inflammatory responses through modulation of HDAC expression and activity. However, the specific effects of individual HDACs remain a subject of debate within the scientific com-

munity, as they appear to have divergent functions on inflammatory genes, leading to both pro-inflammatory and anti-inflammatory outcomes.

The study by Mullican et al., 2011 highlights the unique role of HDAC3 in macrophage polarisation. Macrophages deficient in HDAC3 exhibited a polarisation state akin to the alternative activation induced by IL4, indicating that HDAC3 might act as a regulatory brake on this process. Furthermore, these HDAC3-lacking macrophages showed increased responsiveness to IL4 stimulation, emphasising the epigenomic modifications, including histone acetylation, that influence transcriptional programs leading to alternative macrophage activation (Leus et al., 2016). This supports my findings on the HDAC3 inhibitor RGFP966, which did not demonstrate a repolarisation effect in BMDM.

Conversely, Entinostat, another HDAC inhibitor identified through high-throughput phenotypic screening, was found to activate primary human macrophages toward an M1-like state (Hu et al., 2021), highlighting the varied effects of different HDAC inhibitors on macrophage polarisation. In the context of cancer therapy, the work of Sidiropoulos et al., 2022 further delineates the potential of HDAC inhibitors, such as Entinostat, in reprogramming the TME from a pro-tumour to an anti-tumour signature. This is notably achieved through the epigenetic reprogramming of tumour-associated macrophages from an M2-like phenotype to M1-like phenotype, thereby enhancing antitumour responses and increasing the efficacy of immune checkpoint inhibitors.

Our study's observations, where small molecule inhibitors did not individually repolarise BMDM but did so effectively when combined, underscore the complex interplay of pathways involved in macrophage polarisation. This suggests that a multi-targeted approach, affecting various interconnected pathways, might be necessary to achieve significant repolarisation. This complexity necessitates a broader understanding of the molecular mechanisms at play, where the use of combinations of small molecule inhibitors could offer a more effective strategy for manipulating macrophage phenotypes, especially in therapeutic settings aimed at modulating the immune response within the TME.

3.3 Macrophage polarisation with miRNA

Simultaneously to the search for SMI that could repolarise macrophages by inhibiting transcription regulators of the M2-like phenotype, miRNA sequencing played a vital role in identifying miRNAs upregulated in M1-like macrophages, such as miR-155-5p, miR-9-5p, and miR-147b, known from literature as a negative inflammation regulator (Liu et al., 2009). An *in silico* approach further expanded the pool of potential repolarisation agents, uncovering miRNAs like mmu-miR-709, mmu-miR-694, mmu-miR-144-3p, mmu-miR-125a-5p, and mmu-miR-125b-5p. These were chosen for their predicted ability to target the transcription regulators identified earlier.

These chosen miRNA were candidates for transfection into M2-like macrophages towards a pro inflammatory phenotype.

The study's comprehensive approach, combining baseline establishment, cross-species analysis, and advanced sequencing techniques, facilitated a deeper understanding of macrophage biology. This not only provided insights into potential therapeutic applications for manipulating macrophage states but also underscored the complexities and nuances inherent in macrophage polarisation across different species.

3.3.1 miR-155-5p

In this study, we observed that miR-155-5p was highly expressed in both murine and human macrophages activated with IFN-ɣ+LPS. When transfected into IL4-treated murine BMDMs and human MdMs, miR-155-5p significantly influenced the expression of several genes and proteins associated with the M1-like phenotype. This included the downregulation of MRC1 and the upregulation of CXCL10, TNF-α, Il1b in BMDM, and CCL5 in MdM. At the protein level, there was an increase in CD38 in both murine and human macrophages, a moderate rise in IAb expression in murine BMDM, and an increase in CD80 in human MdM. Additionally, TNF-α secretion was observed in human and murine macrophages, along with the secretion of CXCL10 in human MdMs.

These observations align with previous research in the field. Studies have shown that miR-155 is notably increased in murine and human macrophages when stimulated with inflammatory mediators such as type I interferons (IFNs) and multiple TLR ligands (Cai et al., 2012; Graff et al., 2012; Jablonski et al., 2016; Lu et al., 2016; O'Connell et al., 2007; Zhang et al., 2013). The activation of NF-κB by inflammatory stimuli has been noted to drive miR-155 transcription (Bala et al., 2011; Mann et al., 2017).

miR-155-5p is recognised as a proinflammatory miRNA, enhancing proinflammatory cytokine production in various immune cells, such as macrophages, DCs, T cells and B cells (Tili et al., 2009). It plays a key role in classical macrophage activation by downregulating inhibitors of the proinflammatory response, such as suppressor of cytokine signaling-1 (SOCS1) (Androulidaki et al., 2009), SH-2 containing inositol 5' polyphosphatase 1 (SHIP1) (Mann et al., 2017) and B-cell lymphoma 6 (BCL6) (Nazari-Jahantigh et al., 2012). It also stabilises the TNF-α transcript (Bala et al., 2011), thereby boosting the production of proinflammatory cytokines.

Transfection experiments with miRNA mimics have confirmed miR-155's biological relevance in macrophage polarisation and mirrored our studies' findings. For instance, Graff et al., 2012 showed that miR-155 transfection in human macrophages induced expression of inflammatory gene and protein expression. Similarly, in murine macrophages, Cai et al., 2012 and Jablonski et al., 2016 demonstrated that miR-155-5p induced M1-like phenotype signature while downregulating the M2-like signature.

Notably, miR-155 deficiency resulted in a significant loss of the M1 signature in the mir-155 knockout model (Jablonski et al., 2016) and anti-mir-155 antisense oligonucleotide downregulation (Cai et al., 2012), further underscoring its critical role in macrophage polarisation.

Our study, therefore, corroborated with the literature in this aspect, showing the power of miR-155-5p in orchestrating the pro-inflammatory phenotype in both murine and human macrophages. Our results showed a discrepancy between qRT-PCR and protein expression data in murine BMDM transfected with miR-155-5p, which could be due to various reasons. This variance might be attributed to several factors, including the complexities of post-transcriptional regulation, differences in protein stability and degradation, as well as the varying sensitivities of the qRT-PCR and protein detection methods. Additionally, the temporal gap between peak gene transcription and protein synthesis, along with experimental variability, may contribute to the observed discrepancies between gene and protein expression data.

3.3.2 miR-9-5p

miR-9 is a highly conserved miRNA (Yuva-Aydemir et al., 2011) and is related to the oncogenesis of various tumours (Khafaei et al., 2019). My study found that miR-9-5p was upregulated in murine and human macrophages in response to IFNg+LPS. This finding aligns with previous literature indicating its elevated levels in M1-like macrophages (Bazzoni et al., 2009; Cai et al., 2012; Lu et al., 2016; Wang et al., 2021; Yao et al., 2014).

Various studies have demonstrated that miR-9-5p functions in a pro-inflammatory manner in macrophages: In primary mouse microglia, miR-9 was found to be induced by LPS and identified as a key regulator of the activation process through its suppression of the anti-inflammatory gene monocyte chemotactic protein-induced protein-1 (MCPIP1). Inhibition of miR-9 led to a marked decrease in the inflammatory response induced by LPS. This effect is further linked to the NF-κB signalling pathway, with pharmacological inhibitors of NF-κB significantly reducing miR-9's effect on microglial activation (Yao et al., 2014).

In the context of human head and neck squamous cell carcinoma (HNSCC), miR-9 was found to be enriched in exosomes (Tong et al., 2020). These miR-9-rich exosomes contribute to the induction of M1 macrophage polarisation, subsequently enhancing the radiosensitivity of HNSCC. This process is facilitated by the downregulation of PPARδ, a nuclear receptor involved in inflammation and innate immunity. The inhibition of PPARδ leads to an increase in iNOS expression in M1 macrophages, amplifying nitric oxide levels and thus the radiosensitivity of tumour cells.

Furthermore, high expression levels of miR-9-5p were reported in an osteoarthritis (OA) mouse model (Wang et al., 2021). The knockdown of miR-9-5p was shown to alleviate the symptoms of OA, suggesting its role in promoting the pro-inflammatory M1 macrophage phenotype and suppressing the M2 phenotype, thereby exacerbating OA's inflammatory processes. The study also identified Sirtuin1 (SIRT1) as a target of miR-9-5p, suggesting that its binding and

subsequent degradation of SIRT1 mRNA affects macrophage behavior via the AMP-activated protein kinase (AMPK) and NF-κB signaling pathways.

In a lipopolysaccharide-induced acute lung injury (ALI) model, silencing miR-9 led to a decrease in the pro-inflammatory M1 phenotype and an increase in the anti-inflammatory M2 phenotype (Li et al., 2023). This shift was associated with reduced lung damage, decreased lung water content, lower levels of pro-inflammatory factors in the bronchoalveolar lavage fluid, along with an increase in anti-inflammatory markers.

On the other hand, (Bazzoni et al., 2009) show miR-9-5p to be a regulator of inflammation in macrophages. In their research, miR-9 is characterised as a feedback regulator modulating the NF-κB signalling pathway. This modulation is achieved through inhibiting the NFKB1 transcript, as evidenced by experiments using 3' UTR luciferase reporters. Their findings further reveal that monocytes overexpressing miR-9 show a decrease in the levels of NFKB1/p105, demonstrating miR-9's direct impact on the NF-κB pathway. This study underscores the intricate mechanisms through which miR-9-5p regulates macrophage inflammatory responses.

In my study, however, after transfecting miR-9-5p into human and mouse macrophages, no change in the polarisation state of these macrophages was detected.

3.3.3 miR-709

In my study aimed at identifying miRNAs associated with M1-like polarisation in macrophages, I employed *in silico* methods to predict their binding to key transcriptional regulators. This approach involved searching several databases known for miRNA-target gene interactions to find miRNAs likely to bind and potentially down-regulate transcription factors that promote an M2-like phenotype, thus favouring a shift towards an M1-like state. The miRNAs were ranked based on their predicted binding affinity to these transcriptional regulators, with a higher cumulative score from these databases indicating a stronger regulatory potential. MiRNAs with the highest scores were then chosen for further experimental validation.

miR-709 emerged as a candidate for macrophage repolarisation due to its high binding sum score, showing strong predictions to target Myc across five different databases. In a mouse T-ALL leukemogenesis study, miR-709 was identified as a tumour suppressor that represses key oncogenes, including Myc (Li et al., 2011). This study validated miR-709's specificity in targeting by demonstrating decreased luciferase expression linked to the 3'UTRs of these genes, an effect reversed by mutations in the miR-709 binding sites. Notably, miR-709 significantly reduced Myc mRNA and protein levels in tumour cells.

However, in my study, upon transfecting BMDM with miR-709, no change was observed in Myc levels by qRT-PCR, possibly due to the timing of analysis or differences in models, as the referenced study used the embryonic mouse fibroblast cell line NIH3T3. Additionally, in my project, no polarisation effect of this miRNA in the tested BMDM was detected. This outcome could be attributed to miR-709's role in targeting and downregulating Glycogen synthase

kinase-3beta (GSK-3β) (Chen et al., 2014; Li et al., 2016). Luciferase Reporter assays confirmed the direct interaction between miR-709 and the 3′-UTR of GSK-3β. The inhibition of GSK-3β modulates the LPS-induced inflammatory response by affecting the β-catenin and NF-κB pathways (Li et al., 2016). GSK-3β is also known to suppress STAT3 and STAT6 phosphorylation, promoting M1 polarisation (Patel & Werstuck, 2021). Indeed, miR-709 was found to be upregulated in macrophages in response to LPS stimulation, and its overexpression leads to a reduction in the production of inflammatory cytokines such as IL6, TNF-α, and IL1β (Li et al., 2016).

3.3.4 miR-694

In our bioinformatics analysis, miR-694 also achieved a high sum score, particularly in its predicted binding to Hdac1 and Myc. However, following transfection with miR-694 in our study, no downregulation of Myc was observed. Additionally, current literature lacks validated assays demonstrating miR-694's targeting ability towards Myc or Hdac1. Our experiments involving the transfection of miR-694 into BMDM did not reveal any polarisation function of this miRNA. Interestingly, a study in hepatocellular carcinoma in mice noted that the downregulation of miR-694 correlated with the upregulation of Tumor necrosis factor alpha-induced protein 3 (Tnfaip3), a suppressor of inflammation, which in turn inhibits the NF-kB pathway (Lu et al., 2014). This suggests that while miR-694 may not directly influence macrophage polarisation or Myc expression in our model, it may play a role in inflammatory regulation in other contexts.

3.3.5 miR-144-3p

While miR-144-3p was initially selected for its high binding prediction to Hdac3, Pparg, and Stat6, no significant downregulation of Stat6 was observed following miR-144-3p transfection. However, the targeting of Hdac8 by miR-144-3p, which has sequence homology with Hdac3, was shown previously (Wang et al., 2020a). This finding could suggest potential similar effects on Hdac3.

Interestingly, miR-144-3p did not induce M1-like repolarisation in BMDM, though several studies have highlighted miR-144-3p's role in promoting inflammation. For instance, miR-144-3p accelerates atherosclerosis, a chronic inflammatory condition, by targeting ATP-binding cassette transporter (ABCA1), a receptor known for its anti-inflammatory properties through JAK2-STAT3 signalling (Hu et al., 2014) This targeting led to increased production of pro-inflammatory cytokines, TNF-α, IL1b, and IL6, both *in vitro* and *in vivo*. Furthermore, miR-144-3p expression was correlated with elevated proinflammatory cytokines/chemokines during *M. abscessus* infection in lung macrophages, and overexpression of miR-144-3p resulted in increased inflammation (Kim et al., 2021).

Xu et al., 2021 explored the role of miR-144-3p in septic ALI. They found that miR-144-3p upregulation, which negatively targets Caveolin-2, exacerbated inflammation and cell apoptosis

through the JAK/STAT pathway. This result further supports miR-144-3p's role in enhancing inflammatory responses.

In a study of TAMs from HCC, miR-144-3p was found to promote M1-like macrophage polarisation by targeting factors like Hepatocyte Growth Factor (HGF) and macrophage migration inhibitory factor (MIF), known to influence M2-like macrophage activation. This polarisation was evidenced by increased M1-type and decreased M2-type cytokine production in TAMs and an enhanced capability to activate CTLs (Zhao et al., 2021).

On the other hand, miR-144-4p was shown to regulate inflammation in a rat model by directly binding to the 3′UTR of rat TLR2 mRNA, thereby modulating TLR2 expression. Functional studies in NR8383 rat macrophage cell lines and primary macrophages from E3 rats revealed that miR-144-3p overexpression led to decreased TLR2 expression, reduced activation of NF-κB, and lowered production of pro-inflammatory cytokines such as TNF-α and IFN-γ. Conversely, inhibition of miR-144-3p resulted in the upregulation of TLR2 and enhanced production of these pro-inflammatory cytokines (Li et al., 2015).

3.3.6 miR-125a-5p and miR-125b-5p

The miR-125 family, including miR-125a, miR-125b-1, and miR-125b-2, represents a group of miRNAs that, despite being located at distinct genomic locations and transcribed independently, play crucial roles in cellular processes through varied expression profiles and functions. In my study, the choice of the miR-125 family for investigation was guided by *in silico* analysis, highlighting its potential binding affinity to critical regulatory genes such as Hdac3 and Stat3.

miR-125a has been show to target Stat3 by dual luciferase assay in multiple studies (Wang et al., 2020b; Xu et al., 2018; Zhang et al., 2022). Xu et al., 2018 observed a significant reduction of miR-125a-5p in the livers of diabetic mice and rats, with overexpression of miR-125a-5p decreasing STAT3 levels and downregulating p-STAT3. Zhang et al., 2022 discovered that upregulation of miR-125a targets Stat3, subsequently inhibiting liver regeneration and hepatocyte proliferation through the STAT3/p-STAT3/Jun Proto-Oncogene, AP-1 Transcription Factor Subunit (JUN)/BCL2 axis, as confirmed by dual-luciferase systems and Western blot analysis. Moreover, Wang et al., 2020b extended these observations by demonstrating that miR-125a-5p overexpression can inhibit Stat3 expression in THP-1 cells, implicating miR-125a-5p in the regulation of innate host defences through Stat3 targeting.

In the literature, miR-125a is upregulated by LPS stimulation of macrophages (Graff et al., 2012; Lu et al., 2016), whereas miR-125b is downregulated (Monk et al., 2010; Tili et al., 2007; Xu et al., 2016).

In my study, the transfection of these miRNAs into BMDM did not achieve repolarisation of these macrophages towards the M1-like phenotype.

The literature shows that miR-125b can have a pro-inflammatory function in macrophages. Enforced expression of miR-125b not only altered macrophage morphology and gene expression

but also enhanced their functional roles in immune activation (Chaudhuri et al., 2011). Specifically, miR-125b overexpression in macrophages increased CD80 expression and enhanced their responsiveness to IFN-γ, thereby augmenting their capacity to present antigens and stimulate T-cell activation. This effect is further correlated with an increased ability of miR-125b-expressing macrophages to kill tumour cells, both *in vitro* and *in vivo*. The study also identified IRF4 as a target of miR-125b, where IRF4 downregulation mimicked the effects of miR-125b overexpression, suggesting that miR-125b promotes an activated macrophage phenotype by inhibiting IRF4, a known suppressor of inflammatory responses in macrophages.

Building on this understanding, Gerloff et al., 2020 explored the impact of miR-125b within the tumour microenvironment, particularly in the context of melanoma. They reported that melanoma-derived exosomes carrying miR-125b-5p can reinforce the activation of M1-like TAMs, as evidenced by the induced expression of pro-inflammatory cytokines and chemokines such as IL1β, CCL1, and CCL2. This miR-125b-5p-mediated activation contributes to enhanced myeloid cell recruitment and cancer-associated inflammation. Furthermore, the study highlighted the potential of miR-125b to modulate T cell-mediated immune responses through the upregulation of CD80 expression on macrophages, which may interact with CTLA4 on activated T cells to modulate T cell proliferation and function.

While some studies highlight the pro-inflammatory and tumour-promoting effects of miR-125b, a body of evidence also points to its significant anti-inflammatory actions across various models.

Silencing of miR-125b-5p in human macrophages infected with *Mycobacterium tuberculosis* (Mtb) not only mitigates the inflammatory response but also promotes apoptosis through targeting DNA damage regulated autophagy modulator 2 (DRAM2) (Liu et al., 2020). This suggests a potential anti-inflammatory and antimicrobial role of miR-125b-5p against Mtb infection.

Overexpression of mmu-miR-125b in activated macrophages suppresses NO production, a critical mediator of inflammatory responses (Xu et al., 2016). This suppression is associated with enhanced tumour cell proliferation and growth *in vitro* and *in vivo*.

Overexpressed miR-125a-5p also promotes M2 polarisation of macrophages (Wang & Guo, 2020). This polarisation is characterised by decreased expression of TRAF6 and phosphorylation of Transforming growth factor-β-activated kinase 1 (TAK1), alongside alterations in the levels of IL6, iNOS, IL10, and Arg1, suggesting a skewing towards a resolution phase of inflammation and tissue repair.

In the context of ulcerative colitis, upregulation of mir-125-5p decreased IL6 receptor expression and inflammatory factor levels in THP-1 cells while inhibiting the activation of the JAK1/STAT3 and NF-κB pathways (Yao et al., 2021). These results further support the anti-inflammatory capabilities of certain members of miR-125 family, showing its potential to modulate key inflammatory pathways negatively.

Collectively, these studies present a nuanced view of miR-125a and miR-125b functions, indicating that their roles in inflammation and immune responses can be context-dependent.

3.4 Microarray upregulated DEGs

The microarray analysis conducted in our study aimed to elucidate the complex pathways governing macrophage polarisation, focusing on the impact of miR-155-5p and a pool of inhibitors, including Niclosamide, Entinostat, AS1517499, and 10074-G5. This comprehensive analysis allowed to identify key genes and pathways influenced by these agents in both human and murine macrophages, providing valuable insights into the mechanisms of macrophage repolarisation.

A notable finding from the study was the unique up-regulation of Sod2 in both human and murine macrophages repolarised with miR-155-5p and the inhibitor pool. Sod2, or superoxide dismutase 2, is crucial for the detoxification of superoxide radicals, protecting macrophages from oxidative stress during inflammation processes (Rakkola et al., 2007).

Additionally, miR-155-5p led to the up-regulation of PDE4B in both human and murine models. PDE4B plays a crucial role in the regulation of inflammation and the production of pro-inflammatory cytokines. The activation of PDE4B in response to LPS stimulation is a key mechanism through which macrophages modulate the synthesis and secretion of pro-inflammatory cytokines, such as TNF-α.

Given the role of PDE4B in modulating cyclic AMP (cAMP) levels and its involvement in inflammatory responses, as previously discussed, this finding underscores the significance of miR-155-5p in influencing macrophage function through modulation of PDE4B expression (Jin & Conti, 2002; Peter et al., 2007).

Furthermore, the analysis identified a shared up-regulation in five genes—TRAF1, IDO1, CFB, SLC2A6, and CD274—among the most effectively repolarised macrophages treated with miR-155-5p in human models and the inhibitor pool in murine macrophages. These genes are involved in various critical inflammatory processes:

- **TRAF1**: tumour necrosis factor receptor-associated factor 1, implicated in NF-κB signalling and immune responses (Bradley & Pober, 2001).
- **IDO1**: Indoleamine 2,3-dioxygenase 1, playing a role in tryptophan metabolism and immune regulation (Munn & Mellor, 2013).
- **CFB**: Complement factor B, part of the alternative complement pathway, important for innate immunity (Walport, 2001).
- **SLC2A6**: A glucose transporter, indicating alterations in metabolic pathways (Mueckler & Thorens, 2013).

- **CD274 (PD-L1)**: Programmed death-ligand 1, involved in the immune checkpoint pathway and immune escape mechanisms of tumours (Pardoll, 2012).

The shared up-regulation of these genes suggests a combinatorial effect of miR-155-5p and the inhibitor pool, leading to the enhancement of anti-inflammatory and immunomodulatory responses in macrophages. This could potentially offer new targets for therapeutic interventions aimed at regulating macrophage polarisation and function in various disease contexts.

3.5 Function of repolarised human and mouse macrophages

Experiments conducted to evaluate the impact of repolarisation agents on macrophage function, tumour cell viability, and CTL activation provided insightful outcomes. Specifically, the study focused on the effects of macrophages repolarised with IFN-γ+LPS, miR-155-5p, and a pool of SMIs in various co-culture settings, including direct macrophage-tumour cell interactions, macrophage-CTL co-cultures, and tri-cultures involving macrophages, CTLs, and tumour cells. The intent behind these co-culture arrangements was to simulate the conditions of the tumor microenvironment.

In our study, we embarked on functional experiments to elucidate the effects of macrophage repolarisation on tumour cell viability, CTL activation, and their combined impact on tumour cell killing through co-culture and tri-culture systems. Notably, macrophages repolarised with IFN-γ+LPS exhibited a pronounced ability to kill tumour cells, enhance phagocytosis, and activate CTLs, underscoring the potent anti-tumour functionality of M1-like macrophages. This was further supported by FACS analysis, which revealed a significant reduction in EO771-OVA tumour cell numbers in the presence of IFN-γ+LPS-treated BMDMs. The study also discovered that the supernatant from IFN-γ+LPS repolarised macrophages alone could inhibit tumour cell growth through the action of secreted cytokines like TNF-α and NO, even without direct cell-cell contact.

Furthermore, the study highlighted a stark contrast between human and murine macrophages in their impact on tumour cell growth and response to repolarisation, with human MdMs repolarised with IFN-γ+LPS not showing a tumour killing effect, while still enhancing CAR T-cell activation. This could be explained by the role of NO production and iNOS induction in macrophage-mediated tumour cell killing, as repolarised MdMs do not produce NO. NO's cytotoxic effects on NO-sensitive cancer cells underscore its significance as a part of the immune response against tumours, pointing to the intricate mechanisms through which macrophages can exert anti-tumour effects.

Interestingly, the inhibitor pool-treated BMDMs mediated a slight decrease in tumour cell growth *in vitro*, indicating that certain repolarisation agents require direct interactions to exert their anti-tumour effects. However, miR-155-5p and the inhibitor pool, despite inducing molecular changes in macrophages, did not translate to significant functional outcomes in the

MdMs and cancer cell interaction and T cell activation assays used. These findings emphasise the species dependent differences and complexity of macrophage repolarisation and its functional implications, suggesting that specific repolarisation signals like IFN-γ+LPS are crucial for eliciting effective therapeutic responses, and highlight the need for deeper investigation into the roles and mechanisms of repolarised human macrophages in cancer and immunotherapy.

Even though the assays used in the present study did not show a functional outcome from the repolarisation of human and mouse macrophages with mir-155-5p and the inhibitor pool, the potential of miR-155 to 're-educate' TAMs and endow them with tumour-killing capabilities akin to those of M1 macrophages has been demonstrated through a series studies. By transfecting TAMs isolated from S-180 tumour-implanted mice with pre-miR-155, Cai et al., 2012 observed a significant reduction in tumour cell survival, promotion of tumour cell apoptosis, and inhibition of tumour cell invasion when these modified TAMs were co-cultured with Lewis lung carcinoma (LLC) cells. This finding underscores the efficacy of miR-155 in modifying the tumour microenvironment towards a more hostile setting for cancer cells.

Further exploration into the therapeutic application of miR-155 has shown promising results in targeting tumour immune evasion mechanisms. For instance, the use of pH-responsive nanovectors for targeted delivery of miR-155 has been effective in reprogramming TAMs into immunostimulatory cells, enhancing the activation of T and NK cells and eliciting potent anti-tumour responses (Liu et al., 2017). Similar success was achieved with pH-responsive nanoparticles conjugated with mannose for targeted delivery of miR-155 to TAMs, converting tumour-promoting TAMs into anti-tumour macrophages and reducing tumour sizes *in vivo* (Zang et al., 2019).

Chapter 4

Conclusion

The findings from this study illuminate the complex and dynamic nature of macrophage polarisation, offering insights into the potential for repolarising macrophages towards an M1-like phenotype for therapeutic benefit. The identification of miRNAs and small molecule inhibitors that can modulate macrophage activation states opens new avenues for the development of targeted therapies aimed at harnessing the immune system in the fight against cancer and other diseases characterised by immunosuppressive environments.

4.1 Future perspectives

1. **Precision Targeting of Macrophage Polarisation**: Future research should focus on refining the specificity and efficacy of miRNA and small molecule-based therapies for macrophage repolarisation. This includes developing targeted delivery systems that ensure the selective modulation of macrophage phenotypes within the tumour microenvironment without adversely affecting the broader immune response.

2. **Combination Therapies**: The synergistic potential of combining macrophage repolarisation strategies with existing cancer treatments, such as checkpoint inhibitors, CAR T-cell therapy, and traditional chemotherapeutics, warrants further exploration. By simultaneously targeting multiple facets of tumour immunity, combination therapies could overcome resistance mechanisms and enhance overall treatment efficacy.

3. **Translational and Clinical Research**: Bridging the gap between preclinical findings and clinical application remains a critical challenge. Translational studies using patient-derived cells and tissues, along with clinical trials assessing the safety and therapeutic impact of macrophage repolarisation agents, are essential for validating the potential of these strategies in human health.

4. **Understanding Macrophage Heterogeneity**: Macrophages exhibit remarkable heterogeneity and plasticity, influenced by their tissue microenvironments. Future studies should aim to dissect the diverse roles of macrophages in different tissues and disease contexts, to tailor repolarisation strategies that account for this complexity.

5. **Mechanistic Insights into Macrophage Repolarisation**: While this study has identified key players in macrophage polarisation, the molecular mechanisms underlying these processes are not fully understood. Comprehensive analyses combining transcriptomics, proteomics, and metabolomics are needed to unravel the intricate signalling networks and epigenetic modifications governing macrophage behaviour.

4.2 Concluding remarks

This study contributes to the expanding knowledge of macrophage biology, highlighting the potential of miR-155-5p and specific small molecule inhibitors as promising agents for redirecting macrophage polarisation towards a phenotype conducive to anti-tumour immunity. Despite the challenges ahead, the prospects of manipulating macrophage polarisation for therapeutic purposes are compelling. By continuing to unravel the complexities of macrophage function and harnessing these insights for therapeutic development, we can move closer to realising the full potential of the immune system in combating cancer and other diseases. As we advance, it is imperative to maintain a focus on the ultimate goal: improving patient outcomes through innovative and effective therapies that leverage the body's own defence mechanisms.

Chapter 5

Materials and Methods

5.1 Materials

5.1.1 Chemicals, reagents, and kits

Basal cell culture media used in this study are listed in Table 5.1.1. Other reagents and chemicals used in this study are listed in Table 5.1.2. Kits used in this study are listed in Table 5.1.3.

Component	Cat. No.	Manufacturer
DMEM, high glucose, GlutaMAX Supplement	61965-026	Thermo Fisher Scientific, Waltham, USA
DMEM, low glucose, GlutaMAX Supplement	10567014	Thermo Fisher Scientific, Waltham, USA
Minimum Essential Medium Eagle	M4526	Sigma-Aldrich, St. Louis, USA
RPMI 1640 Medium, GlutaMAX Supplement	61870-010	Thermo Fisher Scientific, Waltham, USA

Table 5.1.1. List of basal cell culture media used in this study.

5.1.2 Equipment and instruments

Equipment and instruments used throughout this thesis are detailed in Table 5.1.4.

5.1.3 Consumables

Consumables, including plasticware and non-reagent materials, are listed in Table 5.1.5.

Component	Cat. No.	Manufacturer
2-Mercaptoethanol	M6250	Sigma-Aldrich, St. Louis, USA
Accutase cell detachment solution	SCR005	Merck KGaA, Darmstadt, Germany
Biocoll	L6115	Merck KGaA, Darmstadt, Germany
Dimethyl sulfoxide (DMSO) Cell culture grade	A3672	AppliChem, Darmstadt, Germany
DPBS, no calcium, no magnesium	14190-094	Thermo Fisher Scientific, Waltham, USA
Fetal calf serum	S 0115	Biochrom, Darmstadt, Germany
Geneticin Selective Antibiotic (G418 Sulfate)	10131035	Thermo Fisher Scientific, Waltham, USA
Humanserum	H4522-20ML	Sigma-Aldrich, St. Louis, USA
L-Glutamine (200 mM)	25030-081	Thermo Fisher Scientific, Waltham, USA
Methyl α-D-mannopyranoside	M6882	Sigma-Aldrich, St. Louis, USA
Penicillin-Streptomycin	P0781	Sigma-Aldrich, St. Louis, USA
Puromycin Dihydrochloride	A1113803	Thermo Fisher Scientific, Waltham, USA
1X RBC Lysis Buffer	00-4333-57	eBioscience, Waltham, USA
TrypLE Select	12563029	Thermo Fisher Scientific, Waltham, USA
Trypsin-EDTA (0.25%), phenol red	25200-056	Thermo Fisher Scientific, Waltham, USA

Table 5.1.2. List of chemicals and reagents used in this study.

Kit	Cat. No.	Manufacturer
ELISA MAX™ Deluxe Set Human CXCL10 (IP-10)	439904	BioLegend, San Diego, USA
ELISA MAX™ Deluxe Set Mouse IFN-γ	430804	BioLegend, San Diego, USA
ELISA MAX™ Deluxe Set Mouse TNF-α	430904	BioLegend, San Diego, USA
ELISA MAX™ Standard Set Human TNF-α	430201	BioLegend, San Diego, USA
Griess Reagent System	G2930	Promega, Madison, USA
High-Capacity cDNA Reverse Transcription Kit	4368814	Applied Biosystems, Foster City, USA
miRNeasy Mini Kit	217004	Qiagen, Venlo, Netherlands
Power SYBR™ Green PCR Master Mix	4368577	Applied Biosystems, Foster City, USA
Qubit™ microRNA Assay Kit	Q32880	Thermo Fisher Scientific, Waltham, USA
Qubit™ RNA High Sensitivity (HS) Kit	Q32852	Thermo Fisher Scientific, Waltham, USA
RNeasy Mini Kit	74106	Qiagen, Venlo, Netherlands

Table 5.1.3. List of experimental kits used in this study.

Instrument	Manufacturer
Biological Safety Cabinet	Heraeus, Hanau, Germany
CO_2 Incubator	BINDER, Tuttlingen, Germany
Centrifuge 5424 R	Eppendorf, Hamburg, Germany
Centrifuge 5810R	Eppendorf, Hamburg, Germany
CLARIOstar Plus Plate reader	BMG LABTECH, Ortenberg, Germany
FACS Canto II Flow Cytometer	Becton Dickinson, Franklin Lakes, USA
Gammacell 1000 Elite	MDS, Ottawa, Canada
Incucyte® S3	Sartorius AG, Göttingen, Germany
Incucyte® SX5	Sartorius AG, Göttingen, Germany
Megafuge 2.0R	Heraeus, Hanau, Germany
Micro-centrifuge 2 CMG-060	neoLab Migge, Heidelberg, Germany
Microscope Olympus CK40	Leica Camera, Wetzlar, Germany
Mini Laboratory Centrifuge	neoLab Migge, Heidelberg, Germany
Multipipette E3x	Eppendorf, Hamburg, Germany
PIPETBOY acu 2	INTEGRA Biosciences, Biebertal, Germany
Pipette (P2, P10, P20, P100, P200, P1000)	Gilson, Middleton, USA
QuantStudio 5 Real-Time PCR System 96-well	Applied Biosystems, Foster City, USA
QuantStudio 5 Real-Time PCR System 384-well	Applied Biosystems, Foster City, USA
Qubit 4 Fluorometer	Thermo Fischer Scientific, Waltham, USA
Spectrophotometer NanoDrop 2000	Thermo Fischer Scientific, Waltham, USA
Thermomixer Comfort	Eppendorf, Hamburg, Germany
Veriti 96-Well Thermal Cycler	Applied Biosystems, Foster City, USA
Vortex-Genie 2	Scientific Industries, New York, USA
Water bath	GFL, Burgwedel, Germany

Table 5.1.4. List of instruments used in this study, and their manufacturers.

Material	Manufacturer
5 ml Polystyrene round bottom tube with cell strainer cap	Corning, New York, USA
BD Discardit II disposable syringe (5, 10 ml)	Becton Dickinson, Franklin Lakes, USA
BD Mircolance 3 (21G, 27G)	Becton Dickinson, Franklin Lakes, USA
Cap for PCR microcentrifuge tubes	nerbe plus, Winsen, Germany
Cell Lifters – UltraCruz®	Santa Cruz, Dallas, USA
Centrifuge tube pp with screw cap PE (15, 50 ml)	Nerbe Plus, Winsen, Germany
Cryogenic vials	Thermo Fischer Scientific, Waltham, USA
Disposable scalpel	Feather, Osaka, Japan
Disposable serological pipette (5, 10, 25, 50 ml)	Corning, New York, USA
easystrainer (40, 70 µm)	Greiner Bio-One, Kremsmünster, Austria
Eppendorf Combitips advanced (0.1, 1, 5, 25 ml)	Eppendorf, Hamburg, Germany
Eppendorf Micro test tube 3810X 1.5 ml	Eppendorf, Hamburg, Germany
Eppendorf Safe-Lock microtubes, PCR clean 2.0 ml	Eppendorf, Hamburg, Germany
Eppendorf Tubes 3810X 1.5 ml	Eppendorf, Hamburg, Germany
Eppendorf tubes 5.0 ml	Eppendorf, Hamburg, Germany
MicroAmp Optical 96-Well Reaction plate	Applied Biosystems, Foster City, USA
MicroAmp Optical 384-Well Reaction plate	Applied Biosystems, Foster City, USA
Nunc™ MaxiSorp™ ELISA Plates, uncoated	BioLegend, San Diego, USA
PCR-grade water	Sigma-Aldrich, St. Louis, USA
PCR microcentrifuge tube PP, 0.2 ml, without cap	nerbe plus, Winsen, Germany
Pipette filter tips (10, 20, 100, 200, 1250 µl)	nerbe plus, Winsen, Germany
Pipette tips PP refill system (10, 200, 1000 µl)	nerbe plus, Winsen, Germany
Plastic serum pipette	Greiner Bio-One, Kremsmünster, Austria
Premium Aluminum Foil	VWR International, Radnor, USA
Reagent Reservoir	Corning, New York, USA
Safe-lock microcentrifuge tubes (1.5, 2 ml)	Eppendorf, Hamburg, Germany
Sealing Tape	Thermo Fischer Scientific, Waltham, USA
Soft-Ject single use syringes	Henke-Sass, Wolf, Tuttlingen, Germany
Syringe Filter Unit, 0.45, 0.22 µm	Sigma-Aldrich, St. Louis, USA
Tissue culture dish 100, 150 mm	TPP, Trasadingen, Switzerland
Tissue culture flask (25, 75, 150 cm2)	TPP, Trasadingen, Switzerland
Tissue culture test plate (96F, 96U)	TPP, Trasadingen, Switzerland
Tissue culture test plates (6, 12, 24, 96 Wells)	TPP, Trasadingen, Switzerland
Vacuum filtration, Filtermax, 500 ml	TPP, Trasadingen, Switzerland

Table 5.1.5. List of general consumables

5.2 Cell culture

Reagents used for cell culture work are listed in Table 5.1.2. All cell lines used within this thesis and their corresponding culture medium are listed in Table 5.2.1 and Table 5.2.2, respectively.

Working with cell lines or primary cells was performed under sterile conditions in a tissue culture hood. Cells were maintained by incubation at 37 °C in a CO2 incubator (5% CO2).

Cell line	Cell type	Modification	Origin	Medium Index	Antibiotic
CTL (OVA257-264; Kb)	mT	-	Osen, Wolfram	8	-
E.G7	mTL	OVA	unknown	2	0.8 mg/ml G418
EL-4	mTL	-	unknown	2	-
EO771	mBC	-	unknown	3	-
EO771/OVA-F	mBC	OVA	generated by David Eisel	3	0.2 mg/ml G418
HT-29	hC	-	unknown	3	-
J7I-53	hT	CEA-CAR; VFP	generated by Eren Boga	3	-
L929	mF	-	unknown	6/7	-
MaMel002	hM	-	unknown	3	-
MaMel002-RFP	hM	RFP	Generated by Rainer Will	3	0.25 µg/ml Puromycin
MDA-MB-231	hBC	-	-	3	-
MDA-MB-231-RFP	HBC	RFP	Generated by Rainer Will	3	0.25 µg/ml Puromycin

Table 5.2.1. Overview of cell lines used in this study.

5.2.1 BMDM isolation, generation, and polarisation

C57BL/6 mice were euthanized and, using surgical scissors and forceps, the femurs and tibias from both legs were excised and freed from muscle tissue for bone marrow extraction. A 5 ml syringe, loaded with bone marrow (BM) culture media (Table 5.2.2) and fitted with a 26G needle, was used to gently flush the bone marrow into a 50 ml falcon tube. Following the flushing of both femurs and tibias, the collected bone marrow was homogenised and passed through a 70 µm cell strainer to eliminate any bone fragments or debris. The cells were then centrifuged at 300 g for 5 minutes and seeded onto 150 mm tissue culture dishes. For 7 days, the bone marrow cells were incubated in a mixture of 30 % L929 cell line-derived culture supernatant, which is enriched with macrophage colony-stimulating factor (M-CSF), and 70 % BM culture media. The resultant bone marrow-derived macrophages (BMDMs) were then harvested and

Index	Name	Medium	Supplements
1	BM culture media	DMEM, low glucose, GlutaMAX Supplement, pyruvate	10% FCS, 1% Penicillin-Streptomycin
2	BMDM culture media	DMEM, low glucose, GlutaMAX Supplement, pyruvate	5% FCS
3	Culture media	RPMI 1640 Medium, GlutaMAX Supplement	10% FCS
4	huM culture media	RPMI 1640 Medium, GlutaMAX Supplement	1% Penicillin-Streptomycin
5	MdM culture media	RPMI 1640 Medium, GlutaMAX Supplement	5% human serum, 1% Penicillin-Streptomycin
6	L929 growth media	DMEM, high glucose, GlutaMAX Supplement	5% FCS, 1% Penicillin-Streptomycin
7	L929 maintaining media	DMEM, high glucose, GlutaMAX Supplement	2% FCS, 1% Penicillin-Streptomycin
8	Complete T cell Medium	Minimum Essential Medium Eagle	10% FCS, 2 mM L-Glutamine, 50 µM 2-Mercaptoethanol, 12.5 mM Methyl α-D-mannopyranoside, 12.5 ml ConA culture supernatant, 1% Penicillin-Streptomycin

Table 5.2.2. Cell culture medium composition.

plated as required for subsequent experiments, utilising BMDM culture media. Harvesting of BMDMs involved incubation with trypsin and dislodgement by gentle scraping. Post-reseeding, BMDMs were either stimulated with 10 ng/ml IL-4) for M2-like macrophage polarisation or with 100 ng/ml LPS) and 50 ng/ml IFN-ɣ for M1-like macrophage polarisation (Table 5.2.3).

5.2.2 Preparation and Collection of L929 Cell Line Supernatant for Macrophage Culture Media

L929 cells were cultured in 175 cm^2 flasks using L929 growth media (Table x) until they achieved 70% confluency. At this point, the growth media was replaced with L929 maintenance media (Table 5.2.2). The cells continued to be cultured for an additional 5 days, after which the supernatant was harvested, filtered and frozen for use in BMDM generation.

5.2.3 Isolation, generation and polarisation of Human Monocyte-Derived Macrophages (MdMs) from Peripheral Blood

Whole blood samples were collected from healthy volunteers through the DRK Blood-donor service in Baden-Württemberg-Hessen, Mannheim, Germany, with informed consent. The blood bag was carefully opened using a sterile scalpel to extract the buffy coat, which was transferred

into a 75 cm² flask and diluted with 1X PBS to a final volume of 125 ml. 15 ml of Biocoll was introduced into 50 ml Leucosept tubes, followed by centrifugation. Subsequently, the diluted PBMC was gently layered on top of the Biocoll gradient, which were then centrifuged without brakes for 15 minutes at 800 g. The upper layer, containing the donor's diluted plasma, was set aside for later use. The Peripheral Blood Mononuclear Cell (PBMC) layer, which contains the monocyte fraction, was collected into a 50 ml falcon tube, rinsed with PBS, and centrifuged for 8 minutes at 400 g. The supernatant was discarded, and the cells were treated with 1X RBC Lysis Buffer for 5 minutes with agitation. After filling the falcon tube with 1X PBS and another centrifugation step at 400 g for 8 minutes two additional washing and centrifugation steps followed. Meanwhile the donor's plasma was filtered through a 0.22 µm syringe filter and heat-inactivated in a water bath at 56°C for 20 minutes. Following the last centrifugation step, human macrophage (huM) culture media was added to the cells, which were then plated in 150 mm tissue culture dishes with 10% of the diluted, strained, and heat-inactivated donor serum and incubated overnight. The next day, monocytes attached to the dish were washed to remove non-adherent cells and debris. These monocytes were cultured for a week, differentiating into Monocyte-Derived Macrophages (MdMs). MdMs were harvested using trypsin and gentle scraping, then reseeded with MdM culture media for subsequent experiments. Macrophage activation was induced with 20 ng/ml IL-4 for M2-like polarization or with 100 ng/ml LPS and 20 ng/ml IFNɣ for M1-like polarisation (Table 5.2.3).

Component	Cat. No.	Manufacturer
Human IFN-gamma Recombinant Protein	PHC4031	Thermo Fisher Scientific, Waltham, USA
Human IL-4 Recombinant Protein	PHC0041	Thermo Fisher Scientific, Waltham, USA
Lipopolysaccharides from Salmonella typhosa	L2387	Sigma-Aldrich, St. Louis, USA
Mouse IFN gamma Recombinant Protein Carrier-Free	34-8311-82	eBioscience, Waltham, USA
Recombinant Mouse IL-4 (carrier-free)	574302	Biolegend, San Diego, USA

Table 5.2.3. Cytokines and TLR ligands

5.3 Flow cytometry

Immunofluorescence staining for flow cytometry involved using reagents detailed in Table 5.3.1, monoclonal antibodies detailed in Table 5.3.6 and appropriate isotype controls as advised by the manufacturers. Centrifugation was consistently performed at 300 g for 2 minutes at room temperature and FACS buffer, composed of 1X PBS with 3 % FCS was used throughout.

Following cell harvesting, the cells were resuspended in a suitable volume of FACS buffer, and 200 µl of this suspension were allocated to each well of a 96-well U-bottom plate. After centrifu-

gation, the supernatant was removed. The cell pellet was then incubated at 4°C for 30 minutes in FACS buffer containing panel-specific fluorochrome-conjugated antibodies, LIVE/DEAD Fixable Yellow Dead Cell stain (diluted 1:1000), True-Stain Monocyte Blocker (50 µL/mL), and, depending on the sample type, rat anti-mouse CD16/CD32 (50 µg/ml) for mouse samples or Human BD Fc Block (25 µg/ml) for human samples. Following another round of centrifugation and two washes with FACS buffer, the cells were resuspended in 200 µl of the same buffer. If cytometer analysis was scheduled for the following day, the samples were fixed with Cytofix/Cytoperm™ solution for 15 minutes, washed with BD Perm/Wash™ Buffer diluted 1:10, and resuspended in 200 µl FACS buffer.

Cell acquisition was conducted using a FACSCanto II system and the FACSDiva software, with data analysed through FlowJo software. For tasks necessitating absolute cell quantification, 40 µl of CountBright Absolute Counting Beads were incorporated into the cell mixture before acquisition. The formula used for calculating cell concentration was:

(Number of cell events / Number of bead events)×(Number of beads added per sample / sample volume (µL))=cell concentration (cells/µL)

Cytometer compensation was achieved with OneComp eBeads following the manufacturer's protocol. In co-culture studies, cells were labelled with CellTrace™ CFSE and CellTrace™ Violet Cell (CTV) according to the manufacturer's instructions before initiating co-culture.

Component	Cat. No.	Manufacturer
BD Perm/Wash™ - Perm/Wash Buffer	51-2091KZ	Becton Dickinson, Franklin Lakes, USA
CellTrace™ CFSE Cell Proliferation Kit	C34554	Thermo Fisher Scientific, Waltham, USA
CellTrace™ Violet Cell Proliferation Kit	C34571	Thermo Fisher Scientific, Waltham, USA
CountBright™ Absolute Counting Beads	C36950	Thermo Fisher Scientific, Waltham, USA
Cy3™ Dye-Labeled Pre-miR Negative Control #1	AM17120	Thermo Fisher Scientific, Waltham, USA
Cytofix/Cytoperm™ - Fixation/Permeabilization Solution	51-2090KZ	Becton Dickinson, Franklin Lakes, USA
Human BD Fc Block™	564219	Becton Dickinson, Franklin Lakes, USA
LIVE/DEAD® Fixable Yellow Dead Cell Stain Kit	L-34959	Thermo Fisher Scientific, Waltham, USA
OneComp eBeads	01-1111-42	eBioscience, Waltham, USA
Purified Rat Anti-Mouse CD16/CD32	553142	Becton Dickinson, Franklin Lakes, USA
True-Stain Monocyte Blocker	426102	BioLegend, San Diego, USA

Table 5.3.1. Reagents for flow cytometry

Fluorescence Channel	Marker
BL530/30	Nos2 AF488
584/42	I-Ab PE
BL670LP	CD11b PerCP-Cy 5.5
RL670/14	CD38 APC
RL780/60	CD86 APC-Cy7
VL450/50	F4/80 BV421
VL510/50	Live/Dead

Table 5.3.2. Mouse BMDM phenotype panel

Fluorescence Channel	Marker
BL530/30	CFSE
BL670LP	CD11b PerCP-Cy 5.5
VL450/50	F4/80 BV421 and CTV
VL510/50	Live/Dead
N/A	Cell Counting Beads

Table 5.3.3. Co-culture panel 1

During the FACS data analysis, cellular doublets were first eliminated using an FSC-H by FSC-A dot plot. Subsequently, the cells of interest were identified on an FSC by SSC dot plot, with exclusion of debris. Live cells were isolated as those negative for the LIVE/DEAD Fixable Yellow Dead Cell Stain. For the characterisation of macrophages, mouse BMDM were identified by CD11b+F4/80+ markers, and human MdM were distinguished by CD11b+CD14+ markers. Within this defined population, both the percentage of cells, in comparison to isotype or unstained controls, and the Median Fluorescence Intensity (MFI) were measured. For cells involved in co-culture experiments, CellTrace dyes facilitated the identification and subsequent analysis of specific cells of interest.

5.4 RNA Isolation

RNA from BMDM and MdMs was isolated using the RNeasy Plus Mini Kit, following the guidelines provided by the manufacturer. For applications such as RNA sequencing (RNAseq), microRNA sequencing (miRNAseq), and microarray analysis, total RNA was extracted from frozen cell pellets using the miRNeasy Mini Kit, adhering to the manufacturer's protocol. The RNA purification process involved silica-membrane spin columns and the final elution was done in 30 µl of nuclease-free water. The concentration and purity of the isolated RNA were determined using a Nanodrop Spectrophotometer or a Qubit Fluorometer, employing either the RNA High

Fluorescence Channel	Marker
BL530/30	CFSE
BL670LP	CD25 PerCP-Cy 5.5
BL780/60	CD69 PE-Cy7
VL450/50	CTV
VL510/50	Live/Dead
N/A	Cell Counting Beads

Table 5.3.4. Co-culture panel 2

Fluorescence Channel	Marker
BL530/30	CD80 AF488
584/42	CD209 PE
BL670LP	CD11b PerCP-Cy 5.5
RL670/14	CD206 APC
VL450/50	CD38 BV421
VL510/50	Live/Dead

Table 5.3.5. Human MdM phenotype panel

Sensitivity kit or the microRNA Assay Kit, in line with the manufacturers' instructions. The RNA samples were then stored at -80°C until further use.

5.5 cDNA Synthesis

For cDNA synthesis, 500 ng of total RNA was reverse transcribed in a 20 µl reaction volume using the High-Capacity cDNA Reverse Transcription Kit, following the manufacturer's instructions. The cDNA synthesis process was performed on a Veriti 96-well Thermal Cycler, with thermal conditions set according to the manufacturer's protocol.

5.6 qRT-PCR Analysis

For quantitative real-time PCR (qRT-PCR) analysis, 2 µl of the cDNA diluted 1:5 with PCR-grade water was used in either a 20 µl or 10 µl reaction volume with 2X Power SYBR™ Green PCR Master Mix. Pipetting scheme is on Table 5.6.1. The human and mouse ribosomal protein L19 (RPL19) gene was employed as the housekeeping gene to normalise the expression levels of the target genes. All primers used for quantitative real-time PCR are shown in Table 5.6.3.

Gene amplification was carried out on the QuantStudio 5 Real-Time PCR System, accommodating both 96-well and 384-well formats, with the specific cycling protocol outlined in Table 5.6.2.

Antigen	Species Reactivity	Coupled	Cat. No.	Manufacturer	Clone
CD11b	Human/Mouse	PerCP-Cy 5.5	101228	BioLegend	M1/70
CD25	Mouse	PerCP-Cy 5.5	45-0251-82	eBioscience	PC61.5
CD38	Mouse	APC	102712	BioLegend	90
CD38	Human	Brilliant Violet 421	562444	Becton Dickinson	HIT2
CD69	Mouse	PE-Cy7	552879	Becton Dickinson	H1.2F3
CD80	Human	Alexa Fluor 488	305214	BioLegend	2D10
CD86	Mouse	APC-Cy7	105030	BioLegend	GL-1
CD206	Human	APC	550889	Becton Dickinson	19.2
CD209	Human	PE	551265	Becton Dickinson	DCN46
F4/80	Mouse	Brilliant Violet 421	123137	BioLegend	BM8
I-Ab	Mouse	PE	553552	Becton Dickinson	AF6-120.1
Nos2	Mouse	Alexa Fluor 488	53-5920-82	eBioscience	CXNFT

Table 5.3.6. Flow cytometry antibodies

Component	Volume per reaction	
	384-well plate	**96-well plate**
cDNA (diluted 1:5 in nuclease free water)	1 μl	2 μl
Power SYBR®Green PCR Master Mix (2X)	5 μl	10 μl
Forward primer (10 μM)	0.2 μl	0.4 μl
Reverse primer (10 μM)	0.2 μl	0.4 μl
Nuclease free water	3.6 μl	7.2 μl
Total volume	**10 μl**	**20 μl**

Table 5.6.1. qPCR pipetting scheme using Power SYBR®Green PCR Master Mix

5.6.1 Primers

All primers used in this thesis were obtained from Sigma-Aldrich (St. Louis, USA) and are listed in Table 5.6.3. The lyophilised primers were resolved in ddH2O to a stock concentration of 100 µM and stored at -20 °C.

5.7 Enzyme-Linked Immunosorbent Assay (ELISA)

The supernatants from MdMs, BMDMs and co-culture experiments were collected, and the concentration of secreted cytokines was quantified using ELISA MAX™ Deluxe kit, following the manufacturer's instructions. The ELISA plates were read using the CLARIOstar Plus Plate reader. The process included subtracting the average absorbance of the blank replicates from the average absorbance of the sample replicates. Cytokine concentrations were ascertained by comparing the sample absorbance values to a standard reference curve, following the manufacturer's instructions.

Step	Temp.	Time
Pre-incubation (1 cycle)	50 °C 95 °C	2 min 10 min
Amplification (40 cycles)	95 °C 60 °C 72 °C	15 s 1 min 30 s
Melting curve (1 cycle)	98 °C 60 °C 95 °C 60 °C	15 s 1 min 15 s 15 s

Table 5.6.2. Cycler protocol for qPCR Using Power SYBR®Green PCR Master Mix

5.7.1 Measurement of NO Using the Griess Reagent System

In a similar manner, supernatants from MdMs, BMDMs, and co-culture experiments were subjected to analysis to quantify the concentration of secreted nitric oxide (NO) using the Griess Reagent System, in line with the manufacturer's recommendations. Absorbance readings were obtained using the CLARIOstar Plus Plate reader. This method involved deducting the average absorbance of the blank replicates from the average absorbance of the sample replicates. The concentrations of NO were then calculated by comparing the sample absorbance to the standard reference curve, enabling the precise quantification of NO levels in the supernatant.

5.8 Whole RNA and small RNA sequencing

Whole RNA and small RNA sequencing of polarised murine BMDM and human MdMs were conducted by GENEWIZ Multiomics & Synthesis Solutions from Azenta Life Sciences, using an Illumina HiSeq, PE 2x150 Sequencing System. GENEWIZ was responsible for library preparation, sequencing, and the subsequent bioinformatics analysis. This analysis involved trimming sequence reads to eliminate potential adapter sequences and low-quality nucleotides with Trimmomatic v.0.36. The trimmed reads were then aligned to the Mus musculus GRCm38 reference genome, using the STAR aligner v.2.5.2b, For the quantification of gene expression, unique gene hit counts were calculated using featureCounts from the Subread package v.1.5.2, based on the 'gene_id' feature in the annotation file, and counting only unique reads that mapped to exon regions. Differential gene expression analysis was carried out on the obtained gene hit counts using DESeq2. This involved comparing gene expression between predefined groups of samples, with the Wald test being utilised to calculate p-values and log2 fold changes. For small RNA sequencing data, read counts were computed using customised scripts. Genes and miRNAs were identified as differentially expressed based on criteria of an adjusted p-value < 0.05 and a log2 fold change > 1 for each comparison.

Target	Sp.	Dir.	Sequence (5'-3')	Product size (bp)	Source
Cxcl10	Mm	F R	TCTGAGTCCTCGCTCAAGTG CCTTGGGAAGATGGTGGTTA	228	Movahedi et al., 2010
Il1b	Mm	F R	GTGTGGATCCAAAGCAATAC GTCTGCTCATTCATGACAAG	282	Movahedi et al., 2010
Mrc1	Mm	F R	GCAAATGGAGCCGTCTGTGC CTCGTGGATCTCCGTGACAC	299	Movahedi et al., 2010
Stat6	Mm	F R	CTGGGGTGGTTTCCTCTTG TGCCCGGTCTCACCTAACTA	94	Shaul et al., 2010
Rpl19	Mm	F R	TACCGGGAATCCAAGAAGATTGA AGGATGCGCTTGTTTTTGAAC	89	PrimerBank 226958656c3
Myc	Mm	F R	ATGCCCCTCAACGTGAACTTC GTCGCAGATGAAATAGGGCTG	78	PrimerBank 293629266c1
Pparg	Mm	F R	TTTTCCGAAGAACCATCCGATT ATGGCATTGTGAGACATCCCC	139	PrimerBank 187960104c3
Trem2	Mm	F R	CCCAAGTGGAACACAGCAC GATGCTGGCTGCAAGAAACT	165	Katzenelenbogen et al., 2020
Tnf	Mm	F R	CCCTCACACTCAGATCATCTTCT GCTACGACGTGGGCTACAG	61	Katzenelenbogen et al., 2020
MRC1	Hs	F R	GGCGGTGACCTCACAAGTAT ACGAAGCCATTTGGTAAACG	168	Jaguin et al., 2013
TREM2	Hs	F R	TGGCACTCTCACCATTACG CCTCCCATCATCTTCCTTCAC	441	Zhang et al., 2016
CXCL10	Hs	F R	TGAAAGCAGTTAGCAAGGAAAGGT AGCCTCTGTGTGGTCCATCC	97	Irvine et al., 2009
TNF	Hs	F R	GGCAGTCAGATCATCTTCTCG CAGCTGGTTATCTCTCAGCTC	148	Mitsuhashi et al., 2013
CCL5	Hs	F R	CGTGCCCACATCAAGGAG GGACAAGAGCAAGCAGAAAC	207	Pham et al., 2012
RPL19	Hs	F R	GGCACATGGGCATAGGTAAG CCATGAGAATCCGCTTGTTT	198	Kordaß, 2022

Table 5.6.3. List of qPCR primers used. Sp. = species, dir. = direction, Mm = *Mus musculus*, Hs = *Homo sapiens*.

5.9 Microarray Analysis of Macrophage Repolarisation

Our study utilised the Microarray Core Facility from the German Cancer Research Center (DKFZ) for gene expression profiling of mouse and human macrophages after repolarisation. We selected the Affymetrix Clariom S platform for both mouse and human samples. The Microarray Core Facility was responsible for the initial quality control of the RNA samples, labelling and hybridisation to the selected microarrays, namely Clariom S Mouse and Clariom S Human and data acquisition. Subsequent analysis encompassed data normalisation, group comparisons, and statistical evaluations. Genes were identified as differentially expressed based on criteria of a p-value < 0.05 and a log2 fold change > 1 for each comparison.

5.10 Bioinformatic analyses

Functional Enrichment Analysis of Differentially Expressed Genes Using g:Profiler To elucidate the biological significance of the DEGs identified in my RNAseq and Microarray data, we employed g:Profiler (Kolberg et al., 2023). g:Profiler mapped DEGs to Gene Ontology (GO) terms, and we specifically focused on Biological Processes (BP) pathways. This analysis allows for the identification of over-represented GO:BP terms, providing insights into the biological mechanisms and processes most impacted by our experimental conditions.

The analysis began with the preparation of a curated list of DEGs, which was then inputted into g:Profiler. We ensured the use of the most up-to-date gene annotations to enhance the accuracy of our analysis. The g:Profiler tool was configured to perform an enrichment analysis, focusing on GO:BP terms to discern the biological pathways that were predominantly influenced by the observed gene expression changes.

5.10.1 Ingenuity pathway analysis of BMDM and MdM mRNA sequencing data

We performed a comprehensive analysis using Ingenuity Pathway Analysis (IPA) Krämer et al., 2014 software to investigate the transcriptional regulation underlying human and mouse M2-like (IL4) macrophage polarisation. Our dataset comprised mRNA sequencing data, specifically differential expression profiles comparing M1-like and M2-like polarisation states in macrophages. The data included gene Ensembl identifiers, log2 fold changes (log2FC) and adjusted p-values. The core analysis was set with default settings except for the following changes: The “confidence” setting was set to “all” including “experimentally observed”, “high (predicted)” as well as “moderate (predicted)”. In addition, the experimental log ratio cutoffs were set to log2FC > 1 (up) or log2FC < -1 (down) and adjusted p-value cutoff was set to <0.05.

Within IPA, we executed an ”Upstream Regulator Analysis” to identify transcription regulators that were likely influencing the observed gene expression patterns in M2-like macrophages.

For the upstream regulators identified as potentially activated in M2-like macrophages, we specifically extracted the "Bias-corrected Activation Z-scores" of the transcription regulators provided by IPA. This metric adjusts for network topology biases, offering a more accurate representation of a regulator's activation state by considering the direction and magnitude of gene expression changes relative to a network-based model.

Further, we conducted a "Network Pathway Analysis" within IPA to visualise the interactions and regulatory relationships of the activated upstream regulators in M2-like macrophages following IL4 stimulation. This analysis allowed us to map out the complex regulatory networks, highlighting key transcription factors and signalling molecules that could serve as potential targets for modulating macrophage polarisation.

5.11 Selection of Small Molecule Inhibitors for Macrophage Repolarisation

In our pursuit to modulate macrophage polarisation towards an M2-like phenotype, we identified key transcription regulators through a multi-faceted approach. Analysis of mRNA sequencing data from both human and mouse samples revealed Myc as significantly upregulated. Additionally, pathway analysis conducted via IPA highlighted Stat6 as an activated regulator. Literature review further pinpointed Stat3 and the Hdac family as critical to the regulation of macrophage phenotypes, with Stat3 acting as a promoter of the anti-inflammatory phenotype and Hdac inhibition leading to M1-like repolarisation ((Hu et al., 2021; Liu et al., 2021; Xia et al., 2023)). Based on these insights, we selected SMIs targeting these regulators to potentially drive macrophages towards an M2-like state. The specific SMIs, along with their experimental concentrations, are detailed in Table 5.11.1. This strategic selection was guided by the dual aims of exploring the biological impact of these regulators on macrophage polarisation and leveraging the availability of commercial inhibitors to ensure the feasibility of our experimental approach.

5.12 Selection of miRNAs for M1-like Macrophage Polarisation

We identified miRNAs upregulated in M1-like mouse and human macrophages, hypothesising their potential to drive repolarisation by downregulating genes associated with the M2-like phenotype, thus enhancing M1-like features. Notably, miR-155-5p and miR-9-5p were identified as candidates. Concurrently, we used *in silico* methods to identify miRNAs capable of downregulating key transcription regulators promoting an M2-like state, such as Hdac1, Hdac3, Myc, Stat6, and Stat3, as discussed in the section "Selection of Small Molecule Inhibitors for M1-like Macrophage Repolarisation." This involved querying multiple databases renowned for miRNA-target gene interaction predictions, including MicroCosm Griffiths-Jones et al., 2007, mirDB (Chen &

Name	Known target(s)	Final conc.	Manufacturer	Cat. No.
10074-G5	Myc	10 µM	Hölzel Diagnostika	SIW-S3686-5mg
AS1517499	Stat6	1 µM	Sigma	SML1906-5MG
FLLL32	Stat3	1 µM	Biomol	Cay10638-1
Mocetinostat (MGCD0103)	HDAC1, HDAC2, HDAC3 and HDAC11	2 µM	Hölzel Diagnostika	TMO-T2512-5mg
Entinostat (MS-275)	HDAC1, HDAC2, and HDAC3	1 µM	Biomol	BPS-27011
Niclosamide (BAY2353)	Stat3	500 nM	Santa Cruz	sc-250564
RGFP966	HDAC3	100 nM	Biomol	Cay16917-1
STAT3 Inhibitor V, Stattic	Stat3	5 µM	Merck	573099-25MG

Table 5.11.1. List of small molecule inhibitors used in this study.

Wang, 2020), miRNAMAP (Hsu, 2006), PITA (Kertesz et al., 2007), and TargetScan Agarwal et al., 2015, aiming to pinpoint miRNAs likely to bind and potentially suppress these transcription regulators. The miRNAs were scored based on the number of databases predicting their binding affinity to the transcription regulators in question. A higher cumulative score across these databases indicated a stronger regulatory potential.

Selected miRNAs with high scores were prioritised for further experimental validation. This approach led to the selection of miR-155-5p and miR-9-5p, observed upregulated in both murine and human M1-like macrophages, along with additional candidates identified through *in silico* analysis: miR-709, miR-694, miR-144-3p, miR-125a-5p, and miR-125b-5p. The sequence details of all selected miRNAs for this study are comprehensively listed in Table 5.12.1.

miRNA	Cat. No.	Sequence
mmu-mir-9-5p	C-310400-07-0002	5'- UCUUUGGUUAUCUAGCUGUAUGA -3'
mmu-mir-125a-5p	C-310392-07-0002	5'- UCCCUGAGACCCUUUAACCUGUGA -3'
mmu-mir-125b-5p	C-310394-05-0002	5'- UCCCUGAGACCCUAACUUGUGA -3'
mmu-mir-144-3p	C-310421-07-0002	5'- UACAGUAUAGAUGAUGUACU -3'
hsa-mir-155-5p	C-300647-05-0002	5'- UUAAUGCUAAUCGUGAUAGGGGUU -3'
mmu-mir-694	C-310745-01-0002	5'- CUGAAAAUGUUGCCUGAAG -3'
mmu-mir-709	C-310707-01-0002	5'- GGAGGCAGAGGCAGGAGGA -3'

Table 5.12.1. Sequences of miRNAs used in this study.

5.13 Transfection of Small RNAs into BMDM and MdMs

All transfection reagents used within this thesis to transfect miRNAs into BMDMs and MdMs are listed in Table 5.13.1. The reagents were used according to manufacturer's instructions.

Transfection Reagent	Cat. No.	Manufacturer
DharmaFECT 4 Transfection Reagent	T-2004-01	Dharmacon, Lafayette, USA
HiPerFect Transfection Reagent	301704	Qiagen, Hilden, Germany
Lipofectamine 3000 Transfection Reagent	L3000001	Thermo Fisher Scientific, Waltham, USA
Lipofectamine RNAiMAX Transfection Reagent	13778-100	Thermo Fisher Scientific, Waltham, USA
METAFECTENE® SI$^+$	T100-1.0	Biontex Laboratories, München, Germany

Table 5.13.1. List of transfection reagents used in this study.

Initially, we evaluated various transfection reagents, to identify the most efficient one for delivering miRNAs into BMDMs. For this purpose, we utilised 20 nM of a Cy3 Dye-Labelled Pre-miR Negative Control, adhering to the manufacturer's instructions for each transfection reagent. Our evaluation criteria included the efficiency of Cy3 incorporation, cell viability assessed 24 hours post-transfection, and the impact of these reagents on the macrophage phenotype, as determined by FACS analysis of Cy3, Live/Dead fixable yellow, and IAB PE.

The results led us to select DharmaFect 4 as our transfection reagent of choice for BMDMs, based on its superior performance in terms of high Cy3 uptake, minimal impact on cell viability, and negligible influence on cell polarisation.

Following this, DharmaFect 4 was employed to transfect the miRNAs listed in Table Y into both IL4-treated BMDMs and MdMs, in accordance with the manufacturer's guidelines. To ensure sustained intracellular levels of small RNA, cells were retransfected at 24-hour intervals after the initial transfection.

5.14 BMDM Co-culture Assay

To understand the functional impact of gene and protein expression changes induced by repolarisation agents in murine BMDMs, we executed a comprehensive co-culture experiment. This experiment aimed to elucidate the effects of BMDM repolarisation on the dynamics between macrophages, EO771 cancer cells engineered to express OVA, and OVA-specific CTLs.

OVA-specific CTLs targeting the OVA257-264 epitope presented by H-2Kb molecules were propagated in 24-well plates, each well containing 2 ml of Complete T cell Medium. To maintain the culture, every seven days, half of the culture medium was removed and replenished with a fresh mix of 5 million irradiated (33 Gy) syngeneic feeder cells and 200,000 irradiated (200 Gy)

stimulator cells (E.G7). A comprehensive list of all chemicals and reagents used for the cultivation of OVA-specific CD8+ T cells is provided in Table 5.1.2.

Initially, BMDMs were cultured in a 6-well plate with a density of 5x10e5 cells per well, and treated with IL4. After a 4-hour incubation to allow cytokine action, the wells were washed, and cells were either treated with IFNg+LPS, transfected with promising miRNAs or treated with inhibitors. Following a 24-hour period to facilitate expression changes, a retransfection or retreatment was conducted, and after an additional 4 hours, EO771-OVA cells and CTLs were introduced to the culture.

EO771-OVA cells were labelled with CFSE for fluorescence tracking, and OVA-specific CTLs were marked with CellTrace™ Violet (CTV), both stained according to manufacturers protocol. These stained cells were added to the macrophage cultures under various conditions to investigate the impact of macrophage repolarisation on tumour immunity.

After an 18-hour incubation period, culture supernatant was collected for analysis of cytokine profiles with ELISA, and cell interactions were analysed using two distinct FACS panels Table 5.3.3 Table 5.3.4 designed for detailed profiling of the cellular outcomes:

Panel 1: Focused on quantifying EO771-OVA tumour cells using absolute cell counting beads, alongside CFSE fluorescence. Macrophage phagocytosis of tumour cells or debris was evaluated using macrophage markers F4/80 and CD11b, identifying CFSE+ events within the macrophage population.

Panel 2: Aimed at assessing CTL activation, employing antibodies against CD25 and CD69. This panel provided insights into T cell activation following their interaction with treated macrophages and the EO771-OVA tumour cells.

5.15 Live-Cell Analysis

5.15.1 BMDM and EO771-OVA Co-Culture

In an experimental setup aimed at observing the dynamic effects of treated BMDMs on tumour cell growth, BMDM were co-cultured with EO771-OVA cells in a Live-cell analysis system.

BMDMs were treated with IL4 for 24 hours to induce an M2 phenotype. Following this induction period, the cytokines were washed away, and the M2-like BMDMs were repolarised with IFN-g+LPS, transfected with candidate miRNAs or treated with specific SMIs. After a 48-hour period post-treatment the BMDMs were harvested for co-culture assays. In a 96-well flat-bottom plate, BMDMs and EO771-OVA cells were seeded at densities of 35,000 and 10,000 cells per well, respectively. EO771-OVA cells were either co-cultured directly with repolarised BMDMs or with the supernatant from repolarised BMDMs. All experiments were conducted with five or six technical replicates.

Monitoring of culture conditions was performed using the IncuCyte® S3 or SX5 Live-Cell Analysis Systems across a 48-hour period, with images captured every 3 hours. Cell confluence and proliferation dynamics were analyzed using IncuCyte® 2019B and 2020B software versions. Key metrics analyzed included Phase Object Confluence (%) and Phase Object Confluence Normalized to Hour 0, enabling observation of the dynamic effects of treated BMDMs on tumour cell growth.

5.15.2 MdM, MDA-MB-231, and MaMel002 Co-Culture

In an experimental setup aimed at observing the dynamic effects of treated MdMs on tumour cell growth, MdMs were co-cultured with MDA-MB-231 or MaMel002 cells in a Live-cell analysis system.

To induce an M2 phenotype, the MdMs were treated with IL-4 for 24 hours. After this induction period, the cells were washed to remove cytokines, and then repolarised with IFNg+LPS, transfected with candidate miRNAs or treated with specific SMIs. After a 48-hour period post-treatment the MdMs were harvested for co-culture assays.

MDA-MB231 or MaMel002 cancer cell lines expressing Red Fluorescent Protein (RFP) were seeded into 96-well flat-bottom plate at 5000 cells per well, in co-culture with the treated MdMs, also at 5000 cells per well. All experiments were conducted with five or six technical replicates.

The culture conditions were monitored using the SX5 Live-Cell Analysis System. The system captured images of the cultures every 3 hours over a 72-hour period, utilising the orange channel to detect RFP levels in the cancer cell lines. Analysis of cell confluence, proliferation dynamics, and RFP detection was performed using the IncuCyte® 2019B and 2020B software versions.

The key metrics analyzed included Phase Object Confluence (%) to assess the overall cell confluence in each well, and orange object count to quantify the RFP-expressing cells in the co-cultures. These metrics allowed for the assessment of the effects of macrophage polarization on co-cultured cancer cells.

5.15.3 MdMs, HT-29, and J7i-53 Co-Culture

In a separate set of experiments, the impact of repolarised MdMs on T-cell activation, particularly focusing on activation of CAR-T cells, was assessed.

For this, the carcinoembryonic antigen (CEA)-expressing tumour cell line HT-29 was co-cultured with Jurkat cells modified to express an anti-CEA chimeric antigen receptor (CAR) and Venus Fluorescent Protein (VFP), which activates upon stimulation by the CAR construct, in the presence of repolarized MdMs. HT-29 cells and MdMs were seeded in a 96-well flat-bottom plate at 5000 cells per well, while J7i-53 cells were seeded at 20.000 cells per well.

The culture conditions and cell interactions within these co-cultures were closely monitored using the SX5 Live-Cell Analysis System. This system was tasked with capturing images of the

cultures every 3 hours across a span of 72 hours. It utilised the green channel specifically for the detection of VFP levels within the T cell line, allowing for a detailed observation of CAR-T cell activation in the presence of macrophages. The analysis of cell confluence, proliferation dynamics, and the detection of VFP was conducted using the IncuCyte® software, versions 2019B and 2020B. Key metrics that were meticulously analysed included the Phase Object Confluence (%), which provided a measure of the overall cell confluence within each well, the green object count and the total green object integrated intensity (GCU x μm²/Image), which were used to quantify the number of VFP-expressing cells and the expression changes in the co-cultures.

Software	Provider
BioRender	BioRender, Toronto, Canada
Excel version 14.0	Microsoft Corporation, Redmond, WA, USA
FACSDiva™ v9.0	Becton Dickinson, Franklin Lakes, USA
FlowJo V10	Becton Dickinson, Franklin Lakes, USA
GraphPad Prism 5	GraphPad Software, Inc., San Diego, USA
IncuCyte 2019B and 2020B	Sartorius AG, Göttingen, Germany
Ingenuity Pathway Analysis	QIAGEN, Venlo, The Netherlands
R 3.0.1	http://www.r-project.org/

Table 5.15.1. List of software used in this study.

5.16 Statistical analysis

Data are presented as mean ± SD unless stated otherwise. No statistical methods were used to predetermine sample size. The exact number of technical and biological replicates, and the statistical tests used, are indicated in figure legends. The biological replicates for RNA-sequencing data are listed. Statistical analysis was performed in R, GraphPad Prism, and with command line tools. Statistical testing was performed using t-test, Dunnett's test, or analysis of variance (ANOVA) test with correction for multiple testing depending on study design.

References

Aegerter, H., Lambrecht, B. N., & Jakubzick, C. V. (2022). Biology of lung macrophages in health and disease [Publisher: Elsevier]. *Immunity*, *55*(9), 1564–1580.

Agarwal, V., Bell, G. W., Nam, J.-W., & Bartel, D. P. (2015). Predicting effective microRNA target sites in mammalian mRNAs. *eLife*, *4*, e05005. https://doi.org/10.7554/eLife.05005

Ahuja, A., Kim, E., Sung, G.-H., & Cho, J. Y. (2020). STAT3 Differentially Regulates TLR4-Mediated Inflammatory Responses in Early or Late Phases. *International Journal of Molecular Sciences*, *21*(20), 7675. https://doi.org/10.3390/ijms21207675

Androulidaki, A., Iliopoulos, D., Arranz, A., Doxaki, C., Schworer, S., Zacharioudaki, V., Margioris, A. N., Tsichlis, P. N., & Tsatsanis, C. (2009). The Kinase Akt1 Controls Macrophage Response to Lipopolysaccharide by Regulating MicroRNAs. *Immunity*, *31*(2), 220–231. https://doi.org/10.1016/j.immuni.2009.06.024

Appleton, E., Hassan, J., Chan Wah Hak, C., Sivamanoharan, N., Wilkins, A., Samson, A., Ono, M., Harrington, K. J., Melcher, A., & Wennerberg, E. (2021). Kickstarting Immunity in Cold Tumours: Localised Tumour Therapy Combinations With Immune Checkpoint Blockade. *Frontiers in Immunology*, *12*, 754436. https://doi.org/10.3389/fimmu.2021.754436

Arango Duque, G., & Descoteaux, A. (2014). Macrophage Cytokines: Involvement in Immunity and Infectious Diseases. *Frontiers in Immunology*, *5*. https://doi.org/10.3389/fimmu.2014.00491

Bala, S., Marcos, M., Kodys, K., Csak, T., Catalano, D., Mandrekar, P., & Szabo, G. (2011). Up-regulation of MicroRNA-155 in Macrophages Contributes to Increased Tumor Necrosis Factor α (TNFα) Production via Increased mRNA Half-life in Alcoholic Liver Disease. *Journal of Biological Chemistry*, *286*(2), 1436–1444. https://doi.org/10.1074/jbc.M110.145870

Batlle, E., & Massagué, J. (2019). Transforming Growth Factor-β Signaling in Immunity and Cancer. *Immunity*, *50*(4), 924–940. https://doi.org/10.1016/j.immuni.2019.03.024

Bazzoni, F., Rossato, M., Fabbri, M., Gaudiosi, D., Mirolo, M., Mori, L., Tamassia, N., Mantovani, A., Cassatella, M. A., & Locati, M. (2009). Induction and regulatory function of miR-9 in human monocytes and neutrophils exposed to proinflammatory signals. *Proceedings of the National Academy of Sciences*, *106*(13), 5282–5287. https://doi.org/10.1073/pnas.0810909106

Bill, M. A., Fuchs, J. R., Li, C., Yui, J., Bakan, C., Benson, D. M., Schwartz, E. B., Abdelhamid, D., Lin, J., Hoyt, D. G., Fossey, S. L., Young, G. S., Carson, W. E., Li, P.-K., & Lesinski, G. B. (2010). The small molecule curcumin analog FLLL32 induces apoptosis in melanoma cells via STAT3 inhibition and retains the cellular response to cytokines with anti-tumor activity. *Molecular Cancer*, *9*(1), 165. https://doi.org/10.1186/1476-4598-9-165

Bingle, L., Brown, N. J., & Lewis, C. E. (2002). The role of tumour-associated macrophages in tumour progression: Implications for new anticancer therapies. *The Journal of Pathology*, *196*(3), 254–265. https://doi.org/10.1002/path.1027

Binnemars-Postma, K., Bansal, R., Storm, G., & Prakash, J. (2018). Targeting the Stat6 pathway in tumor-associated macrophages reduces tumor growth and metastatic niche formation in breast cancer. *The FASEB Journal*, *32*(2), 969–978. https://doi.org/10.1096/fj.201700629R

Bonnardel, J., T'Jonck, W., Gaublomme, D., Browaeys, R., Scott, C. L., Martens, L., Vanneste, B., De Prijck, S., Nedospasov, S. A., Kremer, A., et al. (2019). Stellate cells, hepatocytes, and endothelial cells imprint the Kupffer cell identity on monocytes colonizing the liver macrophage niche [Publisher: Elsevier]. *Immunity*, *51*(4), 638–654.

Boutilier, A. J., & Elsawa, S. F. (2021). Macrophage Polarization States in the Tumor Microenvironment. *International Journal of Molecular Sciences*, *22*(13), 6995. https://doi.org/10.3390/ijms22136995

Bradley, J. R., & Pober, J. S. (2001). Tumor necrosis factor receptor-associated factors (TRAFs). *Oncogene*, *20*(44), 6482–6491. https://doi.org/10.1038/sj.onc.1204788

Cai, X., Yin, Y., Li, N., Zhu, D., Zhang, J., Zhang, C.-Y., & Zen, K. (2012). Re-polarization of tumor-associated macrophages to pro-inflammatory M1 macrophages by microRNA-155. *Journal of Molecular Cell Biology*, *4*(5), 341–343. https://doi.org/10.1093/jmcb/mjs044

Cappell, K. M., & Kochenderfer, J. N. (2023). Long-term outcomes following CAR T cell therapy: What we know so far. *Nature Reviews Clinical Oncology*, *20*(6), 359–371. https://doi.org/10.1038/s41571-023-00754-1

Chaudhuri, A. A., So, A. Y.-L., Sinha, N., Gibson, W. S. J., Taganov, K. D., O'Connell, R. M., & Baltimore, D. (2011). MicroRNA-125b Potentiates Macrophage Activation. *The Journal of Immunology*, *187*(10), 5062–5068. https://doi.org/10.4049/jimmunol.1102001

Chauhan, J., Wang, H., Yap, J. L., Sabato, P. E., Hu, A., Prochownik, E. V., & Fletcher, S. (2014). Discovery of Methyl 4′-Methyl-5-(7-nitrobenzo[*c*][1,2,5]oxadiazol-4-yl)-[1,1′-biphenyl]-3-carboxylate, an Improved Small-Molecule Inhibitor of c-Myc–Max Dimerization. *ChemMedChem*, *9*(10), 2274–2285. https://doi.org/10.1002/cmdc.201402189

Chen, H., Mo, D., Li, M., Zhang, Y., Chen, L., Zhang, X., Li, M., Zhou, X., & Chen, Y. (2014). miR-709 inhibits 3T3-L1 cell differentiation by targeting GSK3β of Wnt/β-catenin signaling. *Cellular Signalling*, *26*(11), 2583–2589. https://doi.org/10.1016/j.cellsig.2014.07.017

Chen, Y., Song, Y., Du, W., Gong, L., Chang, H., & Zou, Z. (2019). Tumor-associated macrophages: An accomplice in solid tumor progression. *Journal of Biomedical Science*, *26*(1), 78. https://doi.org/10.1186/s12929-019-0568-z

Chen, Y., & Wang, X. (2020). miRDB: An online database for prediction of functional microRNA targets. *Nucleic Acids Research*, *48*(D1), D127–D131. https://doi.org/10.1093/nar/gkz757

Chiba, Y., Todoroki, M., Nishida, Y., Tanabe, M., & Misawa, M. (2009). A Novel STAT6 Inhibitor AS1517499 Ameliorates Antigen-Induced Bronchial Hypercontractility in Mice. *American Journal of Respiratory Cell and Molecular Biology*, *41*(5), 516–524. https://doi.org/10.1165/rcmb.2008-0163OC

Clausen, D. M., Guo, J., Parise, R. A., Beumer, J. H., Egorin, M. J., Lazo, J. S., Prochownik, E. V., & Eiseman, J. L. (2010). In Vitro Cytotoxicity and In Vivo Efficacy, Pharmacokinetics, and Metabolism of 10074-G5, a Novel Small-Molecule Inhibitor of c-Myc/Max Dimerization. *Journal of Pharmacology and Experimental Therapeutics*, *335*(3), 715–727. https://doi.org/10.1124/jpet.110.170555

Creagh, E. M., & O'Neill, L. A. (2006). TLRs, NLRs and RLRs: A trinity of pathogen sensors that co-operate in innate immunity. *Trends in Immunology*, *27*(8), 352–357. https://doi.org/10.1016/j.it.2006.06.003

Das, A. S., Mishra, R., & Bhattacharya, S. (2020). Age-related blunting of the phagocyte arsenal and its art of killing. *Current Molecular Biology Reports*, *6*(3), 126–138. https://doi.org/10.1007/s40610-020-00135-y

Economopoulos, V., Pannell, M., Johanssen, V. A., Scott, H., Andreou, K. E., Larkin, J. R., & Sibson, N. R. (2022). Inhibition of Anti-Inflammatory Macrophage Phenotype Reduces Tumour Growth in Mouse Models of Brain Metastasis. *Frontiers in Oncology*, *12*, 850656. https://doi.org/10.3389/fonc.2022.850656

El-Khoury, V., Moussay, E., Janji, B., Palissot, V., Aouali, N., Brons, N. H., Van Moer, K., Pierson, S., Van Dyck, E., & Berchem, G. (2010). The Histone Deacetylase Inhibitor MGCD0103 Induces Apoptosis in B-Cell Chronic Lymphocytic Leukemia Cells through a Mitochondria-Mediated Caspase Activation Cascade. *Molecular Cancer Therapeutics*, *9*(5), 1349–1360. https://doi.org/10.1158/1535-7163.MCT-09-1000

Essandoh, K., Li, Y., Huo, J., & Fan, G.-C. (2016). MiRNA-Mediated Macrophage Polarization and its Potential Role in the Regulation of Inflammatory Response. *Shock*, *46*(2), 122–131. https://doi.org/10.1097/SHK.0000000000000604

Fournel, M., Bonfils, C., Hou, Y., Yan, P. T., Trachy-Bourget, M.-C., Kalita, A., Liu, J., Lu, A.-H., Zhou, N. Z., Robert, M.-F., Gillespie, J., Wang, J. J., Ste-Croix, H., Rahil, J., Lefebvre, S., Moradei, O., Delorme, D., MacLeod, A. R., Besterman, J. M., & Li, Z. (2008). MGCD0103, a novel isotype-selective histone deacetylase inhibitor, has broad spectrum antitumor activity *in vitro* and *in vivo*. *Molecular Cancer Therapeutics*, *7*(4), 759–768. https://doi.org/10.1158/1535-7163.MCT-07-2026

Funes, S. C., Rios, M., Escobar-Vera, J., & Kalergis, A. M. (2018). Implications of macrophage polarization in autoimmunity. *Immunology*, *154*(2), 186–195. https://doi.org/10.1111/imm.12910

Galli, S. J., Borregaard, N., & Wynn, T. A. (2011). Phenotypic and functional plasticity of cells of innate immunity: Macrophages, mast cells and neutrophils. *Nature Immunology*, *12*(11), 1035–1044. https://doi.org/10.1038/ni.2109

Geiß, C., Salas, E., Guevara-Coto, J., Régnier-Vigouroux, A., & Mora-Rodríguez, R. A. (2022). Multistability in Macrophage Activation Pathways and Metabolic Implications. *Cells*, *11*(3), 404. https://doi.org/10.3390/cells11030404

Gerloff, D., Lützkendorf, J., Moritz, R. K., Wersig, T., Mäder, K., Müller, L. P., & Sunderkötter, C. (2020). Melanoma-Derived Exosomal miR-125b-5p Educates Tumor Associated Macrophages (TAMs) by Targeting Lysosomal Acid Lipase A (LIPA). *Cancers*, *12*(2), 464. https://doi.org/10.3390/cancers12020464

Gordon, S., & Plüddemann, A. (2018). Macrophage Clearance of Apoptotic Cells: A Critical Assessment. *Frontiers in Immunology*, *9*, 127. https://doi.org/10.3389/fimmu.2018.00127

Graff, J. W., Dickson, A. M., Clay, G., McCaffrey, A. P., & Wilson, M. E. (2012). Identifying Functional MicroRNAs in Macrophages with Polarized Phenotypes. *Journal of Biological Chemistry*, *287*(26), 21816–21825. https://doi.org/10.1074/jbc.M111.327031

Gratchev, A. (2017). TGF-β signalling in tumour associated macrophages. *Immunobiology*, *222*(1), 75–81. https://doi.org/10.1016/j.imbio.2015.11.016

Griffiths-Jones, S., Saini, H. K., Van Dongen, S., & Enright, A. J. (2007). miRBase: Tools for microRNA genomics. *Nucleic Acids Research*, *36*(Database), D154–D158. https://doi.org/10.1093/nar/gkm952

Guilliams, M., Bruhns, P., Saeys, Y., Hammad, H., & Lambrecht, B. N. (2014). The function of Fcγ receptors in dendritic cells and macrophages. *Nature Reviews Immunology*, *14*(2), 94–108. https://doi.org/10.1038/nri3582

Günthner, R., & Anders, H.-J. (2013). Interferon-Regulatory Factors Determine Macrophage Phenotype Polarization. *Mediators of Inflammation*, *2013*, 1–8. https://doi.org/10.1155/2013/731023

Halama, N., Zoernig, I., Berthel, A., Kahlert, C., Klupp, F., Suarez-Carmona, M., Suetterlin, T., Brand, K., Krauss, J., Lasitschka, F., Lerchl, T., Luckner-Minden, C., Ulrich, A., Koch, M., Weitz, J., Schneider, M., Buechler, M. W., Zitvogel, L., Herrmann, T., Benner, A., Kunz, C., Luecke, S., Springfeld, C., Grabe, N., Falk, C. S., & Jaeger, D. (2016). Tumoral Immune Cell Exploitation in Colorectal Cancer Metastases Can Be Targeted Effectively by Anti-CCR5 Therapy in Cancer Patients. *Cancer Cell*, *29*(4), 587–601. https://doi.org/10.1016/j.ccell.2016.03.005

Hanahan, D., & Weinberg, R. A. (2011). Hallmarks of Cancer: The Next Generation. *Cell*, *144*(5), 646–674. https://doi.org/10.1016/j.cell.2011.02.013

Hourani, T., Holden, J. A., Li, W., Lenzo, J. C., Hadjigol, S., & O'Brien-Simpson, N. M. (2021). Tumor Associated Macrophages: Origin, Recruitment, Phenotypic Diversity, and Targeting. *Frontiers in Oncology*, *11*, 788365. https://doi.org/10.3389/fonc.2021.788365

Hsu, P. W. (2006). miRNAMap: Genomic maps of microRNA genes and their target genes in mammalian genomes. *Nucleic Acids Research*, *34*(90001), D135–D139. https://doi.org/10.1093/nar/gkj135

Hu, G., Su, Y., Kang, B. H., Fan, Z., Dong, T., Brown, D. R., Cheah, J., Wittrup, K. D., & Chen, J. (2021). High-throughput phenotypic screen and transcriptional analysis identify new compounds and targets for macrophage reprogramming. *Nature Communications*, *12*(1), 773. https://doi.org/10.1038/s41467-021-21066-x

Hu, Y.-W., Hu, Y.-R., Zhao, J.-Y., Li, S.-F., Ma, X., Wu, S.-G., Lu, J.-B., Qiu, Y.-R., Sha, Y.-H., Wang, Y.-C., Gao, J.-J., Zheng, L., & Wang, Q. (2014). An Agomir of miR-144-3p Accelerates Plaque Formation through Impairing Reverse Cholesterol Transport and Promoting Pro-Inflammatory Cytokine Production (O. Kocher, Ed.). *PLoS ONE*, *9*(4), e94997. https://doi.org/10.1371/journal.pone.0094997

Hume, D. A., Millard, S. M., & Pettit, A. R. (2023). Macrophage heterogeneity in the single-cell era: Facts and artifacts [Publisher: American Society of Hematology Washington, DC]. *Blood*, *142*(16), 1339–1347.

Irvine, K. M., Andrews, M. R., Fernandez-Rojo, M. A., Schroder, K., Burns, C. J., Su, S., Wilks, A. F., Parton, R. G., Hume, D. A., & Sweet, M. J. (2009). Colony-stimulating factor-1 (CSF-1) delivers a proatherogenic signal to human macrophages. *Journal of Leukocyte Biology*, *85*(2), 278–288. https://doi.org/10.1189/jlb.0808497

Jablonski, K. A., Amici, S. A., Webb, L. M., Ruiz-Rosado, J. D. D., Popovich, P. G., Partida-Sanchez, S., & Guerau-de-Arellano, M. (2015). Novel Markers to Delineate Murine M1 and M2 Macrophages (M. A. Olszewski, Ed.). *PLOS ONE*, *10*(12), e0145342. https://doi.org/10.1371/journal.pone.0145342

Jablonski, K. A., Gaudet, A. D., Amici, S. A., Popovich, P. G., & Guerau-de-Arellano, M. (2016). Control of the Inflammatory Macrophage Transcriptional Signature by miR-155 (G. Zissel, Ed.). *PLOS ONE*, *11*(7), e0159724. https://doi.org/10.1371/journal.pone.0159724

Jaguin, M., Houlbert, N., Fardel, O., & Lecureur, V. (2013). Polarization profiles of human M-CSF-generated macrophages and comparison of M1-markers in classically activated macrophages from GM-CSF and M-CSF origin. *Cellular Immunology*, *281*(1), 51–61. https://doi.org/10.1016/j.cellimm.2013.01.010

Jin, S.-L. C., & Conti, M. (2002). Induction of the cyclic nucleotide phosphodiesterase PDE4B is essential for LPS-activated TNF-α responses [Publisher: National Acad Sciences]. *Proceedings of the National Academy of Sciences*, *99*(11), 7628–7633.

Kaneko, N., Kurata, M., Yamamoto, T., Morikawa, S., & Masumoto, J. (2019). The role of interleukin-1 in general pathology. *Inflammation and Regeneration*, *39*(1), 12. https://doi.org/10.1186/s41232-019-0101-5

Katzenelenbogen, Y., Sheban, F., Yalin, A., Yofe, I., Svetlichnyy, D., Jaitin, D. A., Bornstein, C., Moshe, A., Keren-Shaul, H., Cohen, M., Wang, S.-Y., Li, B., David, E., Salame, T.-M., Weiner, A., & Amit, I. (2020). Coupled scRNA-Seq and Intracellular Protein Activity Reveal an Immunosuppressive Role of TREM2 in Cancer. *Cell*, *182*(4), 872–885.e19. https://doi.org/10.1016/j.cell.2020.06.032

Kawasaki, T., & Kawai, T. (2014). Toll-like receptor signaling pathways [Publisher: Frontiers]. *Frontiers in immunology*, *5*, 461.

Kerneur, C., Cano, C. E., & Olive, D. (2022). Major pathways involved in macrophage polarization in cancer. *Frontiers in Immunology*, *13*, 1026954. https://doi.org/10.3389/fimmu.2022.1026954

Kertesz, M., Iovino, N., Unnerstall, U., Gaul, U., & Segal, E. (2007). The role of site accessibility in microRNA target recognition. *Nature Genetics*, *39*(10), 1278–1284. https://doi.org/10.1038/ng2135

Khafaei, M., Rezaie, E., Mohammadi, A., Shahnazi Gerdehsang, P., Ghavidel, S., Kadkhoda, S., Zorrieh Zahra, A., Forouzanfar, N., Arabameri, H., & Tavallaie, M. (2019). miR-9: From function to therapeutic potential in cancer. *Journal of Cellular Physiology*, *234*(9), 14651–14665. https://doi.org/10.1002/jcp.28210

Khan, F., Pang, L., Dunterman, M., Lesniak, M. S., Heimberger, A. B., & Chen, P. (2023). Macrophages and microglia in glioblastoma: Heterogeneity, plasticity, and therapy. *Journal of Clinical Investigation*, *133*(1), e163446. https://doi.org/10.1172/JCI163446

Kielbassa, K., Vegna, S., Ramirez, C., & Akkari, L. (2019). Understanding the Origin and Diversity of Macrophages to Tailor Their Targeting in Solid Cancers. *Frontiers in Immunology*, *10*, 2215. https://doi.org/10.3389/fimmu.2019.02215

Kim, H. J., Kim, I. S., Lee, S.-G., Kim, Y. J., Silwal, P., Kim, J. Y., Kim, J. K., Seo, W., Chung, C., Cho, H. K., Huh, H. J., Shim, S. C., Park, C., Jhun, B. W., & Jo, E.-K. (2021). MiR-144-3p is associated with pathological inflammation in patients infected with Mycobacteroides abscessus. *Experimental & Molecular Medicine*, *53*(1), 136–149. https://doi.org/10.1038/s12276-020-00552-0

Kim, M.-J., Lee, Y.-J., Yoon, Y.-S., Lim, J. H., Park, E.-M., Chong, Y. H., & Kang, J. L. (2018). A STAT6 Inhibitor AS1517499 Reduces Preventive Effects of Apoptotic Cell Instillation on Bleomycin-Induced Lung Fibrosis by Suppressing PPARγ. *Cellular Physiology and Biochemistry*, *45*(5), 1863–1877. https://doi.org/10.1159/000487877

Kloc, M. (Ed.). (2017). *Macrophages: Origin, Functions and Biointervention* (Vol. 62). Springer International Publishing. https://doi.org/10.1007/978-3-319-54090-0

Kolberg, L., Raudvere, U., Kuzmin, I., Adler, P., Vilo, J., & Peterson, H. (2023). G: Profiler—interoperable web service for functional enrichment analysis and gene identifier mapping (2023 update) [Publisher: Oxford University Press]. *Nucleic Acids Research*, gkad347.

Kordaß, T. (2022). *Controlling the immune suppressors: miRNAs regulating NT5E, ENTPD1 and CD274* [PhD Thesis].

Krämer, A., Green, J., Pollard, J., & Tugendreich, S. (2014). Causal analysis approaches in Ingenuity Pathway Analysis. *Bioinformatics*, *30*(4), 523–530. https://doi.org/10.1093/bioinformatics/btt703

Kumar, S., Ramesh, A., & Kulkarni, A. (2020). Targeting macrophages: A novel avenue for cancer drug discovery. *Expert Opinion on Drug Discovery*, *15*(5), 561–574. https://doi.org/10.1080/17460441.2020.1733525

Lamb, Y. N. (2019). Pexidartinib: First Approval. *Drugs*, *79*(16), 1805–1812. https://doi.org/10.1007/s40265-019-01210-0

Laoui, D., Movahedi, K., Van Overmeire, E., Van den Bossche, J., Schouppe, E., Mommer, C., Nikolaou, A., Morias, Y., De Baetselier, P., & Van Ginderachter, J. A. (2011). Tumor-associated macrophages in breast cancer: Distinct subsets, distinct functions. *The International Journal of Developmental Biology*, *55*(7-8-9), 861–867. https://doi.org/10.1387/ijdb.113371dl

Lauffer, B. E., Mintzer, R., Fong, R., Mukund, S., Tam, C., Zilberleyb, I., Flicke, B., Ritscher, A., Fedorowicz, G., Vallero, R., Ortwine, D. F., Gunzner, J., Modrusan, Z., Neumann, L., Koth, C. M., Lupardus, P. J., Kaminker, J. S., Heise, C. E., & Steiner, P. (2013). Histone Deacetylase (HDAC) Inhibitor Kinetic Rate Constants Correlate with Cellular Histone Acetylation but Not Transcription and Cell Viability. *Journal of Biological Chemistry*, *288*(37), 26926–26943. https://doi.org/10.1074/jbc.M113.490706

Lee, Y.-J., Kim, K., Kim, M., Ahn, Y.-H., & Kang, J. L. (2022). Inhibition of STAT6 Activation by AS1517499 Inhibits Expression and Activity of PPARγ in Macrophages to Resolve Acute Inflammation in Mice. *Biomolecules*, *12*(3), 447. https://doi.org/10.3390/biom12030447

Lendeckel, U., Venz, S., & Wolke, C. (2022). Macrophages: Shapes and functions. *ChemTexts*, *8*(2), 12. https://doi.org/10.1007/s40828-022-00163-4

Leus, N. G., Van Der Wouden, P. E., Van Den Bosch, T., Hooghiemstra, W. T., Ourailidou, M. E., Kistemaker, L. E., Bischoff, R., Gosens, R., Haisma, H. J., & Dekker, F. J. (2016). HDAC 3-selective inhibitor RGFP966 demonstrates anti-inflammatory properties in RAW 264.7 macrophages and mouse precision-cut lung slices by attenuating NF-κB p65 transcriptional activity. *Biochemical Pharmacology*, *108*, 58–74. https://doi.org/10.1016/j.bcp.2016.03.010

Ley, K., Pramod, A. B., Croft, M., Ravichandran, K. S., & Ting, J. P. (2016). How Mouse Macrophages Sense What Is Going On. *Frontiers in Immunology*, *7*. https://doi.org/10.3389/fimmu.2016.00204

Li, D., Wang, X., Lan, X., Li, Y., Liu, L., Yi, J., Li, J., Sun, Q., Wang, Y., Li, H., Zhong, N., Holmdahl, R., & Lu, S. (2015). Down-regulation of miR-144 elicits proinflammatory cytokine production by targeting toll-like receptor 2 in nonalcoholic steatohepatitis of high-fat-diet-induced metabolic syndrome E3 rats. *Molecular and Cellular Endocrinology*, *402*, 1–12. https://doi.org/10.1016/j.mce.2014.12.007

Li, H., Hu, W., Lin, Y., Xu, T., Zhang, X., & Wang, C. (2023). MicroRNA-9-5p Is Involved in Lipopolysaccharide-Induced Acute Lung Injury Via the Regulation of Macrophage Polarization. *International Journal of Toxicology*, *42*(2), 156–164. https://doi.org/10.1177/10915818221146446

Li, M., Chen, H., Chen, L., Chen, Y., Liu, X., & Mo, D. (2016). miR-709 modulates LPS-induced inflammatory response through targeting GSK-3β. *International Immunopharmacology*, *36*, 333–338. https://doi.org/10.1016/j.intimp.2016.04.005

Li, W., Wu, F., Zhao, S., Shi, P., Wang, S., & Cui, D. (2022a). Correlation between PD-1/PD-L1 expression and polarization in tumor-associated macrophages: A key player in tumor immunotherapy. *Cytokine & Growth Factor Reviews*, *67*, 49–57. https://doi.org/10.1016/j.cytogfr.2022.07.004

Li, X., Chen, L., Peng, X., & Zhan, X. (2022b). Progress of tumor-associated macrophages in the epithelial-mesenchymal transition of tumor. *Frontiers in Oncology*, *12*, 911410. https://doi.org/10.3389/fonc.2022.911410

Li, X., Sanda, T., Look, A. T., Novina, C. D., & Von Boehmer, H. (2011). Repression of tumor suppressor miR-451 is essential for NOTCH1-induced oncogenesis in T-ALL. *Journal of Experimental Medicine*, *208*(4), 663–675. https://doi.org/10.1084/jem.20102384

Lin, L., Hutzen, B., Zuo, M., Ball, S., Deangelis, S., Foust, E., Pandit, B., Ihnat, M. A., Shenoy, S. S., Kulp, S., Li, P.-K., Li, C., Fuchs, J., & Lin, J. (2010). Novel STAT3 Phosphorylation Inhibitors Exhibit Potent Growth-Suppressive Activity in Pancreatic and Breast Cancer Cells. *Cancer Research*, *70*(6), 2445–2454. https://doi.org/10.1158/0008-5472.CAN-09-2468

Lin, L., Jou, D., Wang, Y., Ma, H., Liu, T., Fuchs, J., Li, P.-K., Lü, J., Li, C., & Lin, J. (2016). STAT3 as a potential therapeutic target in ALDH+ and CD44+/CD24+ stem cell-like pancreatic cancer cells. *International Journal of Oncology*, *49*(6), 2265–2274. https://doi.org/10.3892/ijo.2016.3728

Lindsten, T., Hedbrant, A., Ramberg, A., Wijkander, J., Solterbeck, A., Eriksson, M., Delbro, D., & Erlandsson, A. (2017). Effect of macrophages on breast cancer cell proliferation, and on expression of hormone receptors, uPAR and HER-2. *International Journal of Oncology*, *51*(1), 104–114. https://doi.org/10.3892/ijo.2017.3996

Liu, G., Friggeri, A., Yang, Y., Park, Y.-J., Tsuruta, Y., & Abraham, E. (2009). miR-147, a microRNA that is induced upon Toll-like receptor stimulation, regulates murine macrophage inflammatory responses. *Proceedings of the National Academy of Sciences*, *106*(37), 15819–15824. https://doi.org/10.1073/pnas.0901216106

Liu, G., Wan, Q., Li, J., Hu, X., Gu, X., & Xu, S. (2020). Silencing miR-125b-5p attenuates inflammatory response and apoptosis inhibition in mycobacterium tuberculosis-infected human macrophages by targeting DNA damage-regulated autophagy modulator 2 (DRAM2). *Cell Cycle*, *19*(22), 3182–3194. https://doi.org/10.1080/15384101.2020.1838792

Liu, J., Zhou, F., Guan, Y., Meng, F., Zhao, Z., Su, Q., Bao, W., Wang, X., Zhao, J., Huo, Z., Zhang, L., Zhou, S., Chen, Y., & Wang, X. (2022). The Biogenesis of miRNAs and Their Role in the Development of Amyotrophic Lateral Sclerosis. *Cells*, *11*(3), 572. https://doi.org/10.3390/cells11030572

Liu, X., Zhang, J., Zeigler, A. C., Nelson, A. R., Lindsey, M. L., & Saucerman, J. J. (2021). Network Analysis Reveals a Distinct Axis of Macrophage Activation in Response to Conflicting Inflammatory Cues. *The Journal of Immunology*, *206*(4), 883–891. https://doi.org/10.4049/jimmunol.1901444

Liu, Y., Kubiak, J. Z., Li, X. C., Ghobrial, R. M., & Kloc, M. (2017). Macrophages and RhoA Pathway in Transplanted Organs. In M. Kloc (Ed.), *Macrophages: Origin, Functions and Biointervention* (pp. 365–376). Springer International Publishing. https://doi.org/10.1007/978-3-319-54090-0_15

Lu, L., McCurdy, S., Huang, S., Zhu, X., Peplowska, K., Tiirikainen, M., Boisvert, W. A., & Garmire, L. X. (2016). Time Series miRNA-mRNA integrated analysis reveals critical miRNAs and targets in macrophage polarization. *Scientific Reports*, *6*(1), 37446. https://doi.org/10.1038/srep37446

Lu, X., Chen, Y., Zeng, T., Chen, L., Shao, Q., & Qin, W. (2014). Knockout of the HCC suppressor gene Lass2 downregulates the expression level of miR-694. *Oncology Reports*, *32*(6), 2696–2702. https://doi.org/10.3892/or.2014.3527

Ma, W.-T., Gao, F., Gu, K., & Chen, D.-K. (2019). The Role of Monocytes and Macrophages in Autoimmune Diseases: A Comprehensive Review. *Frontiers in Immunology*, *10*, 1140. https://doi.org/10.3389/fimmu.2019.01140

Malvaez, M., McQuown, S. C., Rogge, G. A., Astarabadi, M., Jacques, V., Carreiro, S., Rusche, J. R., & Wood, M. A. (2013). HDAC3-selective inhibitor enhances extinction of cocaine-seeking behavior in a persistent manner. *Proceedings of the National Academy of Sciences*, *110*(7), 2647–2652. https://doi.org/10.1073/pnas.1213364110

Mann, M., Mehta, A., Zhao, J. L., Lee, K., Marinov, G. K., Garcia-Flores, Y., Lu, L.-F., Rudensky, A. Y., & Baltimore, D. (2017). An NF-κB-microRNA regulatory network tunes macrophage inflammatory responses. *Nature Communications*, *8*(1), 851. https://doi.org/10.1038/s41467-017-00972-z

Mantovani, A., Sica, A., Sozzani, S., Allavena, P., Vecchi, A., & Locati, M. (2004). The chemokine system in diverse forms of macrophage activation and polarization. *Trends in Immunology*, *25*(12), 677–686. https://doi.org/10.1016/j.it.2004.09.015

Mass, E., Nimmerjahn, F., Kierdorf, K., & Schlitzer, A. (2023). Tissue-specific macrophages: How they develop and choreograph tissue biology. *Nature Reviews Immunology*, *23*(9), 563–579. https://doi.org/10.1038/s41577-023-00848-y

McDonald, M. M., Kim, A. S., Mulholland, B. S., & Rauner, M. (2021). New insights into osteoclast biology [Publisher: Wiley Online Library]. *Jbmr Plus*, *5*(9), e10539.

McGettrick, A. F., & O'Neill, L. A. (2020). The Role of HIF in Immunity and Inflammation. *Cell Metabolism*, *32*(4), 524–536. https://doi.org/10.1016/j.cmet.2020.08.002

Mills, C. D., Kincaid, K., Alt, J. M., Heilman, M. J., & Hill, A. M. (2000). M-1/M-2 Macrophages and the Th1/Th2 Paradigm. *The Journal of Immunology*, *164*(12), 6166–6173. https://doi.org/10.4049/jimmunol.164.12.6166

Mitsuhashi, A., Goto, H., Kuramoto, T., Tabata, S., Yukishige, S., Abe, S., Hanibuchi, M., Kakiuchi, S., Saijo, A., Aono, Y., Uehara, H., Yano, S., Ledford, J. G., Sone, S., & Nishioka, Y. (2013). Surfactant Protein A Suppresses Lung Cancer Progression by Regulating the Polarization of Tumor-Associated Macrophages. *The American Journal of Pathology*, *182*(5), 1843–1853. https://doi.org/10.1016/j.ajpath.2013.01.030

Monk, C. E., Hutvagner, G., & Arthur, J. S. C. (2010). Regulation of miRNA Transcription in Macrophages in Response to Candida albicans (D. Hartl, Ed.). *PLoS ONE*, *5*(10), e13669. https://doi.org/10.1371/journal.pone.0013669

Monnier, M., Paolini, L., Vinatier, E., Mantovani, A., Delneste, Y., & Jeannin, P. (2022). Antitumor strategies targeting macrophages: The importance of considering the differences in differentiation/polarization processes between human and mouse macrophages. *Journal for ImmunoTherapy of Cancer*, *10*(10), e005560. https://doi.org/10.1136/jitc-2022-005560

Movahedi, K., Laoui, D., Gysemans, C., Baeten, M., Stangé, G., Van den Bossche, J., Mack, M., Pipeleers, D., In't Veld, P., De Baetselier, P., et al. (2010). Different tumor microenvironments contain functionally distinct subsets of macrophages derived from Ly6C (high) monocytes [Publisher: AACR]. *Cancer research*, *70*(14), 5728–5739.

Mueckler, M., & Thorens, B. (2013). The SLC2 (GLUT) family of membrane transporters. *Molecular Aspects of Medicine*, *34*(2-3), 121–138. https://doi.org/10.1016/j.mam.2012.07.001

Mullican, S. E., Gaddis, C. A., Alenghat, T., Nair, M. G., Giacomin, P. R., Everett, L. J., Feng, D., Steger, D. J., Schug, J., Artis, D., & Lazar, M. A. (2011). Histone deacetylase 3 is an epigenomic brake in macrophage alternative activation. *Genes & Development*, *25*(23), 2480–2488. https://doi.org/10.1101/gad.175950.111

Munn, D. H., & Mellor, A. L. (2013). Indoleamine 2,3 dioxygenase and metabolic control of immune responses. *Trends in Immunology*, *34*(3), 137–143. https://doi.org/10.1016/j.it.2012.10.001

Muntjewerff, E. M., & Meesters, L. D. (2020). Antigen Cross-Presentation by Macrophages. *Frontiers in Immunology*, *11*.

Murphy, K., & Weaver, C. (2016). *Janeway's immunobiology*. Garland science.

Murray, P. J. (2017). Macrophage Polarization. *Annual Review of Physiology*, *79*(1), 541–566. https://doi.org/10.1146/annurev-physiol-022516-034339

Mussbacher, M., Derler, M., Basílio, J., & Schmid, J. A. (2023). NF-κB in monocytes and macrophages – an inflammatory master regulator in multitalented immune cells. *Frontiers in Immunology*, *14*, 1134661. https://doi.org/10.3389/fimmu.2023.1134661

Nagashima, S., Yokota, M., Nakai, E.-i., Kuromitsu, S., Ohga, K., Takeuchi, M., Tsukamoto, S.-i., & Ohta, M. (2007). Synthesis and evaluation of 2-{[2-(4-hydroxyphenyl)-ethyl]amino}pyrimidine-5-carboxamide derivatives as novel STAT6 inhibitors. *Bioorganic & Medicinal Chemistry*, *15*(2), 1044–1055. https://doi.org/10.1016/j.bmc.2006.10.015

Nazari-Jahantigh, M., Wei, Y., Noels, H., Akhtar, S., Zhou, Z., Koenen, R. R., Heyll, K., Gremse, F., Kiessling, F., Grommes, J., Weber, C., & Schober, A. (2012). MicroRNA-155 promotes atherosclerosis by repressing Bcl6 in macrophages. *Journal of Clinical Investigation*, *122*(11), 4190–4202. https://doi.org/10.1172/JCI61716

O'Connell, R. M., Taganov, K. D., Boldin, M. P., Cheng, G., & Baltimore, D. (2007). MicroRNA-155 is induced during the macrophage inflammatory response. *Proceedings of the National Academy of Sciences*, *104*(5), 1604–1609. https://doi.org/10.1073/pnas.0610731104

Paolicelli, R. C., Bolasco, G., Pagani, F., Maggi, L., Scianni, M., Panzanelli, P., Giustetto, M., Ferreira, T. A., Guiducci, E., Dumas, L., et al. (2011). Synaptic pruning by microglia is necessary for normal brain development [Publisher: American Association for the Advancement of Science]. *science*, *333*(6048), 1456–1458.

Parameswaran, N., & Patial, S. (2010). Tumor Necrosis Factor-α Signaling in Macrophages. *Critical Reviews™ in Eukaryotic Gene Expression*, *20*(2), 87–103. https://doi.org/10.1615/CritRevEukarGeneExpr.v20.i2.10

Pardoll, D. M. (2012). The blockade of immune checkpoints in cancer immunotherapy. *Nature Reviews Cancer*, *12*(4), 252–264. https://doi.org/10.1038/nrc3239

Patel, S., & Werstuck, G. H. (2021). Macrophage Function and the Role of GSK3. *International Journal of Molecular Sciences*, *22*(4), 2206. https://doi.org/10.3390/ijms22042206

Patnaik, A., Spreafico, A., Paterson, A. M., Peluso, M., Chung, J.-K., Bowers, B., Niforos, D., O'Neill, A. M., Beeram, M., Iafolla, M., et al. (2020). Results of a first-in-human phase I study of SRF231, a fully human, high-affinity anti-CD47 antibody.

Paz-Ares, L., Forster, M., Boni, V., Szyldergemajn, S., Corral, J., Turnbull, S., Cubillo, A., Teruel, C. F., Calderero, I. L., Siguero, M., et al. (2017). Phase I clinical and pharmacokinetic study of PM01183 (a tetrahydroisoquinoline, Lurbinectedin) in combination with gemcitabine in patients with advanced solid tumors [Publisher: Springer]. *Investigational new drugs*, *35*, 198–206.

Pello, O. M. (2016). Macrophages and c-Myc cross paths. *OncoImmunology*, *5*(6), e1151991. https://doi.org/10.1080/2162402X.2016.1151991

Pello, O. M., Chèvre, R., Laoui, D., De Juan, A., Lolo, F., Andrés-Manzano, M. J., Serrano, M., Van Ginderachter, J. A., & Andrés, V. (2012a). In Vivo Inhibition of c-MYC in Myeloid Cells Impairs Tumor-Associated Macrophage Maturation and Pro-Tumoral Activities (D. D. Roberts, Ed.). *PLoS ONE*, *7*(9), e45399. https://doi.org/10.1371/journal.pone.0045399

Pello, O. M., De Pizzol, M., Mirolo, M., Soucek, L., Zammataro, L., Amabile, A., Doni, A., Nebuloni, M., Swigart, L. B., Evan, G. I., Mantovani, A., & Locati, M. (2012b). Role of c-MYC in alternative activation of human macrophages and tumor-associated macrophage biology. *Blood*, *119*(2), 411–421. https://doi.org/10.1182/blood-2011-02-339911

Peter, D., Jin, S. L. C., Conti, M., Hatzelmann, A., & Zitt, C. (2007). Differential Expression and Function of Phosphodiesterase 4 (PDE4) Subtypes in Human Primary CD4+ T Cells: Predominant Role of PDE4D. *The Journal of Immunology*, *178*(8), 4820–4831. https://doi.org/10.4049/jimmunol.178.8.4820

Pham, K., Luo, D., Liu, C., & Harrison, J. K. (2012). CCL5, CCR1 and CCR5 in murine glioblastoma: Immune cell infiltration and survival rates are not dependent on individual expression of either CCR1 or CCR5. *Journal of Neuroimmunology*, *246*(1-2), 10–17. https://doi.org/10.1016/j.jneuroim.2012.02.009

Piaggio, F., Kondylis, V., Pastorino, F., Di Paolo, D., Perri, P., Cossu, I., Schorn, F., Marinaccio, C., Murgia, D., Daga, A., Raggi, F., Loi, M., Emionite, L., Ognio, E., Pasparakis, M., Ribatti, D., Ponzoni, M., & Brignole, C. (2016). A novel liposomal Clodronate depletes tumor-associated macrophages in primary and metastatic melanoma: Anti-angiogenic and anti-tumor effects. *Journal of Controlled Release*, *223*, 165–177. https://doi.org/10.1016/j.jconrel.2015.12.037

Platanitis, E., & Decker, T. (2018). Regulatory Networks Involving STATs, IRFs, and NFκB in Inflammation. *Frontiers in Immunology*, *9*, 2542. https://doi.org/10.3389/fimmu.2018.02542

Rakkola, R., Matikainen, S., & Nyman, T. A. (2007). Proteome analysis of human macrophages reveals the upregulation of manganese-containing superoxide dismutase after toll-like receptor activation [Publisher: Wiley Online Library]. *Proteomics*, *7*(3), 378–384.

Ren, X., Duan, L., He, Q., Zhang, Z., Zhou, Y., Wu, D., Pan, J., Pei, D., & Ding, K. (2010). Identification of Niclosamide as a New Small-Molecule Inhibitor of the STAT3 Signaling Pathway. *ACS Medicinal Chemistry Letters*, *1*(9), 454–459. https://doi.org/10.1021/ml100146z

Richards, D. M., Hettinger, J., & Feuerer, M. (2013). Monocytes and Macrophages in Cancer: Development and Functions. *Cancer Microenvironment*, *6*(2), 179–191. https://doi.org/10.1007/s12307-012-0123-x

Roa-Vidal, N., Rodríguez-Aponte, A. S., Lasalde-Dominicci, J. A., Capó-Vélez, C. M., & Delgado-Vélez, M. (2023). Cholinergic Polarization of Human Macrophages. *International Journal of Molecular Sciences*, *24*(21), 15732. https://doi.org/10.3390/ijms242115732

Roche, P. A., & Furuta, K. (2015). The ins and outs of MHC class II-mediated antigen processing and presentation. *Nature Reviews Immunology*, *15*(4), 203–216. https://doi.org/10.1038/nri3818

Rosato, R. R., Almenara, J. A., & Grant, S. (2003). The Histone Deacetylase Inhibitor MS-275 Promotes Differentiation or Apoptosis in Human Leukemia Cells through a Process Regulated by Generation of Reactive Oxygen Species and Induction of p21CIP1/WAF1.

Ross, E. A., Devitt, A., & Johnson, J. R. (2021). Macrophages: The Good, the Bad, and the Gluttony. *Frontiers in Immunology*, *12*, 708186. https://doi.org/10.3389/fimmu.2021.708186

Rőszer, T. (2015). Understanding the Mysterious M2 Macrophage through Activation Markers and Effector Mechanisms. *Mediators of Inflammation*, *2015*, 1–16. https://doi.org/10.1155/2015/816460

Roussel, M., Ferrell Jr, P. B., Greenplate, A. R., Lhomme, F., Le Gallou, S., Diggins, K. E., Johnson, D. B., & Irish, J. M. (2017). Mass cytometry deep phenotyping of human mononuclear phagocytes and myeloid-derived suppressor cells from human blood and bone marrow [Publisher: Oxford University Press]. *Journal of leukocyte biology*, *102*(2), 437–447.

Saenger, Y. M., Sabado, R. L., Holman, R. M., Lehrer, D., Salazar, A. M., & Bhardwaj, N. (2014). Treatment of solid tumors with intratumoral poly-ICLC: A phase II clinical study.

Saraiva Camara, N. O., & Braga, T. T. (2022). *Macrophages in the human body a tissue level approach* [OCLC: 1328128473]. Academic Press.

Schust, J., Sperl, B., Hollis, A., Mayer, T. U., & Berg, T. (2006). Stattic: A Small-Molecule Inhibitor of STAT3 Activation and Dimerization. *Chemistry & Biology*, *13*(11), 1235–1242. https://doi.org/10.1016/j.chembiol.2006.09.018

Seidel, J. A., Otsuka, A., & Kabashima, K. (2018). Anti-PD-1 and Anti-CTLA-4 Therapies in Cancer: Mechanisms of Action, Efficacy, and Limitations. *Frontiers in Oncology*, *8*, 86. https://doi.org/10.3389/fonc.2018.00086

Shapouri-Moghaddam, A., Mohammadian, S., Vazini, H., Taghadosi, M., Esmaeili, S.-A., Mardani, F., Seifi, B., Mohammadi, A., Afshari, J. T., & Sahebkar, A. (2018). Macrophage plasticity, polarization, and function in health and disease. *Journal of Cellular Physiology*, *233*(9), 6425–6440. https://doi.org/10.1002/jcp.26429

Shaul, M. E., Bennett, G., Strissel, K. J., Greenberg, A. S., & Obin, M. S. (2010). Dynamic, M2-like remodeling phenotypes of CD11c+ adipose tissue macrophages during high-fat diet–induced obesity in mice [Publisher: Am Diabetes Assoc]. *Diabetes*, *59*(5), 1171–1181.

Shobaki, N., Sato, Y., Suzuki, Y., Okabe, N., & Harashima, H. (2020). Manipulating the function of tumor-associated macrophages by siRNA-loaded lipid nanoparticles for cancer immunotherapy. *Journal of Controlled Release*, *325*, 235–248. https://doi.org/10.1016/j.jconrel.2020.07.001

Sidiropoulos, D. N., Rafie, C. I., Jang, J. K., Castanon, S., Baugh, A. G., Gonzalez, E., Christmas, B. J., Narumi, V. H., Davis-Marcisak, E. F., Sharma, G., Bigelow, E., Vaghasia, A., Gupta,

A., Skaist, A., Considine, M., Wheelan, S. J., Ganesan, S. K., Yu, M., Yegnasubramanian, S., Stearns, V., Connolly, R. M., Gaykalova, D. A., Kagohara, L. T., Jaffee, E. M., Fertig, E. J., & Roussos Torres, E. T. (2022). Entinostat Decreases Immune Suppression to Promote Antitumor Responses in a HER2+ Breast Tumor Microenvironment. *Cancer Immunology Research*, *10*(5), 656–669. https://doi.org/10.1158/2326-6066.CIR-21-0170

Siouti, E., & Andreakos, E. (2019). The many facets of macrophages in rheumatoid arthritis. *Biochemical Pharmacology*, *165*, 152–169. https://doi.org/10.1016/j.bcp.2019.03.029

Solís-Martínez, R., Cancino-Marentes, M., Hernández-Flores, G., Ortiz-Lazareno, P., Mandujano-Álvarez, G., Cruz-Gálvez, C., Sierra-Díaz, E., Rodríguez-Padilla, C., Jave-Suárez, L., Aguilar-Lemarroy, A., & Bravo-Cuellar, A. (2018). Regulation of immunophenotype modulation of monocytes-macrophages from M1 into M2 by prostate cancer cell-culture supernatant via transcription factor STAT3. *Immunology Letters*, *196*, 140–148. https://doi.org/10.1016/j.imlet.2018.02.009

Szanto, A., Balint, B. L., Nagy, Z. S., Barta, E., Dezso, B., Pap, A., Szeles, L., Poliska, S., Oros, M., Evans, R. M., Barak, Y., Schwabe, J., & Nagy, L. (2010). STAT6 Transcription Factor Is a Facilitator of the Nuclear Receptor PPARγ-Regulated Gene Expression in Macrophages and Dendritic Cells. *Immunity*, *33*(5), 699–712. https://doi.org/10.1016/j.immuni.2010.11.009

Taylor, P., Martinez-Pomares, L., Stacey, M., Lin, H.-H., Brown, G., & Gordon, S. (2005). MACROPHAGE RECEPTORS AND IMMUNE RECOGNITION. *Annual Review of Immunology*, *23*(1), 901–944. https://doi.org/10.1146/annurev.immunol.23.021704.115816

Thepmalee, C., Panya, A., Junking, M., Chieochansin, T., & Yenchitsomanus, P.-t. (2018). Inhibition of IL-10 and TGF-β receptors on dendritic cells enhances activation of effector T-cells to kill cholangiocarcinoma cells. *Human Vaccines & Immunotherapeutics*, *14*(6), 1423–1431. https://doi.org/10.1080/21645515.2018.1431598

Thomas, D. A., & Massagué, J. (2005). TGF-β directly targets cytotoxic T cell functions during tumor evasion of immune surveillance. *Cancer Cell*, *8*(5), 369–380. https://doi.org/10.1016/j.ccr.2005.10.012

Tili, E., Michaille, J.-J., Cimino, A., Costinean, S., Dumitru, C. D., Adair, B., Fabbri, M., Alder, H., Liu, C. G., Calin, G. A., & Croce, C. M. (2007). Modulation of miR-155 and miR-125b Levels following Lipopolysaccharide/TNF-α Stimulation and Their Possible Roles in Regulating the Response to Endotoxin Shock. *The Journal of Immunology*, *179*(8), 5082–5089. https://doi.org/10.4049/jimmunol.179.8.5082

Tili, E., Croce, C. M., & Michaille, J.-J. (2009). *miR-155* : On the Crosstalk Between Inflammation and Cancer. *International Reviews of Immunology*, *28*(5), 264–284. https://doi.org/10.1080/08830180903093796

Tommasi, C., Pellegrino, B., Diana, A., Palafox Sancez, M., Orditura, M., Scartozzi, M., Musolino, A., & Solinas, C. (2022). The Innate Immune Microenvironment in Metastatic Breast Cancer. *Journal of Clinical Medicine*, *11*(20), 5986. https://doi.org/10.3390/jcm11205986

Tong, F., Mao, X., Zhang, S., Xie, H., Yan, B., Wang, B., Sun, J., & Wei, L. (2020). HPV + HNSCC-derived exosomal miR-9 induces macrophage M1 polarization and increases tumor radiosensitivity. *Cancer Letters*, *478*, 34–44. https://doi.org/10.1016/j.canlet.2020.02.037

Van Duijn, A., Van Der Burg, S. H., & Scheeren, F. A. (2022). CD47/SIRPα axis: Bridging innate and adaptive immunity. *Journal for ImmunoTherapy of Cancer*, *10*(7), e004589. https://doi.org/10.1136/jitc-2022-004589

Vandenborre, K., Van Gool, S. W., Kasran, A., Ceuppens, J. L., Boogaerts, M. A., & Vandenberghe, P. (1999). Interaction of CTLA-4 (CD152) with CD80 or CD86 inhibits human T-cell activation. *Immunology*, *98*(3), 413–421. https://doi.org/10.1046/j.1365-2567.1999.00888.x

Walport, M. J. (2001). Complement. First of two parts. [Place: United States]. *The New England journal of medicine*, *344*(14), 1058–1066. https://doi.org/10.1056/NEJM200104053441406

Wang, B., Xu, L., Zhang, J., Cheng, X., Xu, Q., Wang, J., & Mao, F. (2020a). LncRNA NORAD accelerates the progression and doxorubicin resistance of neuroblastoma through up-regulating HDAC8 via sponging miR-144-3p. *Biomedicine & Pharmacotherapy*, *129*, 110268. https://doi.org/10.1016/j.biopha.2020.110268

Wang, J., Wang, J., Wang, J., Yang, B., Weng, Q., & He, Q. (2019). Targeting Microglia and Macrophages: A Potential Treatment Strategy for Multiple Sclerosis. *Frontiers in Pharmacology*, *10*, 286. https://doi.org/10.3389/fphar.2019.00286

Wang, J., Ma, S., Yu, J., Zuo, D., He, X., Peng, H., Shi, X., Huang, W., & Li, Q. (2021). MiR-9-5p promotes M1 cell polarization in osteoarthritis progression by regulating NF-κB and AMPK signaling pathways by targeting SIRT1. *International Immunopharmacology*, *101*, 108207. https://doi.org/10.1016/j.intimp.2021.108207

Wang, N., Liang, H., & Zen, K. (2014). Molecular mechanisms that influence the macrophage M1–M2 polarization balance [Publisher: Frontiers Media SA]. *Frontiers in immunology*, *5*, 614.

Wang, W., & Guo, Z.-H. (2020). Downregulation of lncRNA NEAT1 Ameliorates LPS-Induced Inflammatory Responses by Promoting Macrophage M2 Polarization via miR-125a-5p/TRAF6/TAK1 Axis. *Inflammation*, *43*(4), 1548–1560. https://doi.org/10.1007/s10753-020-01231-y

Wang, Y., Chen, C., Xu, X.-d., Li, H., Cheng, M.-h., Liu, J., & Tang, L.-j. (2020b). Levels of miR-125a-5p are altered in Mycobacterium avium-infected macrophages and associate with the triggering of an autophagic response. *Microbes and Infection*, *22*(1), 31–39. https://doi.org/10.1016/j.micinf.2019.07.002

Wells, C. E., Bhaskara, S., Stengel, K. R., Zhao, Y., Sirbu, B., Chagot, B., Cortez, D., Khabele, D., Chazin, W. J., Cooper, A., Jacques, V., Rusche, J., Eischen, C. M., McGirt, L. Y., & Hiebert,

S. W. (2013). Inhibition of Histone Deacetylase 3 Causes Replication Stress in Cutaneous T Cell Lymphoma (S. Cotterill, Ed.). *PLoS ONE*, *8*(7), e68915. https://doi.org/10.1371/journal.pone.0068915

Xia, T., Zhang, M., Lei, W., Yang, R., Fu, S., Fan, Z., Yang, Y., & Zhang, T. (2023). Advances in the role of STAT3 in macrophage polarization. *Frontiers in Immunology*, *14*, 1160719. https://doi.org/10.3389/fimmu.2023.1160719

Xiao, H., Guo, Y., Li, B., Li, X., Wang, Y., Han, S., Cheng, D., & Shuai, X. (2020). M2-like tumor-associated macrophage-targeted codelivery of STAT6 inhibitor and IKKβ siRNA induces M2-to-M1 repolarization for cancer immunotherapy with low immune side effects [Publisher: ACS Publications]. *ACS central science*, *6*(7), 1208–1222.

Xu, L., Li, Y., Yin, L., Qi, Y., Sun, H., Sun, P., Xu, M., Tang, Z., & Peng, J. (2018). miR-125a-5p ameliorates hepatic glycolipid metabolism disorder in type 2 diabetes mellitus through targeting of STAT3. *Theranostics*, *8*(20), 5593–5609. https://doi.org/10.7150/thno.27425

Xu, R., Shao, Z., & Cao, Q. (2021). MicroRNA-144-3p enhances LPS induced septic acute lung injury in mice through downregulating Caveolin-2. *Immunology Letters*, *231*, 18–25. https://doi.org/10.1016/j.imlet.2020.12.015

Xu, Z., Zhao, L., Yang, X., Ma, S., Ge, Y., Liu, Y., Liu, S., Shi, J., & Zheng, D. (2016). Mmu-miR-125b overexpression suppresses NO production in activated macrophages by targeting eEF2K and CCNA2. *BMC Cancer*, *16*(1), 252. https://doi.org/10.1186/s12885-016-2288-z

Yang, Y., Ye, Y.-C., Chen, Y., Zhao, J.-L., Gao, C.-C., Han, H., Liu, W.-C., & Qin, H.-Y. (2018). Crosstalk between hepatic tumor cells and macrophages via Wnt/β-catenin signaling promotes M2-like macrophage polarization and reinforces tumor malignant behaviors. *Cell Death & Disease*, *9*(8), 793. https://doi.org/10.1038/s41419-018-0818-0

Yao, D., Zhou, Z., Wang, P., Zheng, L., Huang, Y., Duan, Y., Liu, B., & Li, Y. (2021). MiR-125-5p/IL-6R axis regulates macrophage inflammatory response and intestinal epithelial cell apoptosis in ulcerative colitis through JAK1/STAT3 and NF-κB pathway. *Cell Cycle*, *20*(23), 2547–2564. https://doi.org/10.1080/15384101.2021.1995128

Yao, H., Ma, R., Yang, L., Hu, G., Chen, X., Duan, M., Kook, Y., Niu, F., Liao, K., Fu, M., Hu, G., Kolattukudy, P., & Buch, S. (2014). MiR-9 promotes microglial activation by targeting MCPIP1. *Nature Communications*, *5*(1), 4386. https://doi.org/10.1038/ncomms5386

Yap, J. L., Wang, H., Hu, A., Chauhan, J., Jung, K.-Y., Gharavi, R. B., Prochownik, E. V., & Fletcher, S. (2013). Pharmacophore identification of c-Myc inhibitor 10074-G5. *Bioorganic & Medicinal Chemistry Letters*, *23*(1), 370–374. https://doi.org/10.1016/j.bmcl.2012.10.013

Yu, T., Gan, S., Zhu, Q., Dai, D., Li, N., Wang, H., Chen, X., Hou, D., Wang, Y., Pan, Q., Xu, J., Zhang, X., Liu, J., Pei, S., Peng, C., Wu, P., Romano, S., Mao, C., Huang, M., Zhu, X., Shen, K., Qin, J., & Xiao, Y. (2019). Modulation of M2 macrophage polarization by the crosstalk between Stat6 and Trim24. *Nature Communications*, *10*(1), 4353. https://doi.org/10.1038/s41467-019-12384-2

Yuva-Aydemir, Y., Simkin, A., Gascon, E., & Gao, F.-B. (2011). MicroRNA-9: Functional evolution of a conserved small regulatory RNA. *RNA Biology*, *8*(4), 557–564. https://doi.org/10.4161/rna.8.4.16019

Zang, X., Zhang, X., Zhao, X., Hu, H., Qiao, M., Deng, Y., & Chen, D. (2019). Targeted Delivery of miRNA 155 to Tumor Associated Macrophages for Tumor Immunotherapy. *Molecular Pharmaceutics*, *16*(4), 1714–1722. https://doi.org/10.1021/acs.molpharmaceut.9b00065

Zhang, C., Zhao, Y., Wang, Q., Qin, J., Ye, B., Xu, C., & Yu, G. (2022). Overexpression of miR-125a-5p Inhibits Hepatocyte Proliferation through the STAT3 Regulation In Vivo and In Vitro. *International Journal of Molecular Sciences*, *23*(15), 8661. https://doi.org/10.3390/ijms23158661

Zhang, L., Alizadeh, D., Van Handel, M., Kortylewski, M., Yu, H., & Badie, B. (2009). Stat3 inhibition activates tumor macrophages and abrogates glioma growth in mice. *Glia*, *57*(13), 1458–1467. https://doi.org/10.1002/glia.20863

Zhang, Y., Mei, H., Chang, X., Chen, F., Zhu, Y., & Han, X. (2016). Adipocyte-derived microvesicles from obese mice induce M1 macrophage phenotype through secreted miR-155. *Journal of Molecular Cell Biology*, *8*(6), 505–517. https://doi.org/10.1093/jmcb/mjw040

Zhang, Y., Zhang, M., Zhong, M., Suo, Q., & Lv, K. (2013). Expression profiles of miRNAs in polarized macrophages. *International Journal of Molecular Medicine*, *31*(4), 797–802. https://doi.org/10.3892/ijmm.2013.1260

Zhao, J., Li, H., Zhao, S., Wang, E., Zhu, J., Feng, D., Zhu, Y., Dou, W., Fan, Q., Hu, J., Jia, L., & Liu, L. (2021). Epigenetic silencing of miR-144/451a cluster contributes to HCC progression via paracrine HGF/MIF-mediated TAM remodeling. *Molecular Cancer*, *20*(1), 46. https://doi.org/10.1186/s12943-021-01343-5

Zheng, H., Peng, X., Yang, S., Li, X., Huang, M., Wei, S., Zhang, S., He, G., Liu, J., Fan, Q., Yang, L., & Li, H. (2023). Targeting tumor-associated macrophages in hepatocellular carcinoma: Biology, strategy, and immunotherapy. *Cell Death Discovery*, *9*(1), 65. https://doi.org/10.1038/s41420-023-01356-7